OAK RIDGE
NATIONAL LABORATORY

MANAGED BY UT-BATTELLE
FOR THE DEPARTMENT OF ENERGY

ORNL/TM-2010/322

Final Technical Report

Additional Characterization of Min-K T/E-1400 Thermal Insulation

January 2011

Prepared by

Dr. J. G. Hemrick
Principal Investigator

UT-BATTELLE

ORNL-27 (4-00)

ORNL/TM-2010/322

Materials Science and Technology Division

ADDITIONAL CHARACTERIZATION OF
Min-K TE-1400 THERMAL INSULAITON

J. G. Hemrick and J. F. King

January 2011

Prepared for
Department of Energy Office of Space and Defense Power Systems

Prepared by
OAK RIDGE NATIONAL LABORATORY
Oak Ridge, Tennessee 37831-6079
managed by
UT-BATTELLE, LLC
for the
U.S. DEPARTMENT OF ENERGY
under contract DE-AC05-00OR22725

CONTENTS

LIST OF FIGURES

Figure Page

Figure Page

Figure Page

LIST OF TABLES

ABBRIVATIONS AND ACRONYMS

Min-K	Min-K 1400TE (Thermal Ceramics, Augusta, Georgia)
ORNL	Oak Ridge National Laboratory
TSE	Transient Strain Events

NOTE: Units used in this document are those requested by the program sponsors. Where applicable, equivalent SI units are given.

ADDITIONAL CHARACTERIZATION OF Min-K TE-1400 THERMAL INSULATION[2]

J. G. Hemrick and J. F. King

1.0 EXECUTIVE SUMMARY

Min-K 1400TE (Thermal Ceramics, Augusta, Georgia) insulation material was further characterized at Oak Ridge National Laboratory (ORNL) for use in structural applications under gradient temperature conditions in an inert environment. Original characterization of Min-K was undertaken from April 1997 to July 2008 to determine its high temperature compressive strength and stress relaxation behavior up to 900°C in helium along with the formulation of a general model for the mechanical behavior exhibited by Min-K under these conditions. The additional testing described in this report was undertaken from April 2009 to June 2010 in an effort to further evaluate the mechanical behavior of Min-K when subjected to a variety of conditions including alternative test temperatures and time scales than previously measured. The behavior of Min-K under changing environments (temperature and strain), lateral loads, and additional isothermal temperatures was therefore explored.

Changing Environments Testing was performed to validate the gradient temperature stress relaxation predictions previously made based on generated data from ORNL. Changes in temperature and strain imparted on Min-K components under gradient temperature conditions were simulated and the effects of these changes were evaluated through testing under various changing environmental conditions. Testing was performed with an initial temperature gradient of 680/130^{o}C and an initial stress of ≈180 psi (1,380 kPa).

A modified test procedure was implemented, based on previous gradient stress relaxation testing. Sample loading was performed under strain control at a rate of 5.56% strain/hour utilizing a twelve increment loading scheme with three equal steps of load application during each increment. Steps were spaced two minutes apart and increments occurred every half hour. Loading was followed by stress relaxation under strain control for ≈75 days. After this period, the first "changing environment" event was performed. While maintaining constant displacement on the test sample (as monitored by a LVDT strain monitoring system) the top and bottom temperatures were changed to 600 and 60^{o}C, respectively. After again allowing the test sample to thermally equilibrate over night, 0.72% strain was applied (using same strain rate as above) in four equal increments spaced 60 minutes apart. Strain change was then followed by stress relaxation under strain control for ≈45 days. After this period, the second "changing environment" event was performed. While again maintaining constant displacement on the test sample (as monitored by a LVDT strain monitoring system), the top and bottom temperatures were changed to 690 and 115^{o}C, respectively.

[2]Research sponsored by the U.S. Department of Energy, Office of Space and Defense Power Systems, under contract with UT-Battelle, LLC.

After again allowing the test sample to thermally equilibrate over night, 0.49% strain was applied (using same strain rate as above) in three equal increments spaced 60 minutes apart. Another period of stress relaxation under strain control was then undertaken for a period of at least 20 days.

Seven gradient stress relaxation tests were completed. Total test durations ranged from 240 and 5,765 hours. Three tests had “changing environments” events performed on them and two tests had Transient Strain Events (TSE) simulated on them. TSE simulation consisted of three phases of testing with Phase I raising the strain under displacement control to simulate cooling of a metal shell around the Min-K insulation material, Phase II decreasing the strain under displacement control to simulate the expansion of a metal shell and Phase III returning the strain back to the original level prior to TSE testing. Following Phase III, the test was put back under fixed displacement and allowed to relax until the test was terminated. For these tests, the rate of stress relaxation did not appear to be affected by either the first or second changing environment event, nor by the TSE event. After each of these events, the rate of stress relaxation appeared to return to a level similar to that before the event.

Lateral Load Testing was performed to provide information on the friction created between two pieces of Min-K or a piece of Min-K and a textured aluminum surface at both room temperature and at elevated temperatures. The original test set-up consisted of a test sample of Min-K sandwiched between two other pieces of constrained Min-K. A tangential load was applied on the top of the stack (through use of dead weights), while a lateral load was applied to the center piece of Min-K (by a mechanical actuator moved at one of two speeds) to remove it from the stack while constraining the top and bottom pieces of and Min-K and monitoring the applied lateral load. It was found during initial testing at room temperature that this test set-up did not properly represent the actual intended application of interest for this material, where the Min-K would be in contact with a textured aluminum surface. Therefore, a revised test set-up was constructed where the original test set-up was moved from a horizontal to a vertical orientation and mounted on an existing mechanical test frame. This set-up consisted of an aluminum plate with a “pyramoidal” structure machined into each surface sandwiched between two pieces of Min-K. Axial load was supplied by a stepper motor attached to a push rod below the sample assembly. Lateral load was applied through a metal rod attached to the textured aluminum plate which was passed through a steel front plate assembly. By turning a mounted bolt, the rod attached to the aluminum plate was pulled, thus applying a lateral load. Testing was performed by first loading the sample axially, then applying a set lateral load. The axial load was then removed at a prescribe displacement rate while monitoring the lateral load for a period where it no longer changed.

After further testing, the test set-up was again modified to eliminate lateral loading created by the test frame when axial loads were applied to the test assembly. The further modified set-up had the rear support assembly replaced with a turnbuckle connected to the center aluminum plate and load cell by hooks and eyelets. Additionally, the original metal loading plates were replaced with new plates incorporating aluminum inserts with the same “pyramoidal” texture as the center plate. Also, supports were added to confine lateral movement of the push rods due to flexure. The use of the hooks and eyelets allowed the sample assembly to move without creating a lateral load during the application of the axial loading and by manipulating the turnbuckle, a lateral load could now be applied to the test assembly.

Initial testing with this set-up was performed with samples first loaded axially, then laterally before the axial load was removed at a prescribe displacement rate while monitoring the lateral load and watching for a period of unchanging lateral load. It was decided though that this test method was still not producing the desired data for analysis, therefore the test procedure was modified. Samples were next axially loaded in a step fashion while observing the corresponding lateral load. After each load step the loads (both axial and lateral) were allowed to relax as the sample was held under constant axial displacement. Next, tests were run by applying a lateral load to a test sample in a step fashion through turning of the frame turnbuckle assembly and observing the corresponding axial load. Again, after each load step the loads (both axial and lateral) were allowed to relax as the sample was held under the current conditions. It was found that coupling still existed between the axial and lateral loads. These loads were thought to be due to deflection of the frame push rods, therefore subsequent work was done to stiffen the frame by providing supports to the push rods.

After stiffening the test frame, testing was run by axially loading the test sample to a prescribed load, then performing a lateral step loading while watching for the sample to begin to slip and recording the corresponding lateral load reached. If the target lateral load was reached for a specific axial load, then the lateral load was removed from the sample and the axial load was reduced to a new value. The sample was then reloaded laterally in a step fashion while watching for slipping. Initial validation of the test system was performed at room temperature. Elevated temperature testing was performed at 400^{o}C. Replicate testing was performed at both temperatures.

Results of initial testing performed at room temperature using the original test set-up provided information on the amount of axial stress that the test assembly could accumulate for a specific dead axial load and test speed (speed of actuator to apply lateral load) before slipping between the Min-K layers occurred represented by the maxing out of the measured axial stress. Although this information was of academic interest, these results were determined to not be representative of the actual intended application of interest for this material, where the Min-K would be in contact with a textured aluminum surface and not other Min-K. Therefore this test set-up was abandoned after only eight tests.

Results of testing performed using the test set-up after the first modification (Tests #1-10) where samples were loaded axially and then laterally before the axial load was removed at a constant displacement rate showed a decrease in lateral load until a corresponding axial load was reached at which point the lateral load remained constant for a fixed period before the lateral load began to decrease to zero as the remainder of the axial load was removed. There was good repeatability found between repeat tests run under these conditions. Tests run under varying displacement rates during removal of the axial load indicated that the removal of the axial load at a faster rate resulted in the period of decreased lateral load loss occurring at a higher lateral load value. To confirm that the loss of lateral load was related to the removal of the axial load and not to some other source, a test was run which was loaded both axially and laterally with the axial load removed at a constant displacement rate with holds when the axial load reached set levels. As expected, the lateral load stopped decreasing when the axial load was held constant at each hold. A test was also run where the axial load was intermittently removed and reapplied at various levels again confirming the direct correlation between the axial and lateral loads, along with an increase in the lateral load with the axial reloading events. This indicated coupling between the axial and lateral loads due to problems with the test fixture which needed to be corrected for improved accuracy of the test data analysis. Therefore, the second modification of the test set-up was undertaken.

Results of testing performed using the test set-up after the second modification (Tests #11-61) showed that the lateral loads were found to decrease rapidly at a constant rate with the removal of the axial load, contrary to the behavior seen in previous testing. It was found that coupling still existed between the axial and lateral load, which was thought to be due to deflection of the frame push rods. Subsequently, work was done to stiffen the frame by providing supports to the push rods. After stiffening the test frame, testing showed that in general, samples began to slip when the applied lateral load was roughly twice the applied axial load. This is as expected since a friction factor of ≈1 was expected for this material and the applied lateral load was split over two sample surfaces. Therefore, the lateral load at slippage should be roughly twice the applied axial load. No difference in material behavior was seen when using different sample sizes nor when testing at room temperature or 400^{o}C.

Additional Isothermal Stress Relaxation testing was performed at 450, 500, 550, 600, and 650^{o}C. The purpose of this testing was to provide additional information on the isothermal stress relaxation behavior of Min-K at intermediate temperatures in the range of 400-700^{o}C. As found through previous testing, the behavior of Min-K transitions from “lower temperature behavior” to “higher temperature behavior” at these temperatures as characterized by the rate of stress relaxation. Sample loading was performed in strain control utilizing a twelve-step loading scheme with loading every half hour at a rate of 5.56% strain/hour and initial stresses of ≈200 psi (1,380 kPa). Loading was then followed by stress relaxation at constant strain levels with testing carried out until the initial load was dissipated or had leveled off to a rate of change of less than 0.25 psi/hour (1.7 kPa/hour). Eleven tests were completed with durations ranging from 24 hours to in excess of 4,675 hours.

2.0 INTRODUCTION

Characterization of the thermo-mechanical properties of Thermal Ceramics® Min-K 1400TE (Thermal Ceramics, Augusta, Georgia) material, hereafter referred to as Min-K, was originally undertaken at Oak Ridge National Laboratory (ORNL) from April 1997 to July 2008 in support of its use for structural applications under a gradient temperature regime in an inert environment. In particular, ORNL sought to determine the high temperature compressive strength and stress relaxation behavior of Min-K up to 900°C in helium along with the formulation of a general model for the mechanical behavior exhibited by Min-K under these conditions. Testing consisted of general high temperature compressive mechanical testing, isothermal stress relaxation testing, and stress relaxation testing of samples exposed to a thermal gradient. Results of this testing are discussed in two previously published ORNL Technical Reports[1,2].

Additional testing of Min-K was undertaken from April 2009 to June 2010 in an effort to further evaluate its mechanical behavior when subjected to a variety of conditions. Min-K is a high temperature load-bearing fibrous silica insulation material often used in aerospace applications where it may be called upon to perform under compressive preloading and subsequent functions as a spring. Such application may require the Min-K to store a preload in the form of potential energy, while resisting in-line motion and laterally restraining a heat source via friction. It is known, however, that Min-K is susceptible to load relaxation at elevated temperatures[3].

The need for additional data at alternative test temperatures and time scales than previously measured necessitate additional characterization of Min-K. Therefore, the new round of testing was initiated at ORNL to evaluate the behavior of Min-K under changing environments (temperature and strain), lateral loads, and additional isothermal temperatures. Results of this additional testing are discussed in this report.

3. CHANGING ENVIRONMENTS TESTING

3.1 EXPERIMENTAL PROCEDURES

Changing environments testing was intended to validate the gradient temperature stress relaxation predictions previously made based on generated data from ORNL[1,2]. Changes in temperature and strain imparted on Min-K components under gradient temperature conditions were simulated and the effects of these changes were evaluated through testing under various changing environmental conditions.

Testing was performed with an initial temperature gradient of 680/130°C and an initial stress of ≈180 psi (1,380 kPa). Initial load values, changes in temperature and strain for each test, and test durations are shown in Table 1. All testing was conducted using 6” (15 cm) diameter, 3” (7.5 cm) long cylindrical samples and the set-up shown in Figure 1, Gradient Stress Relaxation Test Frame Used for Changing Environments Testing, which consists of a retrofitted electromechanical testing machine (InstruMet, Inc.) with new heater platens, improved thermal insulation, improved electrical connections, and a back-up power supply system to run all three independent retrofitted experimental stations. The back-up power supply system (208 VAC, 3 PH, 4 W, 60 Hz, 111A, 120 cells) is shown in Figure 2. Each station consisted of a 35 kN load cell, an electromechanical actuator and a computerized system for data acquisition and control. In addition, each experimental station included a heating/cooling system to subject cylindrical test specimens of Min-K to a prescribed temperature gradient. Each heating/cooling unit includes a pair of stiff metallic platens: one with active resistance heating and the other with the capability of active water-cooling. The operation of the platens is controlled using a digital temperature controller and type-K thermocouples. The heating unit is surrounded by ceramic insulation and is enclosed in an environmental chamber (with 99.999% purity helium flow, flow rate of 70 mm) to maintain a prescribed helium atmosphere. Frames were connected to a laboratory water chiller/circulator system to provide constant temperature cooling water to the test frames. Frames were also equipped with an LVDT strain monitoring system (shown in Figure 3) for use during change of temperature and strain to simulate “changing environments”.

Table 1. Changing Environments Test Matrix

(all samples loaded to ≈180 psi./1,380 kPa)

Test #	Initial Hot Side (°C)	Initial Cold Side (°C)	Initial Load (lbf./N)	Changes (Temperature, Strain)	Test Duration (hours)
1_1	680	130	5,887/26,187	None	193
1_2	680	130	5,033/22,388	None	820
1_3	680	130	5,162/22,962	600/60°C, +0.72%	3,129
1_4	680	130	5,243/23,322	None	96
1_5	680	130	5,152/22,917	None	1,250
1_6	680	130	5,107/22,717	600/60°C, +0.72% 690/115°C, -0.49% TSE	5,828
1_7	680	130	5,200/23,131	600/60°C, +0.72% 690/115°C, -0.49% TSE	5,253

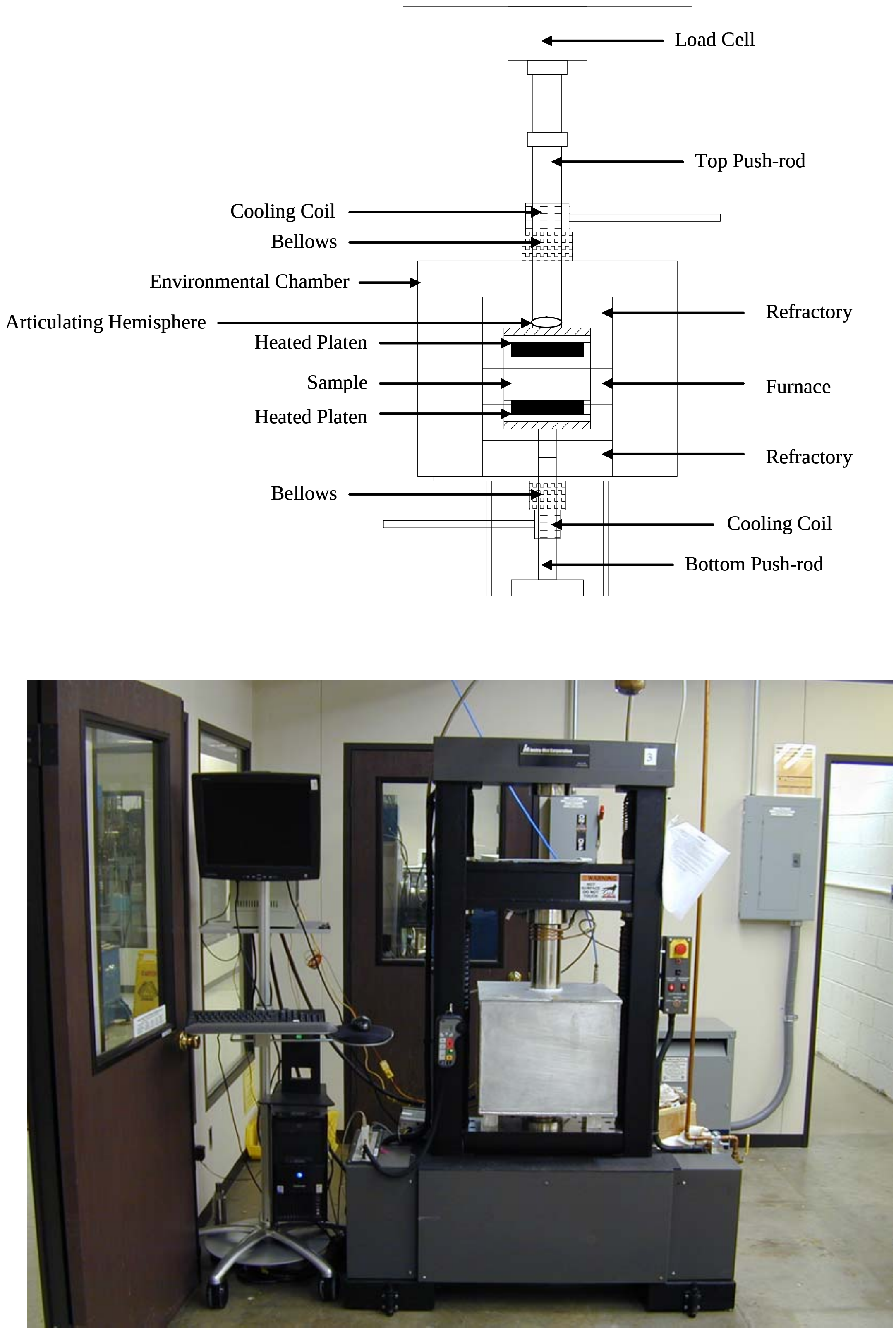

Figure 1. Gradient Stress Relaxation Test Frame Used for Changing Environments Testing.

Figure 2. Installed Back-Up Power Supply System for Gradient Test Systems.

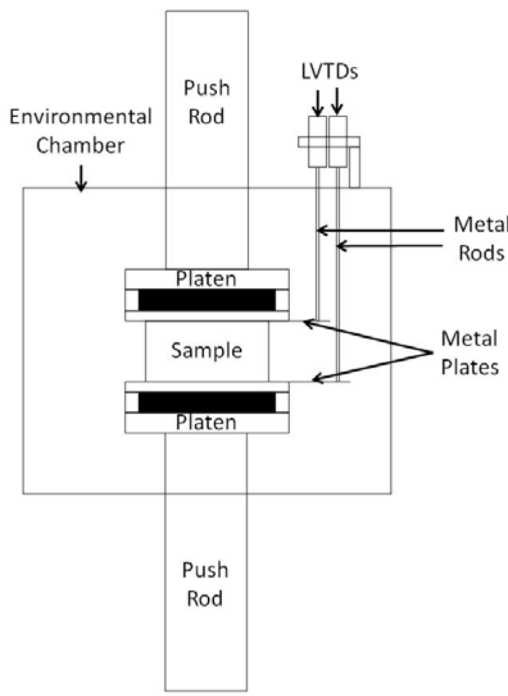

Figure 3. Schematic of LVDT Strain Monitoring System.

A modified test procedure was implemented, based on previous gradient stress relaxation testing[1,2]. Initially, a preload of 4 psi (28 kPa) was applied to the test sample during heating. When the sample was at temperature and allowed to equilibrate over night, the sample was loaded to 2.8% strain at a rate of 5.56% strain/hour in four increments of 0.7% strain with 30 minutes between each load step. The sample was then unloaded at a constant rate, removing the load over ≈15 minute period. Data from this preloading experiment was then used to determine the actual loading needed for the specific test specimen to achieve a preload of ≈180 psi (1,380 kPa).

Full sample loading was then performed under strain control at a rate of 5.56% strain/hour utilizing a twelve increment loading scheme with three equal steps of load application during each increment. Steps were spaced two minutes apart and increments occurred every half hour. Loading was followed by stress relaxation under strain control for ≈75 days. After this period, the first “changing environment” event was performed. While maintaining constant displacement on the test sample (as monitored by the LVDT strain monitoring system) the top and bottom temperatures were changed to 600 and 60^{o}C, respectively. After again allowing the test sample to thermally equilibrate over night, 0.72% strain was applied (using same strain rate as above) in four equal increments spaced 60 minutes apart.

Strain change was then followed by stress relaxation under strain control for ≈45 days. After this period, the second “changing environment” event was performed. While again maintaining constant displacement on the test sample (as monitored by the LVDT strain monitoring system), the top and bottom temperatures were changed to 690 and 115^{o}C, respectively. After again allowing the test sample to thermally equilibrate over night, 0.49% strain was applied (using same strain rate as above) in three equal increments spaced 60 minutes apart. Another period of stress relaxation under strain control was then undertaken for a period of at least 20 days.

Transient Strain Events (TSE) expected during actual material service were also simulated for Test #1_6 and Test #1_7. This effort involved three phases of testing. During Phase I of this testing, the strain was raised under displacement control to simulate cooling of a metal shell around the Min-K insulation material through a 0.25% increase in strain over a two hour period. The test was then allowed to sit over night under constant displacement. After sitting, Phase II was initiated by decreasing the strain under displacement control to simulate the expansion of a metal shell through a 0.79% decrease in strain over a 20 minute period. The test was then allowed to again sit over night under constant displacement. Phase III returned the strain back to the original level prior to TSE testing with a target of 0.54% increase in strain applied over a two hour period. Following Phase III, the test was put back under fixed displacement and allowed to relax until the test was terminated.

3.2 RESULTS

Seven tests were completed under this task with total durations ranging from 240 and 5,765 hours. Three tests had “changing environments” events performed on them and two tests had Transient Strain Events (TSE) simulated on them as shown in Table 1. Results from the seven tests are shown in Figure 4 through Figure 17.

Figure 4 shows the first test (Test #1_1) which was only run for 193 hours and was ended due to problems with the bottom platen cooling system. At the time it was ended it had relaxed from 208 to 156 psi (1,434 to 1,076 kPa) over 180 hours.

Figure 5 shows Test #1_2 which was started on the same frame as Test #1_1 following repair of the cooling system. This test ran for 820 hours before being ended due to a platen failure resulting from a laboratory electrical event which kicked out the furnace controller and water chiller fuse systems. The source of this electrical failure was investigated and the other two test frames were checked for similar failures. At the time the test lost temperature, it had been relaxing for over 720 hours and had moved from an initial stress level of 184 psi to a stress level of 132 psi (1,269 to 910 kPa).

Figure 6 shows Test #1_3 which was started on a second test frame. This test was run for a total of 3,129 hours before a failure of the top heater platen occurred. After relaxing for 1,795 hours to a stress level of 130 psi (896 kPa), a "changing environments" test was performed as shown in Figure 7. The top platen was cooled to 600^{o}C and the bottom platen to 60^{o}C, while the displacement on the test specimen was held constant by controlling off the LVDT sensors monitoring the position of the top and bottom of the test sample. Temperatures in the test chamber were allowed to equilibrate over night at which time the specimen was at a stress level of 133 psi (917 kPa). Following equilibration, 0.72% of additional strain was added to the test specimen in four increments of 0.18% strain at 10 mils/min (0.254 mm/min) spaced 60 minutes apart. Following application of the additional strain, the sample was at a stress level of 159 psi (1,096 kPa) and was again allowed to relax under constant displacement. The rate of stress relaxation appeared to return to a level similar to that before the changing environment event. The failure of the top heater platen occurred while attempting to perform the second "changing environments" test. The final stress level (prior to failure of the top platen) was 154 psi (1,062 kPa).

Figure 8 shows Test #1_4 which was started on a third test frame and ended after only 96 hours due to a failure of the top platen and controller. Prior to the platen failure, the test had been relaxing for ≈50 hours and had moved from an initial stress of 184 psi to a stress level of 157 psi (1,269 to 1,082 kPa).

Test #1_5 (shown in Figure 9) was started on the same frame as Test #1_4 following repair of the top platen. This test ran for 1,250 hours before being ended due to a failure of the top platen. At the time it was ended, it had been relaxing for over 1,225 hours and had relaxed from an initial stress of 182 psi to a stress level of 137 psi (1,255 to 945 kPa).

Test #1_6 (shown in Figure 10) was started on the same frame as Test #1_2. This test was run for a total of 5,828 hours before being ended due to a loss of the cooling water system to the laboratory where the experiment was housed. After relaxing for 1,943 hours to a stress level of 127 psi (876 kPa), a "changing environments" test was performed as shown in Figure 11. The top platen was cooled to 600^{o}C and the bottom platen to 60^{o}C, while the displacement on the test specimen was held constant by controlling off the LVDT sensors monitoring the position of the top and bottom of the test sample. Temperatures in the test chamber were allowed to equilibrate over night at which time the specimen was at a stress level of 128 psi (883 kPa). Following equilibration, 0.72% of additional strain was added to

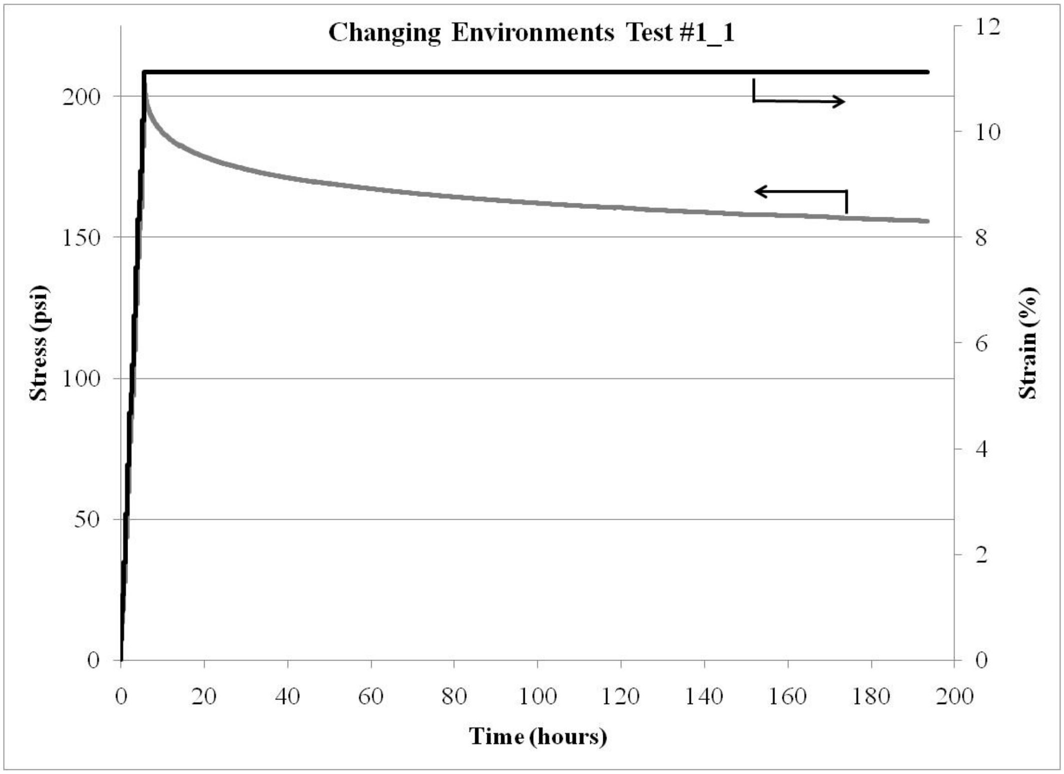

Figure 4. Results from Changing Environments Test #1_1.

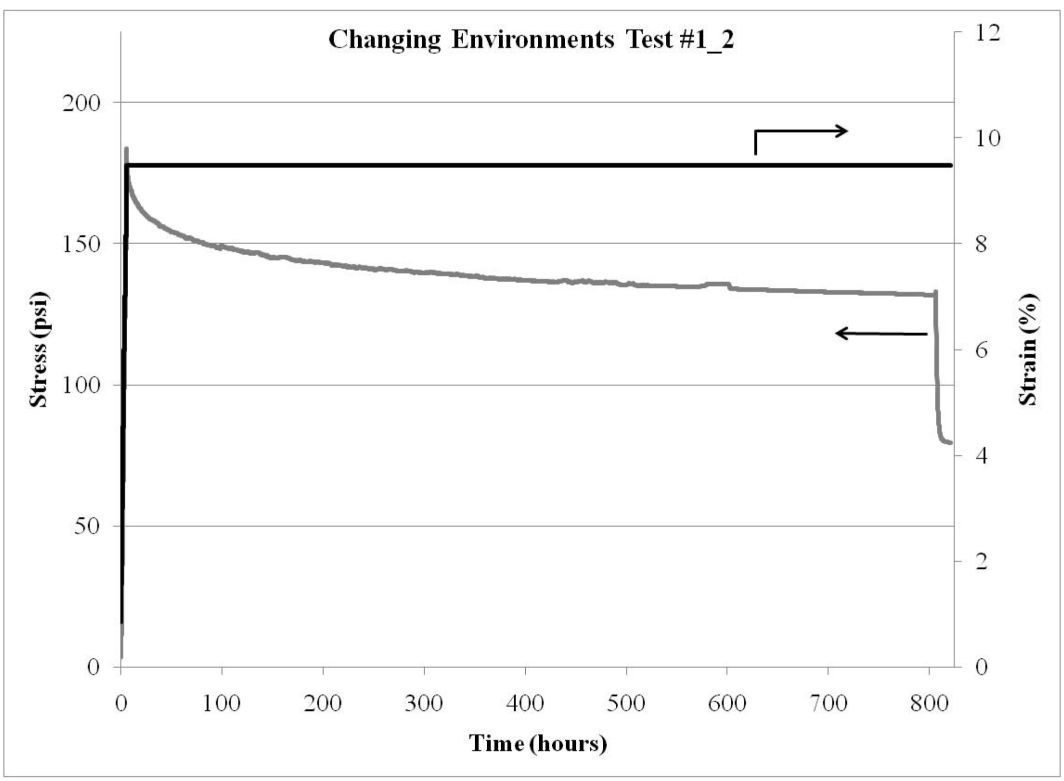

Figure 5. Results from Changing Environments Test #1_2.

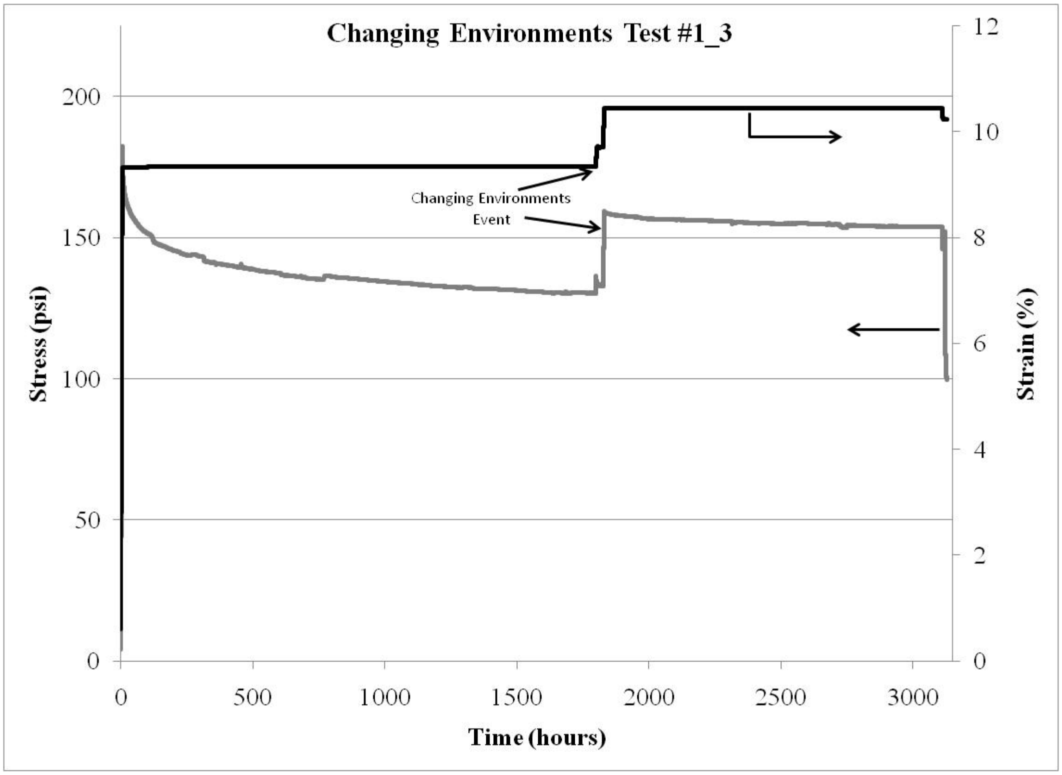

Figure 6. Results from Changing Environments Test #1_3.

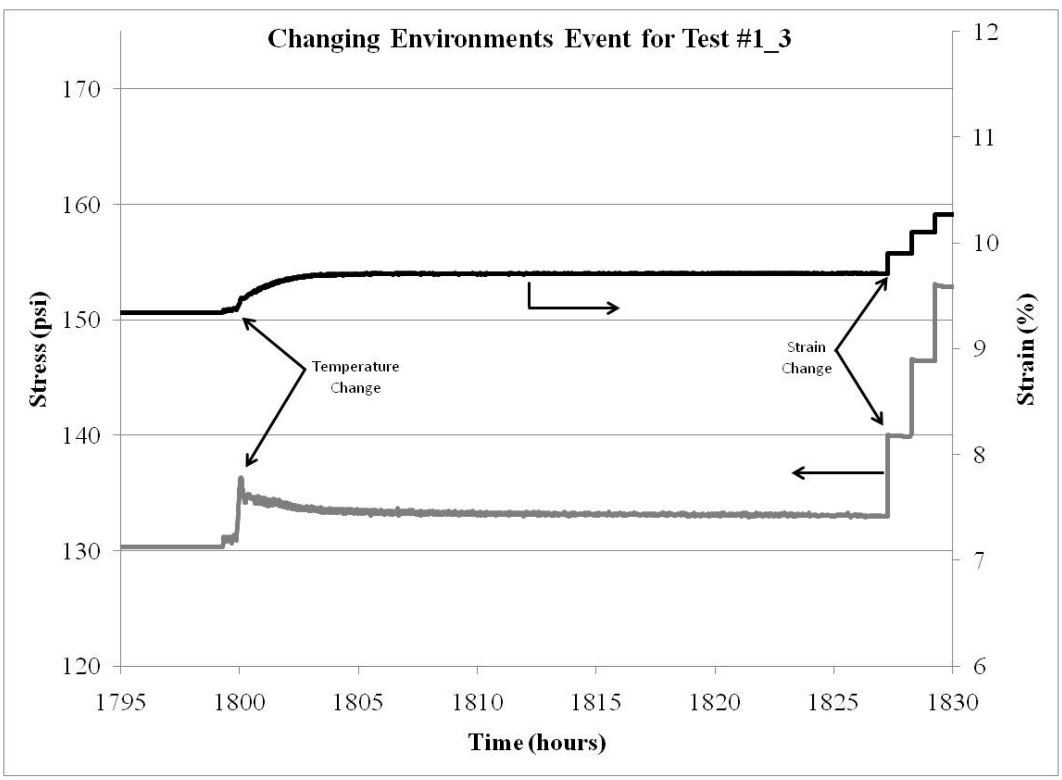

Figure 7. Changing Environment Event for Test #1_3.

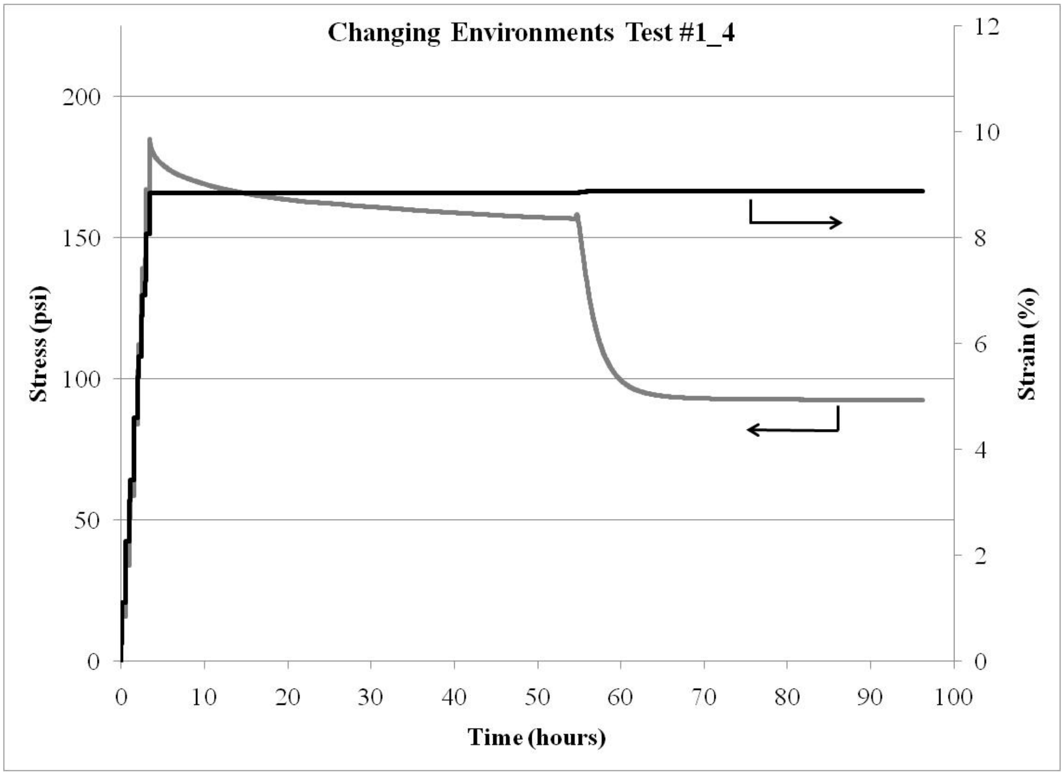

Figure 8. Results from Changing Environments Test #1_4.

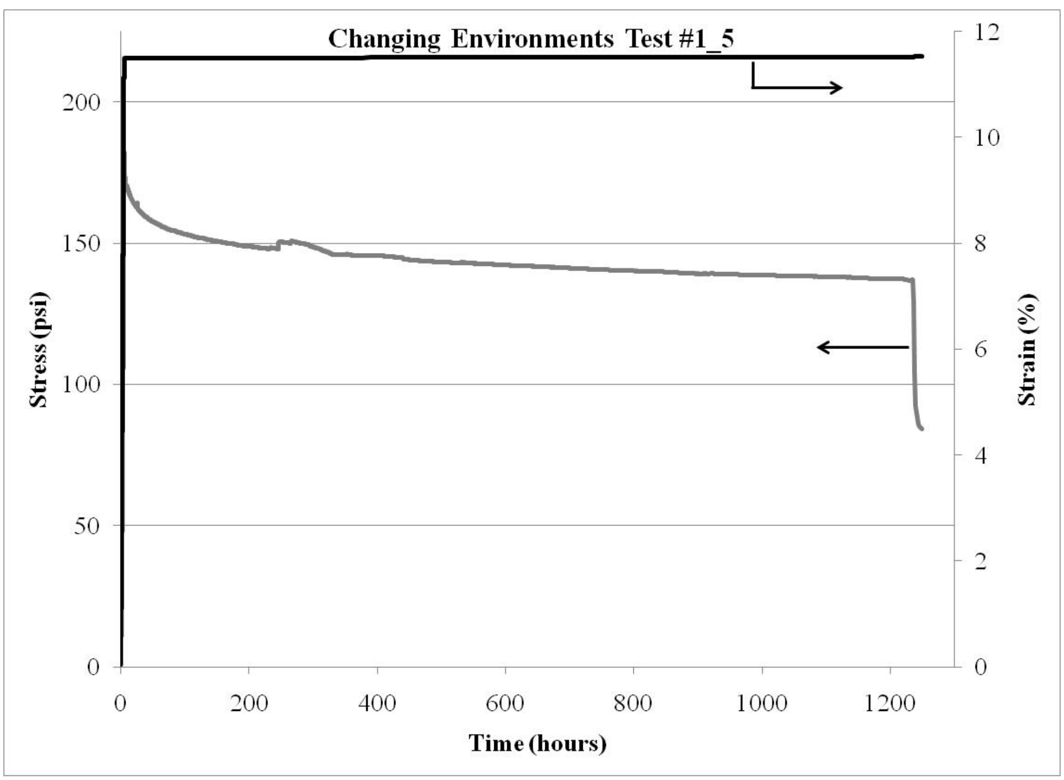

Figure 9. Results from Changing Environments Test #1_5.

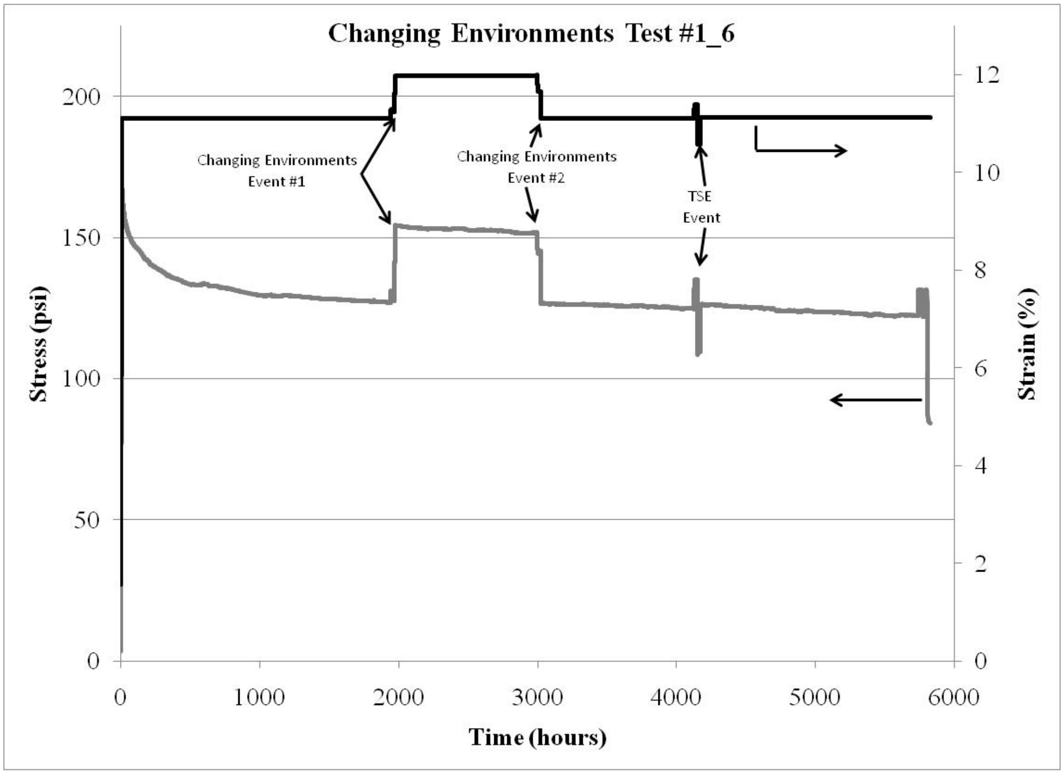

Figure 10. Results from Changing Environments Test #1_6.

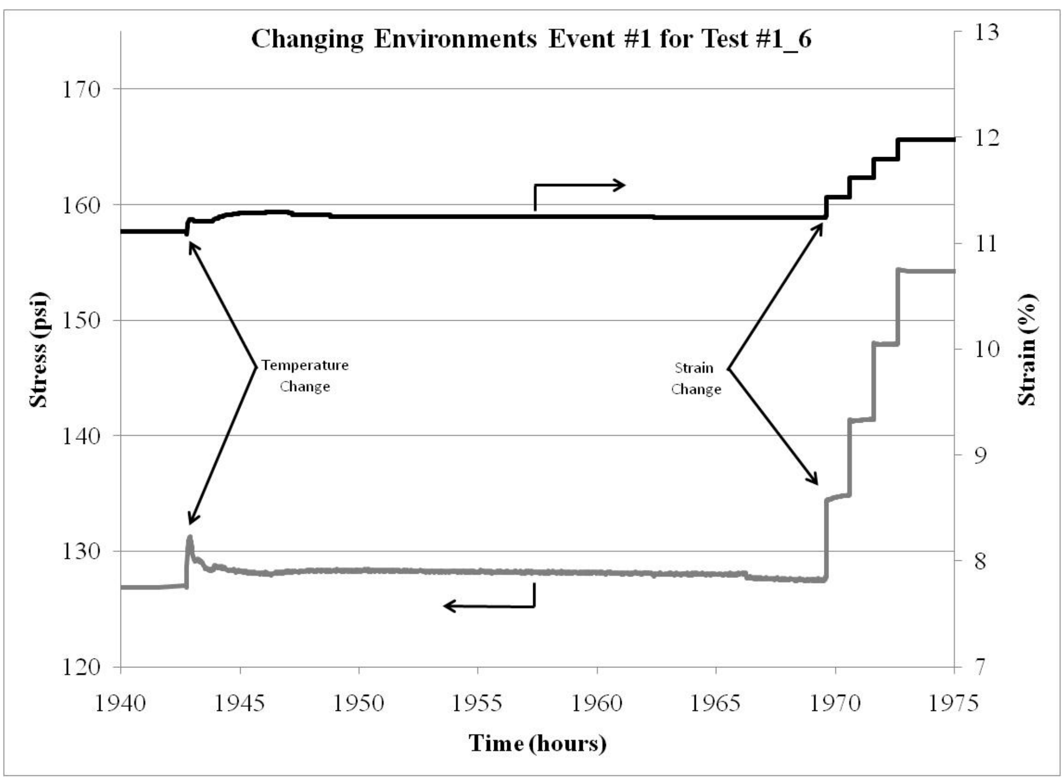

Figure 11. Changing Environment Event One for Test #1_6.

the test specimen in four increments of 0.18% strain at 10 mils/min (0.254 mm/min) spaced 60 minutes apart. Following application of the additional strain, the sample was at a stress level of 154 psi (1,062 kPa) and was again allowed to relax under constant displacement. Following the changing environment event, the rate of stress relaxation appeared to return to a level similar to that before the event.

A second changing environment event (shown in Figure 12) was performed on Test #1_6 after it had been relaxing for 2,999 hours. At the time this event was initiated, the test was at a stress level of 152 psi (1,048 kPa). The top platen was heated to 690^{o}C and the bottom platen to 115^{o}C, while the displacement on the test specimen was held constant by controlling off the LVDT sensors monitoring the position of the top and bottom of the test sample. Temperatures in the test chamber were allowed to equilibrate over night at which time the specimen was at a stress level of 144 psi (993 kPa). Following equilibration, 0.49% of strain was removed from the test specimen in three increments of 0.163% strain at 10 mils/min (0.254 mm/min) spaced 60 minutes apart. Following reduction of the strain, the sample was at a stress level of 126 psi (869 kPa) and was again allowed to relax under constant displacement. Again, following this second changing environment event, the rate of stress relaxation appeared to return to a level similar to that before the event.

After relaxing for 4,125 hours, testing to simulate TSE expected during material service was performed on Test #1_6 as shown in Figure 13. At the time of the initiation of the events, the test was at a stress level of 125 psi (862 kPa). Due to the slow strain rate of the first event, ratcheting was experienced by the test frame during the strain application resulting in an actual application of 0.277% strain over a nearly 3 hour time period (target 0.25% strain over two hours). This resulted in an increase in stress to 135 psi (931 kPa). The test was then allowed to sit over night under constant displacement. The second event had a target of 0.79% decrease in strain over a 20 minute period. Again, due to ratcheting effects, the actual strain application was 0.806% over a 23 minute time period. This resulted in a decrease in stress to 109 psi (752 kPa). The test was then allowed to again sit over night under constant displacement. The final event had a target of 0.53% increase in strain (to bring the test back to the level prior to TSE testing) applied over a two hour period. Similar to the first step, the slow strain rate led to ratcheting experienced by the test frame during the strain application resulting in an actual application of 0.553% strain over a 2.45 hour time period. This resulted in an increase in stress to 126 psi (869 kPa). After the TSE event, the rate of stress relaxation appeared to return to a level similar to that before the event. The test was then allowed to relax under constant displacement until it was ended after relaxing for over 5,780 hours to a final stress level of 122 psi (841 kPa).

Test #1_7 (shown in Figure 14) was started on the same frame as Test #1_5. This test was run for a total of 5,253 hours before being ended due to the failure of the top platen. After relaxing for 1,777 hours to a stress level of 137 psi (945 kPa), a “changing environments” test was performed as shown in Figure 15. The top platen was cooled to 600^{o}C and the bottom platen to 60^{o}C, while the displacement on the test specimen was held constant by controlling off the LVDT sensors monitoring the position of the top and bottom of the test sample. Temperatures in the test chamber were allowed to equilibrate over night at which time the specimen was at a stress level of 141 psi (972 kPa). Following equilibration, 0.72% of additional strain was added to the test specimen in four increments of 0.18% strain at 10

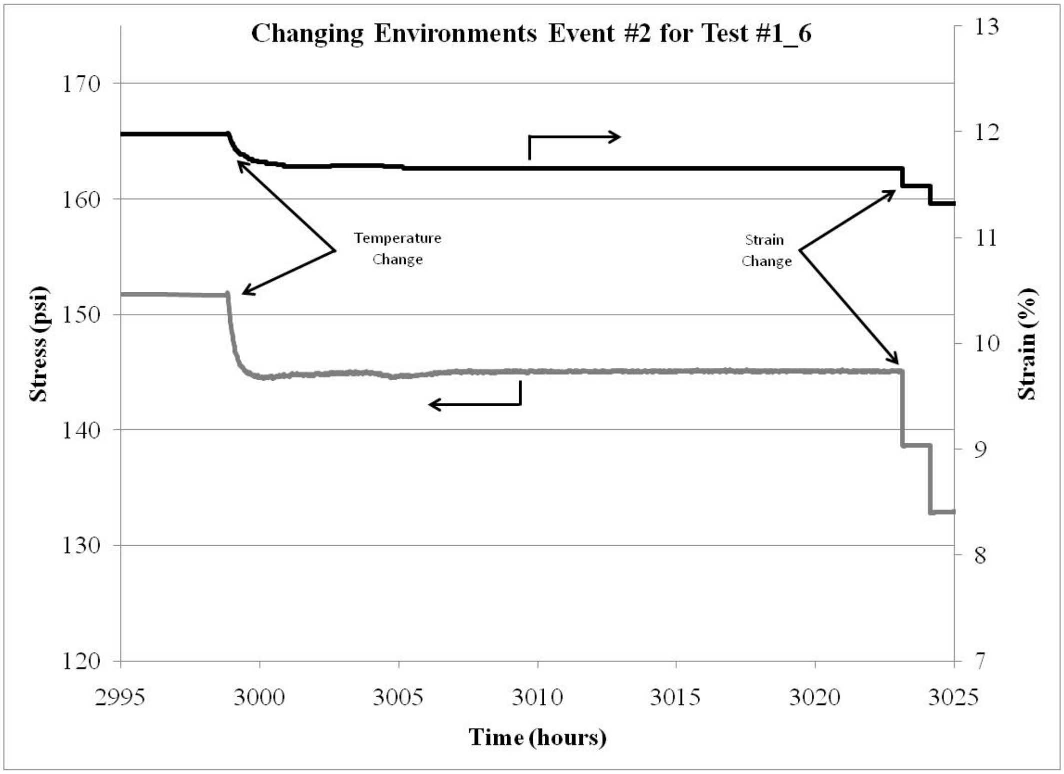

Figure 12. Changing Environment Event Two for Test #1_6.

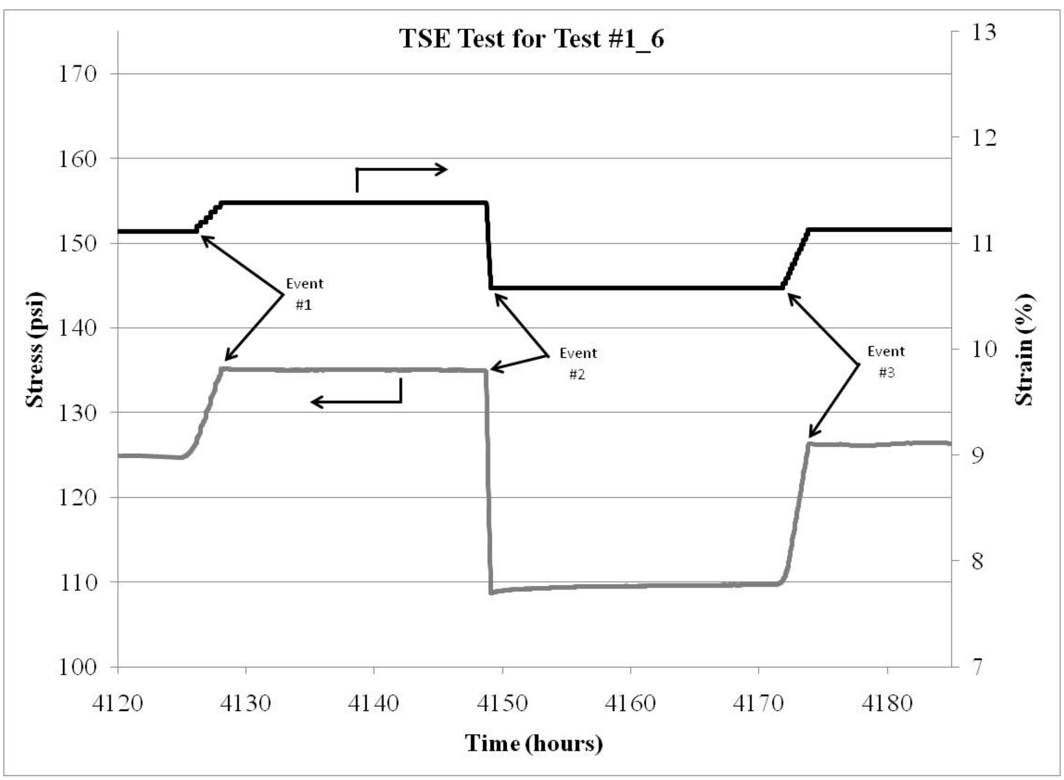

Figure 13. TSE Test for Test #1_6.

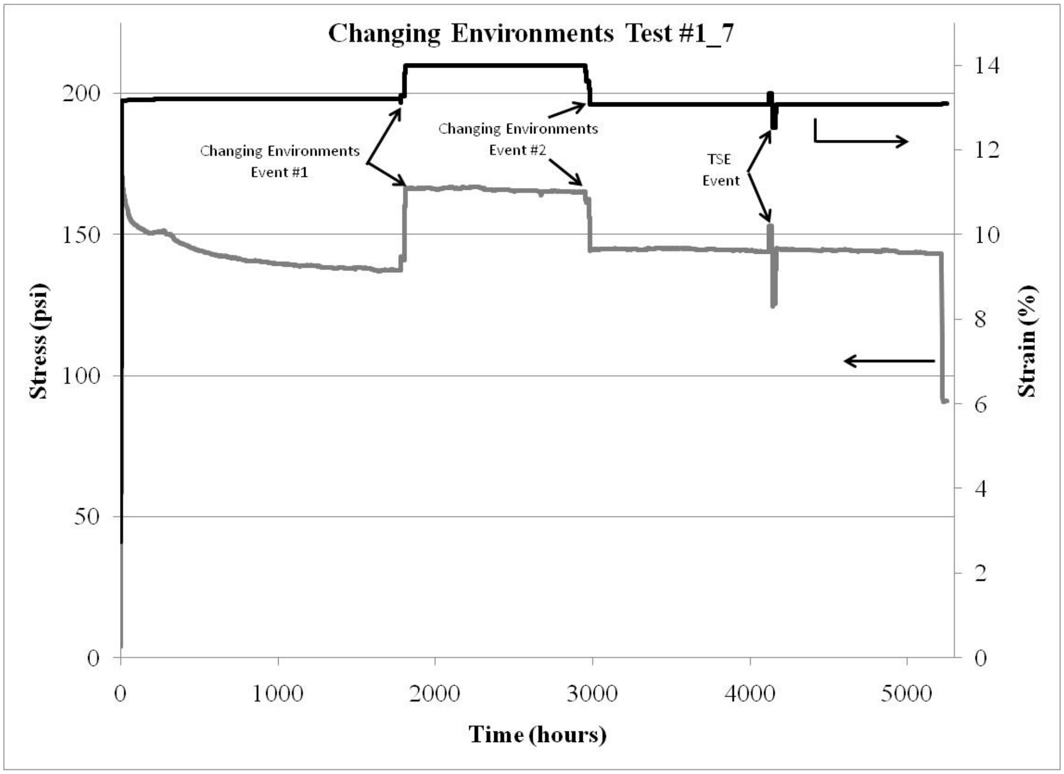

Figure 14. Results from Changing Environments Test #1_7.

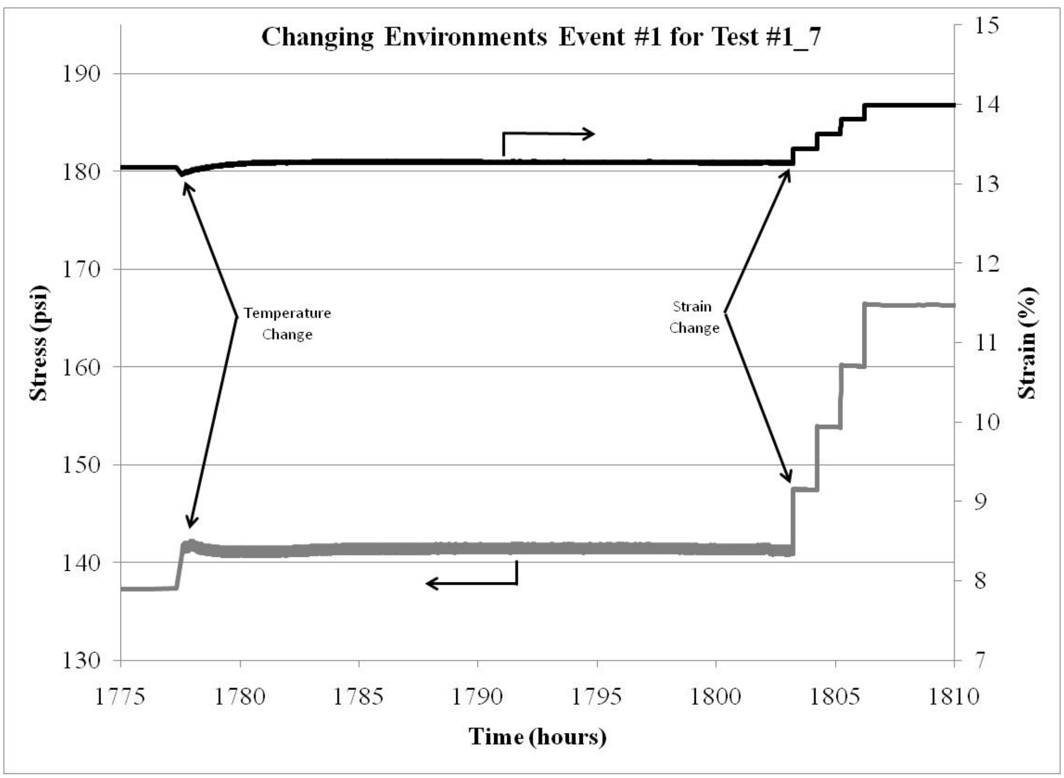

Figure 15. Changing Environment Event One for Test #1_7.

mils/min (0.254 mm/min) spaced 60 minutes apart. Following application of the additional strain, the sample was at a stress level of 166 psi (1,145 kPa) and was again allowed to relax under constant displacement. Following the changing environment event, the rate of stress relaxation appeared to return to a level similar to that before the event.

A second changing environment event (shown in Figure 16) was performed on Test #1_7 after it has been relaxing for 2,955 hours. At the time this event was initiated, the test was at a stress level of 165 psi (1,138 kPa). The top platen was heated to 690^{o}C and the bottom platen to 115^{o}C, while the displacement on the test specimen was held constant by controlling off the LVDT sensors monitoring the position of the top and bottom of the test sample. Temperatures in the test chamber were allowed to equilibrate over night at which time the specimen was at a stress level of 160 psi (1,103 kPa). Following equilibration, 0.49% of strain was removed from the test specimen in three increments of 0.163% strain at 10 mils/min (0.254 mm/min) spaced 60 minutes apart. Following reduction of the strain, the sample was at a stress level of 144 psi (993 kPa) and was again allowed to relax under constant displacement. Again, following this second changing environment event, the rate of stress relaxation appeared to return to a level similar to that before the event.

After relaxing for 4,118 hours, testing to simulate TSE expected during material service was performed on Test #1_7 as shown in Figure 17. At the time of the initiation of the events, the test was at a stress level of 144 psi (993 kPa). Improvements were made in the application of small amounts of strain based on lessons learned during the TSE testing performed during Test #1_6. Event one had a target of 0.25% increase in strain over a two hour period. An actual application of 0.253% strain over a 2.097 hour time period was realized. This resulted in an increase in stress to 153 psi (1,055 kPa). The test was then allowed to sit over night under constant displacement. The second event had a target of 0.79% decrease in strain over a 20 minute period. The actual strain application was 0.792% over a 20.448 minute time period. This resulted in a decrease in stress to 124 psi (855 kPa). The test was then allowed to again sit over night under constant displacement. The final event had a target of 0.539% increase in strain applied over a two hour period. An actual application of 0.542% strain over a 2.060 hour time period was realized. This resulted in an increase in stress to 145 psi (1,000 kPa). After the TSE event, the rate of stress relaxation appeared to return to a level similar to that before the event. The test was then allowed to relax under constant displacement until it was ended after relaxing for over 5,240 hours to a final stress level of 143 psi (986 kPa).

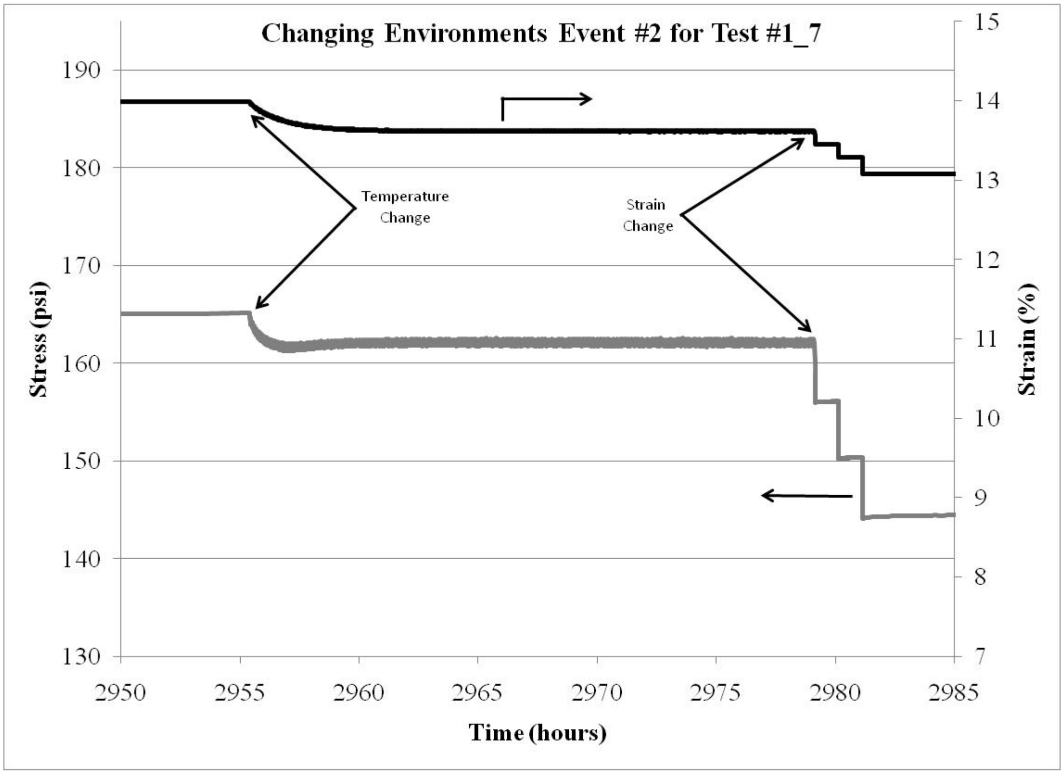

Figure 16. Changing Environment Event Two for Test #1_7.

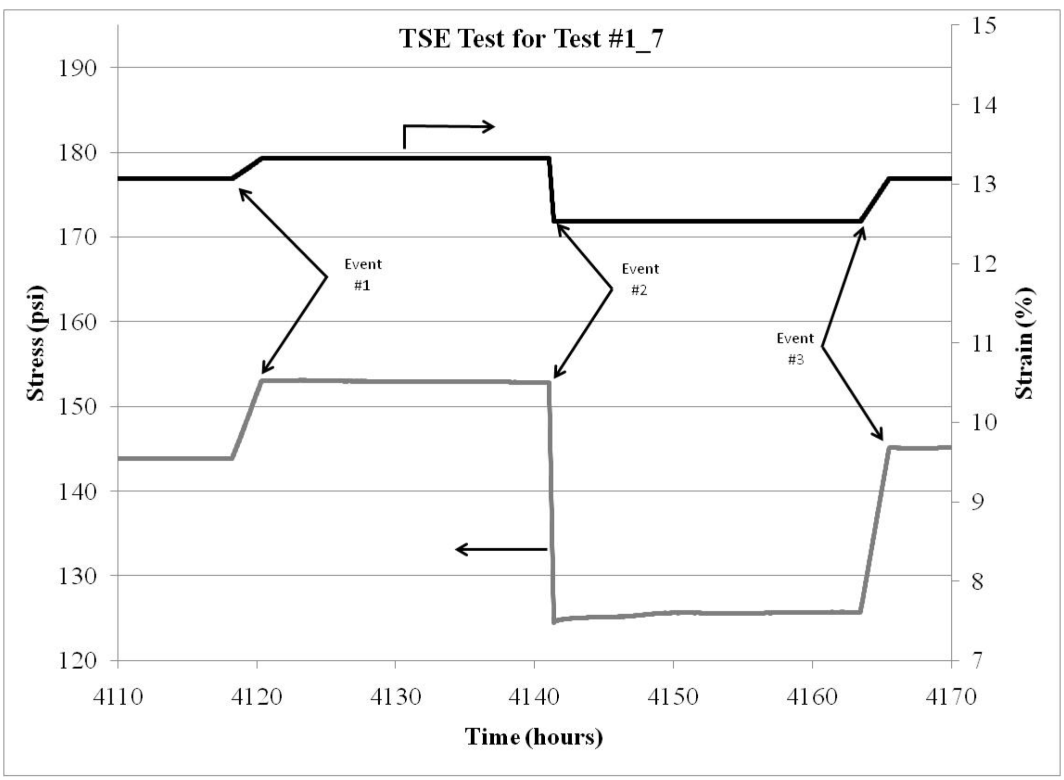

Figure 17. TSE Test for Test #1_7.

4. LATERAL LOAD TESTING

4.1 EXPERIMENTAL PROCEDURES

This testing was requested to provide information on the friction created between two pieces of Min-K or a piece of Min-K and a textured aluminum surface at both room temperature and at elevated temperatures. The original test set-up consisted of a test sample of Min-K (either 1.5” x 1.5” x 1” or 2.5” x 2.5” x 1”) (38.1 x 38.1 x 25.4 mm or 63.5 x 63.5x 25.4 mm) sandwiched between two other pieces of constrained Min-K (with same dimensions) as shown in Figure 18(a). A tangential load was applied on the top of the stack (through use of dead weights), while a lateral load was applied to the center piece of Min-K (by a mechanical actuator moved at one of two speeds) to remove it from the stack while constraining the top and bottom pieces of and Min-K and monitoring the applied lateral load. A picture of the original test set-up is shown in Figure 18(b).

As discussed in the results section below, it was found during initial testing at room temperature that this test set-up did not properly represent the actual intended application of interest for this material, where the Min-K would be in contact with a textured aluminum surface. Therefore, a revised test set-up was constructed as shown in Figure 19. The original test set-up was moved from a horizontal to a vertical orientation and mounted on an existing mechanical test frame. This set-up consisted of an aluminum plate with a “pyramoidal” structure machined into each surface sandwiched between two pieces of Min-K (either 1.0” x 1.0” x 1.0” or 2.25” x 2.25” x 1.0”) (25.4 x 25.4 x 25.4 mm or 57.15 x 57.15 x 25.4 mm). Axial load was supplied by a stepper motor attached to a push rod below the sample assembly. Lateral load was applied through a metal rod attached to the textured aluminum plate which was passed through a steel front plate assembly. By turning a mounted bolt, the rod attached to the aluminum plate was pulled, thus applying a lateral load as shown in Figure 20. Testing was performed by first loading the sample axially, then applying a set lateral load. The axial load was then removed at a prescribe displacement rate (0.01, 0.10, or 0.05 mm/sec) while monitoring the lateral load. A period of unchanging lateral load was then watched for.

After initial testing, the test set-up was again modified to eliminate lateral loading created by the transfer of forces by a moment arm produced on the rear support (see Figure 19(a) and discussion in Section 4.2) when axial loads were applied to the test assembly. The further modified set-up is shown in Figure 21. The rear support assembly was replaced with a turnbuckle connected to the center aluminum plate and load cell by hooks and eyelets. Additionally, the original metal loading plates were replaced with new plates incorporating aluminum inserts with the same “pyramoidal” texture as the center plate. Also, supports were added to confine lateral movement of the push rods due to flexure. The use of the hooks and eyelets allowed the sample assembly to move without creating a lateral load during the application of the axial loading and by manipulating the turnbuckle, a lateral load could now be applied to the test assembly.

Initial testing was performed as above where a 2.25” (57.15 mm) square sample was first loaded axially, then laterally and the axial load was removed at a prescribe displacement rate (0.01 mm/sec) while monitoring the lateral load and watching for a period of unchanging a)

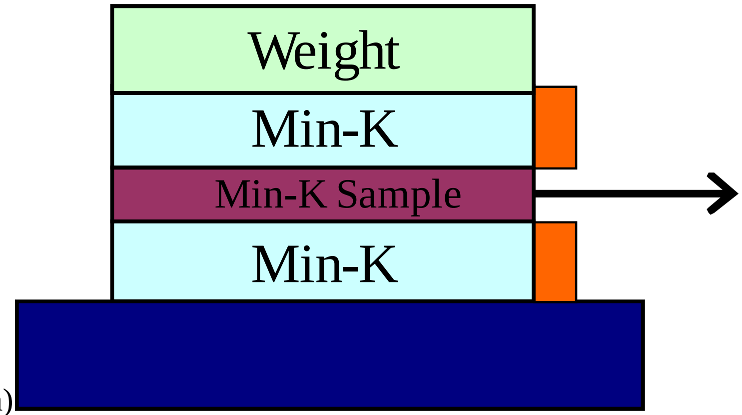

b)

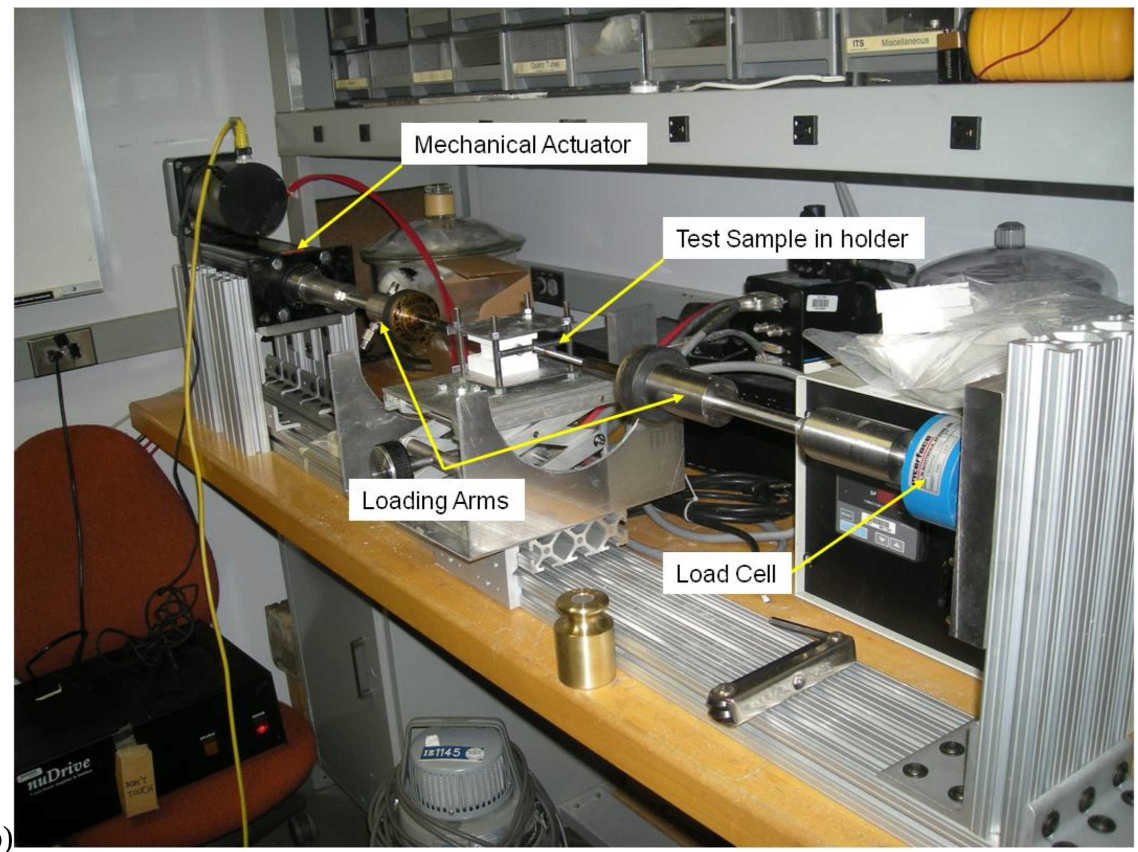

Figure 18. Original Lateral Load Test Set-Up a) Schematically and b) Pictorially.

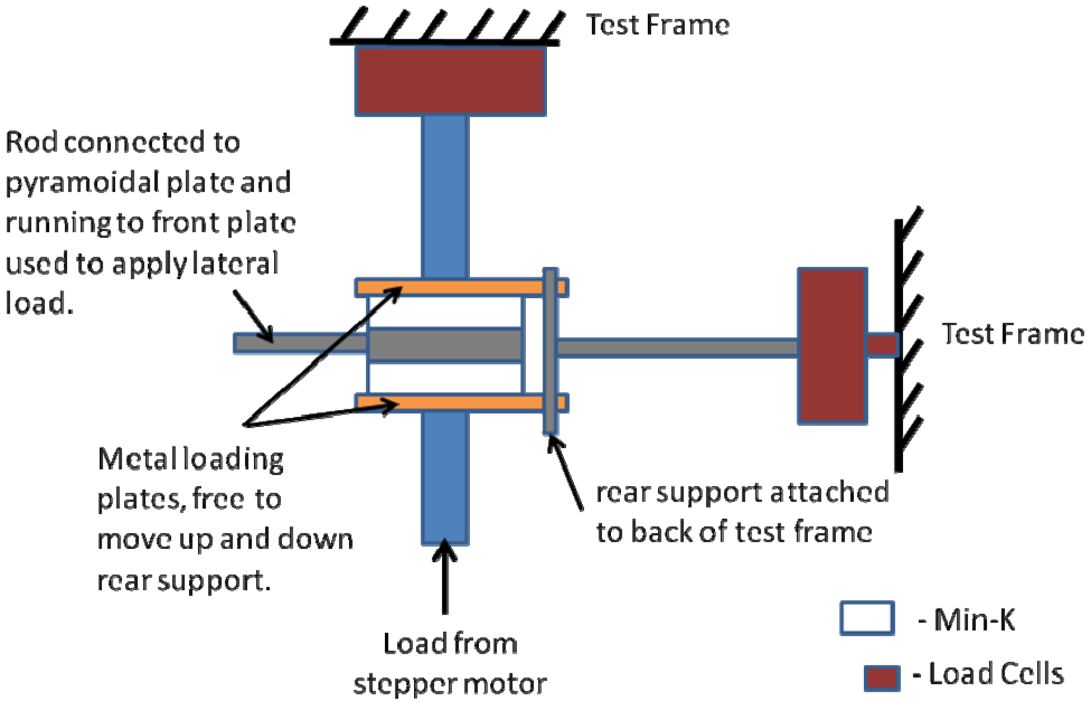

a)

b)

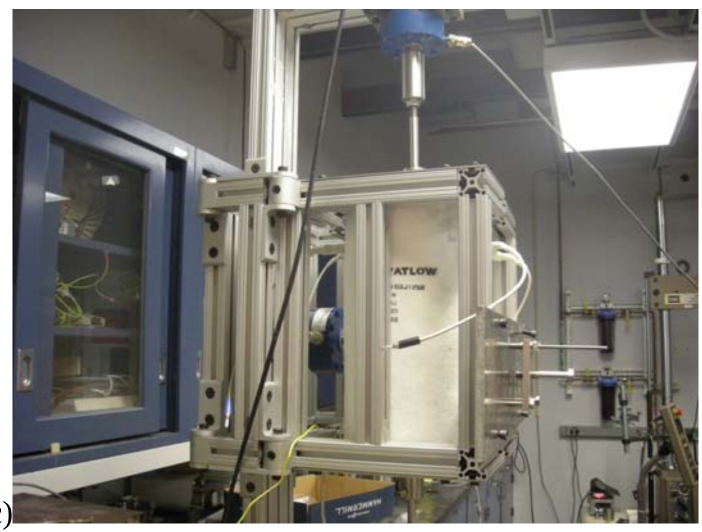

c)

Figure 19. Lateral Load Test Set-Up after First Modification a) Schematically and Pictorially b) Showing Sample Holder and c) Showing Entire Set-Up with Furnace in Place and Front Plate Assembly for Applying Lateral Load.

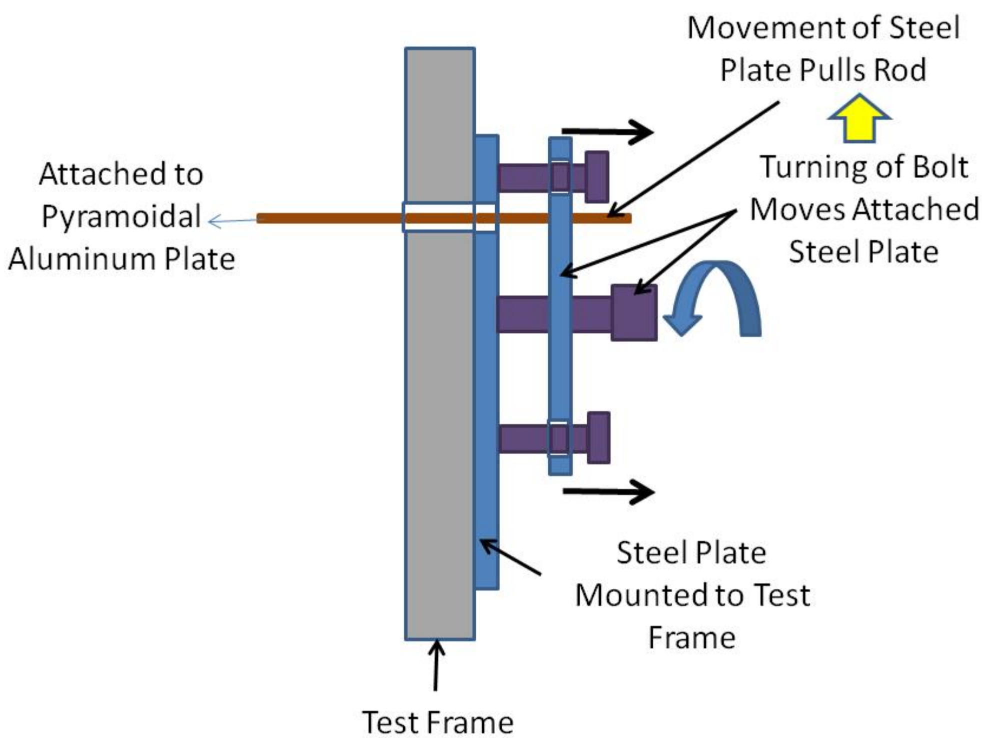

Figure 20. Schematic of Lateral Load Application for Modified Lateral Load Test Set-Up.

a)

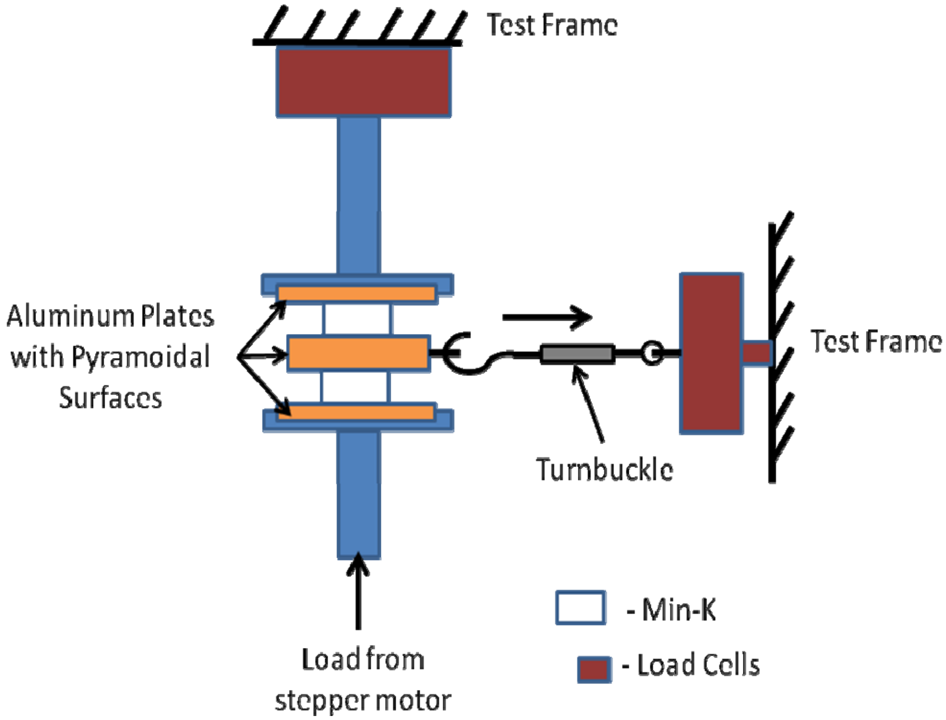

b)

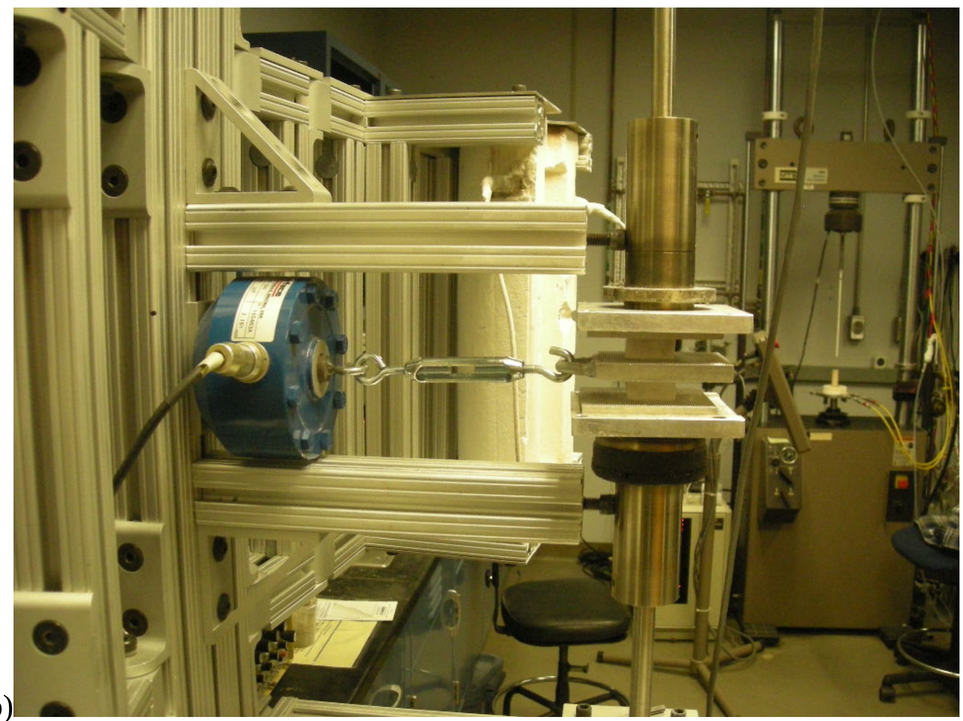

Figure 21. Lateral Load Test Set-Up after Second Modification
a) Schematically and b) Pictorially.

lateral load. It was decided though that this test method was still not producing the desired data for analysis, therefore the test procedure was modified. A test was next run by axially loading a 2.25" (57.15 mm) square test sample in a step fashion and observing the corresponding lateral load. After each load step the loads (both axial and lateral) were allowed to relax as the sample was held under constant axial displacement. This test was followed by two tests run by applying a lateral load to a 1" (25.4 mm) square test sample in a step fashion through turning of the frame turnbuckle assembly and observing the corresponding axial load. Again, after each load step the loads (both axial and lateral) were allowed to relax as the sample was held under the current conditions. It was found that coupling still existed between the axial and lateral loads. These loads were thought to be due to deflection of the frame push rods as discussed below. Subsequently, work was done to stiffen the frame by providing supports to the push rods as shown in Figure 21(b).

After stiffening the test frame, testing was run by axially loading the test sample to a prescribed load, then performing a lateral step loading while watching for the sample to begin to slip and recording the corresponding lateral load reached. If the target lateral load was reached for a specific axial load, then the lateral load was removed from the sample and the axial load was reduced to a new value. The sample was then reloaded laterally in a step fashion while watching for slipping. Sample sizes used for this testing were 1.0" x 1.0" x 1.0" (25.4 x 25.4 x 25.4 mm), 1.0" x 1.0" x 0.5" (25.4 x 25.4 x 12.7 mm), 2.25" x 2.25" x 1.0" (57.15 x 57.15 x 25.4 mm), or 2.25" x 2.25" x 0.5" (57.15 x 57.15 x 12.7 mm). Initial validation of the test system was performed at room temperature. Elevated temperature testing was performed at 400^{o}C. Replicate testing was performed at both temperatures.

4.2 RESULTS

Results of initial testing performed at room temperature using the original test set-up are shown in Table 2 along with characteristic plots for each sample size tested in Figure 22.

Table 2. Initial Lateral Load Testing Results

Small Block (1.5" square)

Test	Weight (kg/lbs.)	Speed (mm/sec.)	Frict. Stress (psi)
1	1/2.2	0.1	1.33
2	1/2.2	0.5	1.19
3	1.75/3.85	0.1	2.88
4	1.75/3.85	0.5	2.92

Large Block (2.5" square)

Test	Weight (kg/lbs.)	Speed (mm/sec.)	Frict. Stress (psi)
5	1/2.2	0.1	0.81
6	1/2.2	0.5	0.72
7	1.75/3.85	0.1	1.32
8	1.75/3.85	0.5	1.52

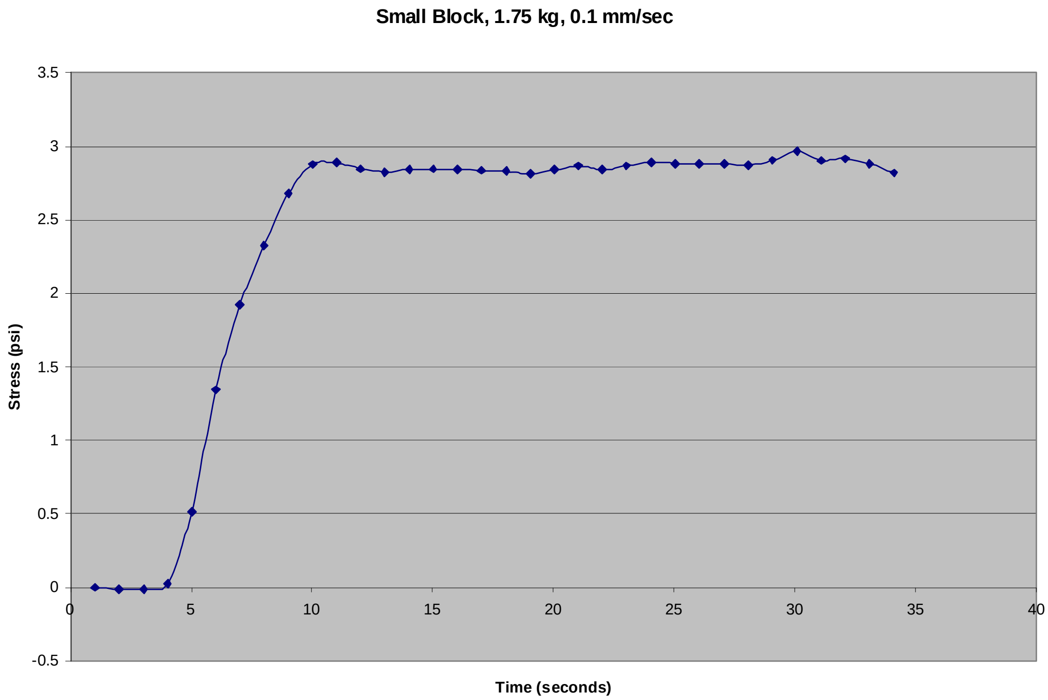

a)

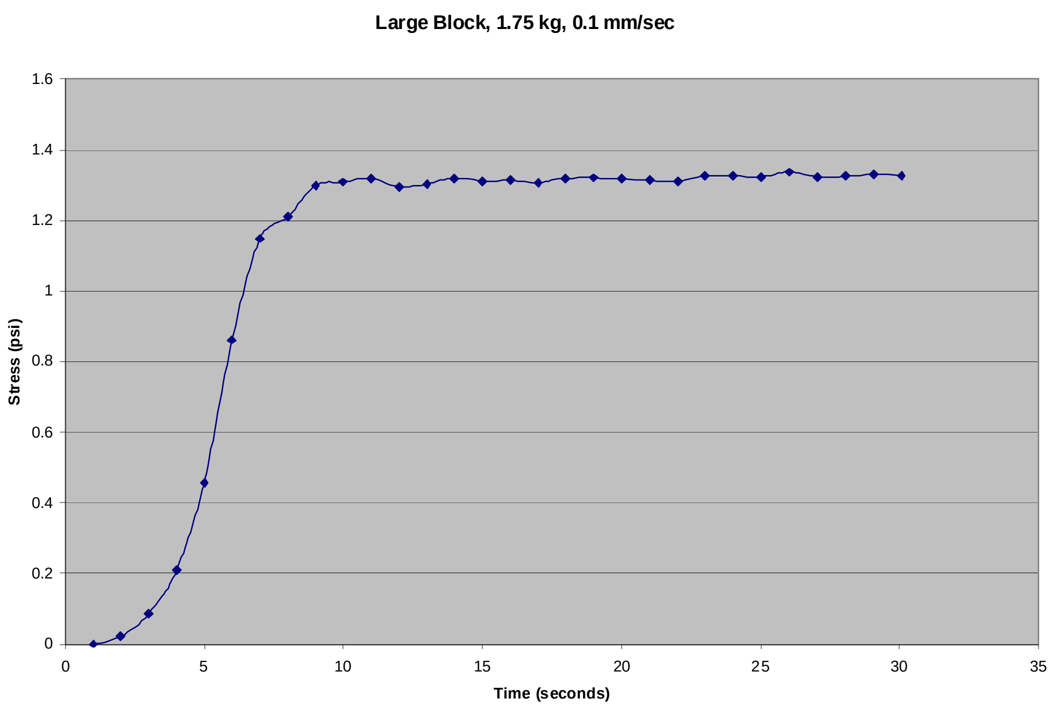

b)

Figure 22. Characteristic Results for Initial Lateral Load Testing (Lateral Stress vs. Time) Using Original Set-Up with a) 1.5” Square “Small Block” Samples and b) 2.5” Square “Large Block” Samples.

This test provided information on the amount of axial stress that the test assembly could accumulate for a specific dead axial load and test speed (speed of actuator to apply lateral load) before slipping between the Min-K layers occurred represented by the maxing out of the measured axial stress. Although this information was of academic interest, these results were determined to not be representative of the actual intended application of interest for this material, where the Min-K would be in contact with a textured aluminum surface and not other Min-K. Therefore this test set-up was abandoned after only eight tests.

A matrix of tests performed using the modified test frame is shown in Table 3. Results of testing performed using the test set-up after the first modification (Tests #1-10) are shown in Figure 23 through Figure 27. Figure 23 shows results from Lateral Load Tests #1 and 2 where 2.25” (57.15 mm) square samples were loaded to 145 lbs. (65.77 kg) axially and 15 lbs. (6.80 kg) laterally before the axial load was removed at a constant displacement rate of 0.01 mm/sec. The lateral load was found to decrease until it reached ≈3 lbs. (1.36 kg) and a corresponding axial load of ≈35 lbs. (15.88 kg) at which point the lateral load remained constant until the axial load was decreased to 10-15 lbs. (4.53-6.80 kg). The lateral load then began to decrease to zero as the remainder of the axial load was removed. There was good repeatability found between Tests #1 and 2. Test #3 was a repeat of these tests started at an initial axial load of 250 lbs. (113.40 kg) as opposed to 145 lbs. (65.77 kg). Results were found to be similar.

Figure 24 shows the results from Lateral Load Tests #4 and 5 where 1.0” (25.4 mm) square samples were loaded to 40 lbs. (18.14 kg) axially and 5 lbs. (2.27 kg) laterally before the axial load was removed at a constant displacement rate of either 0.10 mm/sec (Test #4) or 0.05 mm/sec (Test #5). For Test #4, the lateral load was found to decrease until it reached ≈3.25 lbs. (1.47 kg) and a corresponding axial load of ≈25 lbs. (11.34 kg), at which point the lateral load decreased at a much reduced rate until the axial load was decreased to ≈5 lbs. (2.27 kg). The lateral load then began to decrease at the original rate until it reached zero as the remainder of the axial load was removed. For Test #5, the lateral load was found to decrease until it reached ≈2.25 lbs. (1.02 kg) and a corresponding axial load of ≈20 lbs. (9.07 kg), at which point the lateral load decreased at a much reduced rate until the axial load was decreased to ≈10 lbs. (4.54 kg). The lateral load then began to decrease at the original rate until it reached zero as the remainder of the axial load was removed. This shows the effect of varying the displacement rate during removal of the axial load. The removal of the axial load at a faster rate (Test #4) resulted in the period of decreased lateral load loss occurring at a higher lateral load value. Test #6 (note shown) was similar to Test #4, but utilized an initial axial load of 65 lbs. (29.48 kg) as opposed to 40 lbs. (18.14). Results were found to be similar.

To confirm that the loss of lateral load was related to the removal of the axial load and not to some other source, Test #7 was run on a 2.5” (63.5 mm) square sample which was loaded to 145 lbs. (65.77 kg) axially and 15lbs. (6.80 kg) laterally as shown in Figure 25. The axial load was removed from this sample at a constant displacement rate of 0.10 mm/sec with holds when the axial load reached 75 and 45 lbs. (34.02 and 20.41 kg). As expected, the lateral load stopped decreasing when the axial load was held constant at each of the above values.

Table 3. Lateral Load Test Matrix Utilizing Modified Test Frame

Test #	Temperature	Sample Size (inches)	Axial Load (lbs.)	Lateral Load (lbs.)
1 (9/2)	RT	2.25 x 2.25 x 1.0	145	15 unloaded at 0.01 mm/sec
2 (9/2)	RT	2.25 x 2.25 x 1.0	145	15 unloaded at 0.01 mm/sec
3 (9/2)	RT	2.25 x 2.25 x 1.0	250	15 unloaded at 0.01 mm/sec
4 (9/3)	RT	1.0 x 1.0 x 1.0	40	5 unloaded at 0.10 mm/sec
5 (9/3)	RT	1.0 x 1.0 x 1.0	40	5 unloaded at 0.05 mm/sec
6 (9/3)	RT	1.0 x 1.0 x 1.0	65	5 unloaded at 0.10 mm/sec
7 (9/3)	RT	2.25 x 2.25 x 1.0	145	15 unloaded at 0.10 mm/sec
8 (9/8)	RT	2.25 x 2.25 x 1.0	145	25 unloaded at 0.10 mm/sec
9 (9/8)	RT	2.25 x 2.25 x 1.0	145	25 unloaded at 0.10 mm/sec
10 (9/8)	RT	2.25 x 2.25 x 1.0	145	15 unloaded at 0.10 mm/sec
11 (9/22)	RT	2.25 x 2.25 x 1.0	207	25 unloaded at 0.01 mm/sec
12 (9/22)	RT	2.25 x 2.25 x 1.0	188	9 unloaded at 0.01 mm/sec

() indicates test date; RT = room temperature, ET = 400^{o}C
Note: Tests #1-10 performed after first frame modification, Tests #11-61 performed after second frame modification

(Table 3 Continued)

Test #	Temperature	Sample Size (inches)	Axial Load (lbs.)	Lateral Load (lbs.)
13 (9/24)	RT	2.25 x 2.25 x 1.0	188 step loaded	88
14 (9/24)	RT	1.0 x 1.0 x 1.0	28	23 step loaded
15 (9/24)	RT	1.0 x 1.0 x 1.0	28	34 step loaded
16 (9/24)	RT	1.0 x 1.0 x 1.0	20	30 step loaded
17 (10/8)	RT	1.0 x 1.0 x 1.0	65	70 step loaded
18 (10/12)	RT	1.0 x 1.0 x 0.5	65	75 step loaded
19 (10/12)	RT	1.0 x 1.0 x 0.5	65/25	60 step loaded
20 (10/12)	RT	1.0 x 1.0 x 0.5	65	75 step loaded
21 (10/12)	RT	1.0 x 1.0 x 0.5	65	65 step loaded
22 (10/15)	RT	2.25 x 2.25 x 0.5	270	285 step loaded
23 (10/16)	RT	2.25 x 2.25 x 0.5	270	285 step loaded
24 (10/19)	RT	2.25 x 2.25 x 0.5	270	285 step loaded
25 (10/22)	ET	1.0 x 1.0 x 0.5	65	50 step loaded
26 (10/28)	ET	1.0 x 1.0 x 0.5	65/25	75/30 step loaded
27 (10/28)	ET	1.0 x 1.0 x 0.5	65/25/15	75/30 step loaded
28 (11/11)	ET	1.0 x 1.0 x 0.5	65	60 step loaded
29 (11/11)	ET	1.0 x 1.0 x 0.5	65/25	70/50 step loaded
30 (11/11)	ET	1.0 x 1.0 x 0.5	65/25	50 step loaded
31 (11/13)	ET	1.0 x 1.0 x 0.5	65/25	70/50 step loaded
32 (11/13)	ET	1.0 x 1.0 x 0.5	65/25	50 step loaded

() indicates test date; RT = room temperature, ET = 400^{o}C
Note: Tests #1-10 performed after first frame modification, Tests #11-61 performed after second frame modification

(Table 3 Continued)

Test #	Temperature	Sample Size (inches)	Axial Load (lbs.)	Lateral Load (lbs.)
33 (11/16)	ET	1.0 x 1.0 x 0.5	65/15	50 step loaded
34 (11/17)	ET	1.0 x 1.0 x 0.5	65/15	30 step loaded
35 (11/18)	ET	1.0 x 1.0 x 0.5	65/15	30 step loaded
36 (11/20)	ET	1.0 x 1.0 x 0.5	65/25	70/50 step loaded
37 (11/23)	ET	1.0 x 1.0 x 0.5	65/25	30 step loaded
38 (11/25)	ET	1.0 x 1.0 x 0.5	65/15	30 step loaded
39 (11/30)	ET	1.0 x 1.0 x 0.5	65/10	30 step loaded
40 (12/3)	ET	1.0 x 1.0 x 0.5	65	70 unloaded laterally
41 (12/10)	ET	1.0 x 1.0 x 0.5	65/25	50 step loaded
42 (12/11)	ET	1.0 x 1.0 x 0.5	65/15	40 step loaded
43 (12/14)	ET	1.0 x 1.0 x 0.5	65/10	30 step loaded
44 (12/16)	ET	1.0 x 1.0 x 0.25	65/25	70/50 step loaded
45 (12/21)	ET	1.0 x 1.0 x 0.25	65/25	50 step loaded
46 (12/23)	ET	1.0 x 1.0 x 0.25	65/15	40 step loaded
47 (12/29)	RT	1.0 x 1.0 x 0.25	65/25	70/50 step loaded
48 (1/4)	RT	1.0 x 1.0 x 0.25	65	50 step loaded
49 (1/4)	RT	1.0 x 1.0 x 0.25	65/15	40 step loaded
50 (1/5)	RT	1.0 x 1.0 x 0.25	65/15	40 step loaded
51 (1/12)	RT	1.0 x 1.0 x 0.25	65/25	70/60 step loaded
52 (1/12)	RT	1.0 x 1.0 x 0.25	25	50 step loaded

() indicates test date; RT = room temperature, ET = 400^{o}C

Note: Tests #1-10 performed after first frame modification, Tests #11-61 performed after second frame modification

(Table 3 Continued)

Test #	Temperature	Sample Size (inches)	Axial Load (lbs.)	Lateral Load (lbs.)
53 (1/25)	RT	1.0 x 1.0 x 0.25	65/25	70/50 step loaded
54 (1/26)	RT	1.0 x 1.0 x 0.25	65/25	50 step loaded
55 (2/4)	RT	1.0 x 1.0 x 0.25	65/25	40 step loaded
56 (2/4)	RT	1.0 x 1.0 x 0.25	65/25	50 step loaded
57 (3/26)	RT	2.25 x 2.25 x 0.5	152	330 step loaded
58 (3/26)	RT	2.25 x 2.25 x 0.5	152/95	181 step loaded
59 (3/30)	RT	1.0 x 1.0 x 0.5	25/10	30 step loaded
60 (4/15)	RT	1.0 x 1.0 x 0.5	25/15	40 step loaded
61 (4/15)	RT	1.0 x 1.0 x 0.5	35/15	30 step loaded

() indicates test date; RT = room temperature, ET = 400°C
Note: Tests #1-10 performed after first frame modification, Tests #11-61 performed after second frame modification

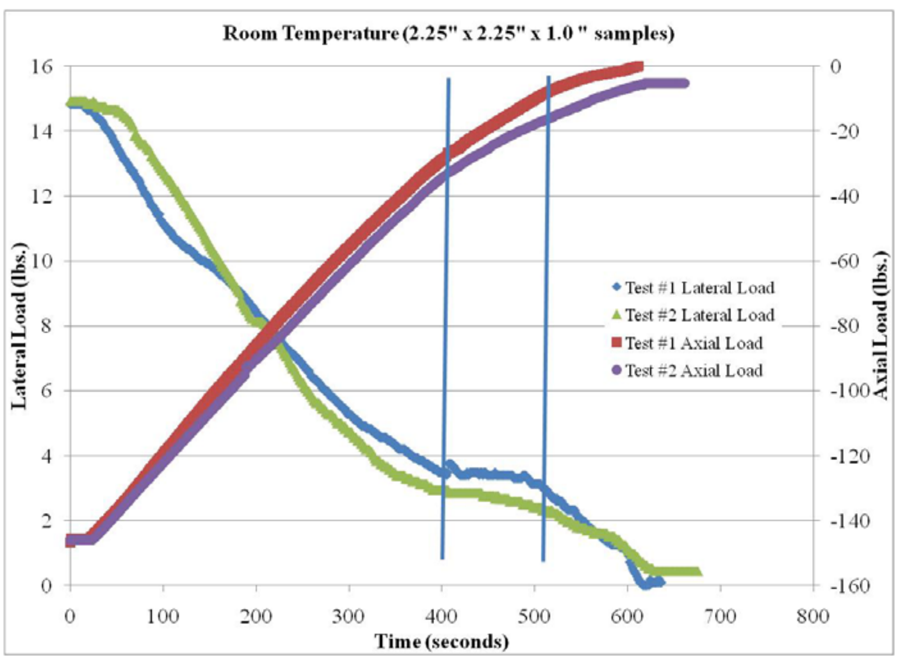

Figure 23. Results for 2.25" Samples Using Lateral Load Testing Set-Up after First Modification (Lateral Load Removed at 0.01 mm/sec).

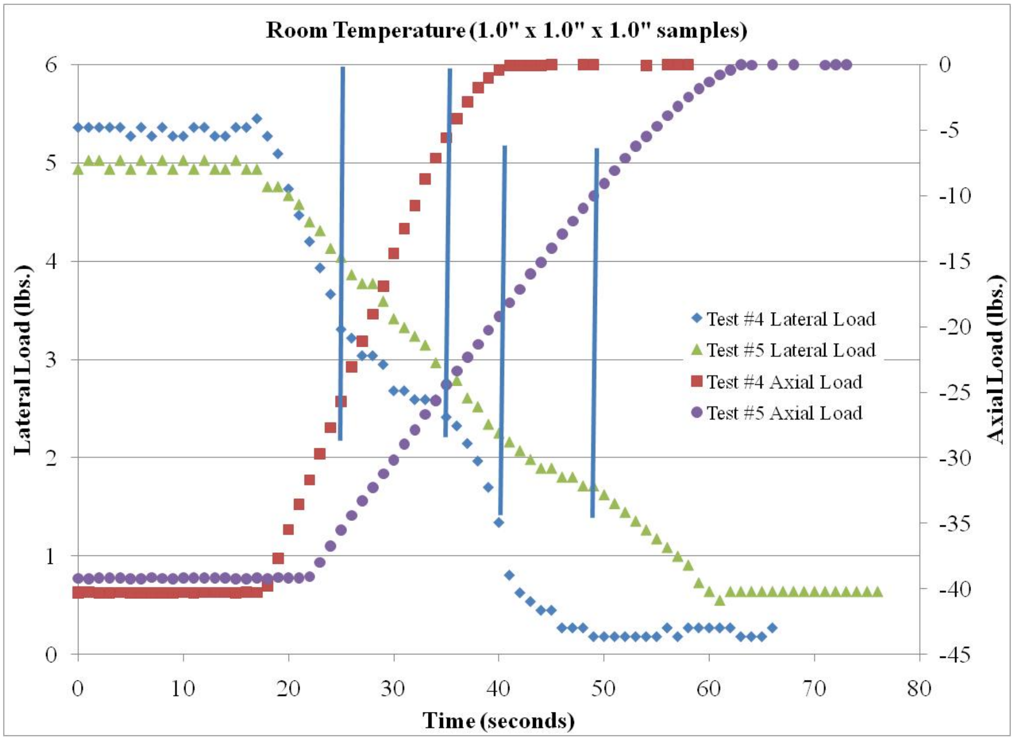

Figure 24. Results for 1” Samples Using Lateral Load Testing Set-Up after First Modification.

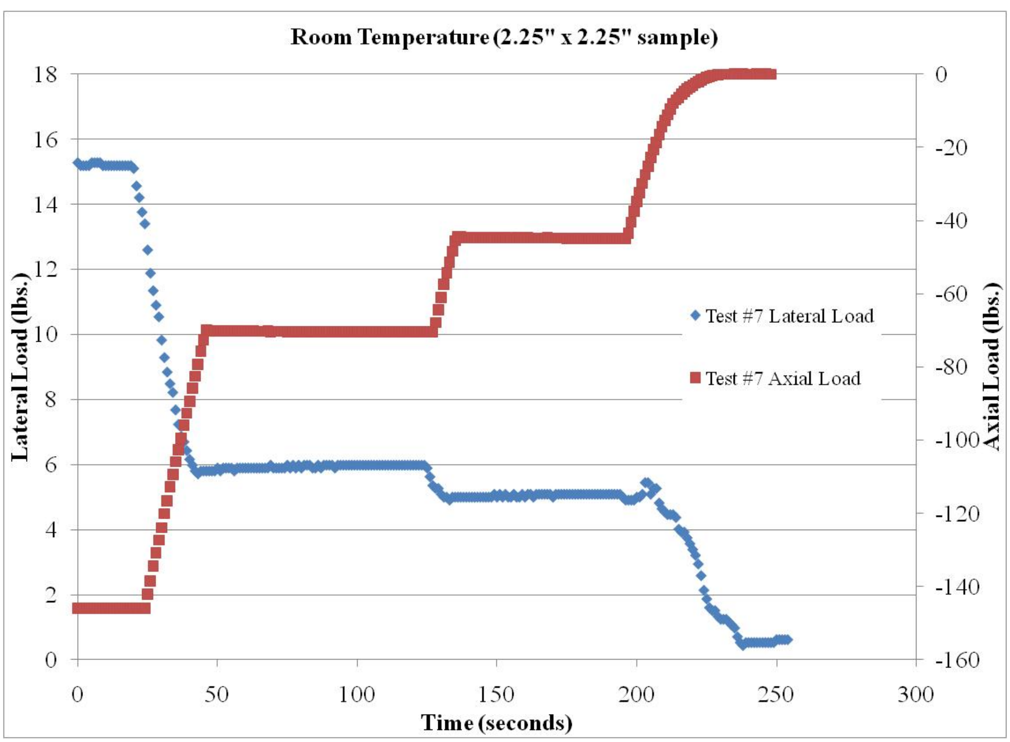

Figure 25. Results for 2.25” Sample Using Lateral Load Testing Set-Up after First Modification Using Step Unloading.

Tests #8 and 9 where run using 2.25” (57.15 mm) square samples loaded to 145 lbs. (65.77 kg) axially and 25 lbs. (11.34 kg) laterally (as opposed to 15 lbs. (6.80 kg) above). Figure 26 shows results from Test #9. Similar to before, the axial load was removed at a constant displacement rate of 0.01 mm/sec. The lateral load was found to decrease until it reached ≈18 lbs. (8.16 kg) and a corresponding axial load of ≈105 lbs. (47.63 kg) at which point the lateral load decreased at a much reduced rate until the axial load was decreased to ≈35 lbs. (15.88 kg). The lateral load then began to decrease to zero at an accelerated rate as the remainder of the axial load was removed. Results of Test #8 were found to be similar.

A test was also run using a 2.25” (57.15 mm) square sample loaded axially to 145 lbs. (65.77 kg) and laterally to 15 lbs. (6.80 kg) where the axial load was intermittently removed and reapplied at various levels as shown in Figure 27 (Test #10). The direct correlation between the axial and lateral loads was again confirmed, along with an increase in the lateral load with the axial reloading events. This indicated coupling between the axial and lateral loads due to problems with the test fixture which needed to be corrected for improved accuracy of the test data analysis. Therefore, the second modification of the test set-up (as described in Section 4.1) was undertaken.

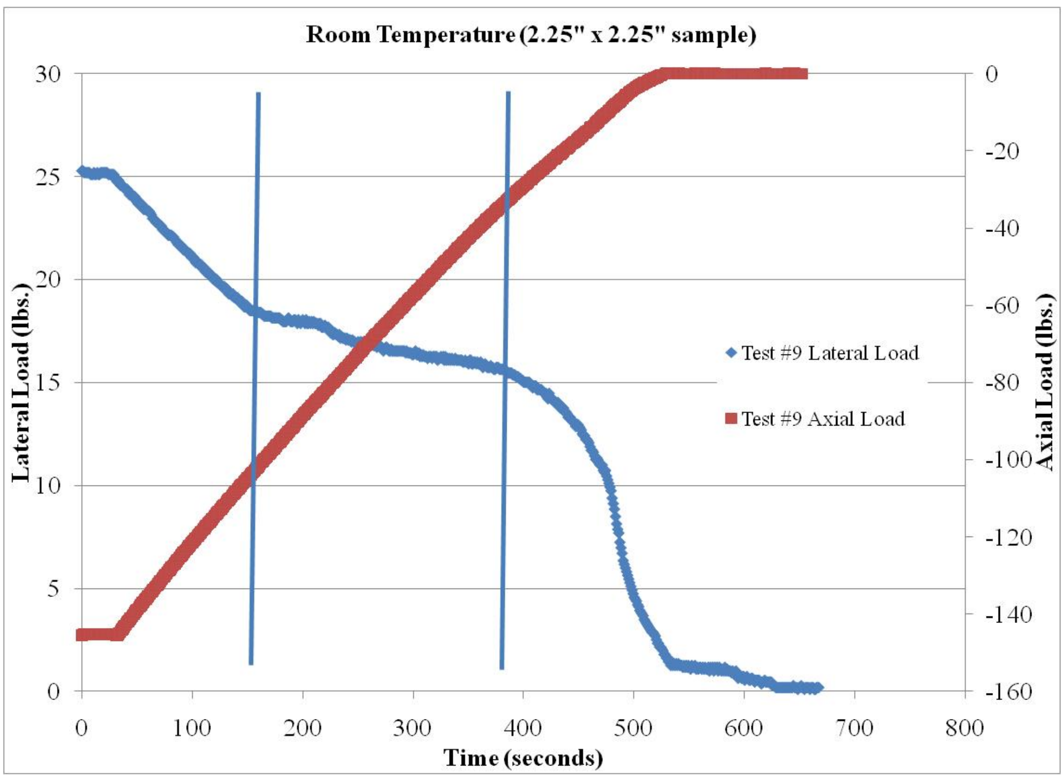

Figure 26. Results for 2.25” Sample Using Lateral Load Testing Set-Up after First Modification with Increased Lateral Load.

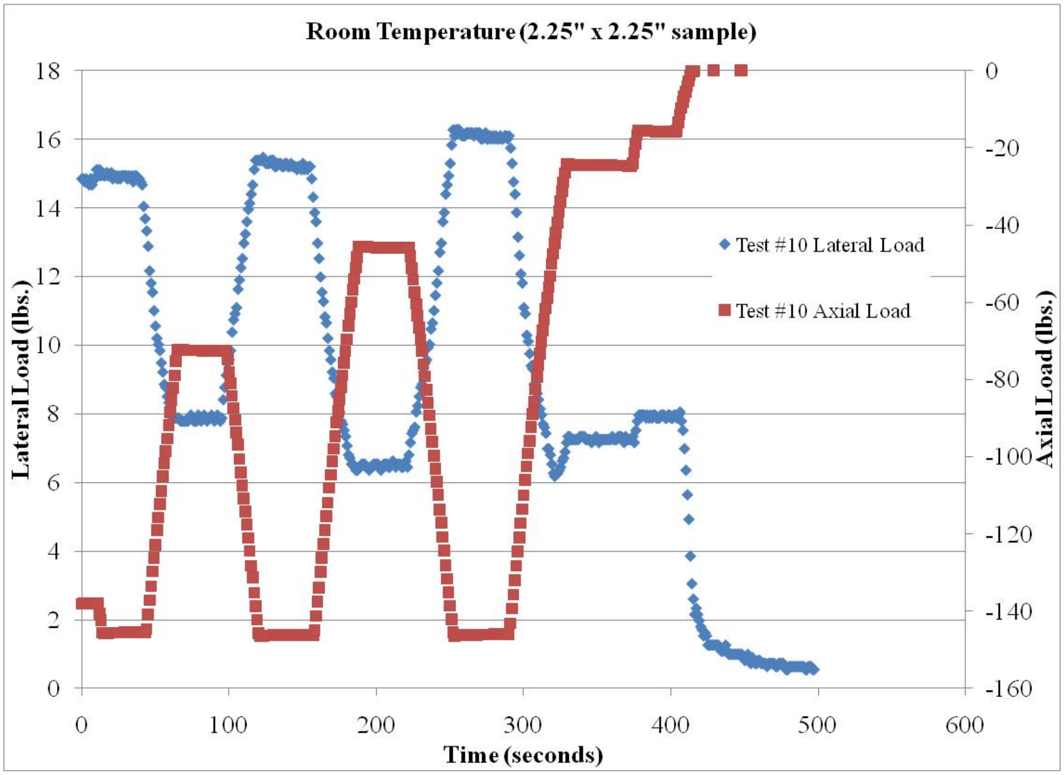

Figure 27. Results for 2.25" Sample Using Lateral Load Testing Set-Up after First Modification with Cyclic Unloading/Loading.

Results of testing performed using the test set-up after the second modification (Tests #11-61) are shown in Figure 28 through Figure 48. Figure 28 shows Tests #11 and 12 run using 2.25" (57.15 mm) square samples. Test #11 was loaded axially to 207 lbs. (93.89 kg) and laterally to 25 lbs. (11.34 kg), while Test #12 was loaded axially to 188 lbs. (85.28 kg) and laterally to 9 lbs. (4.08 kg). Load removal from these tests was performed at 0.01 mm/sec. The lateral loads were found to decrease rapidly in both tests at a constant rate with the removal of the axial load, contrary to the behavior seen in previous testing discussed above. It was decided though that this test method was still not producing the desired data for analysis, therefore the test procedure was modified.

Tests #13 (as shown in Figure 29) was run by axially loading a 2.25" (57.15 mm) square test sample in a step fashion and observing the corresponding lateral load. After each load step the loads (both axial and lateral) were allowed to relax as the sample was held under constant axial displacement. Tests #14-16 were run by applying a lateral load to a 1" (25.4 mm) square test sample in a step fashion through turning of the frame turnbuckle assembly and observing the corresponding axial load. Again, after each load step the loads (both axial and lateral) were allowed to relax as the sample was held under the current conditions. As shown in Figure 30 for Test #14 (and also seen in Tests #15 and 16), it was found that coupling still existed between the axial and lateral loads. This was thought to be due to deflection of the frame push rods. Subsequently, work was done to stiffen the frame by providing supports to the push rods as shown in Figure 21(b).

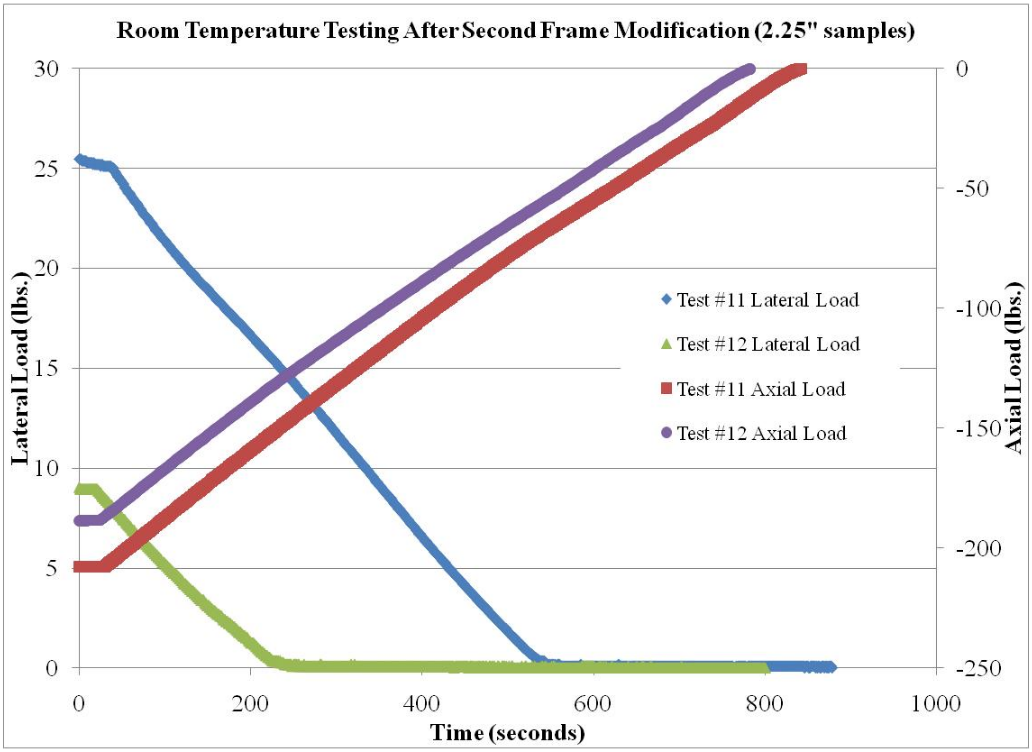

Figure 28. Results for 2.25” Samples Using Lateral Load Testing Set-Up after Second Modification.

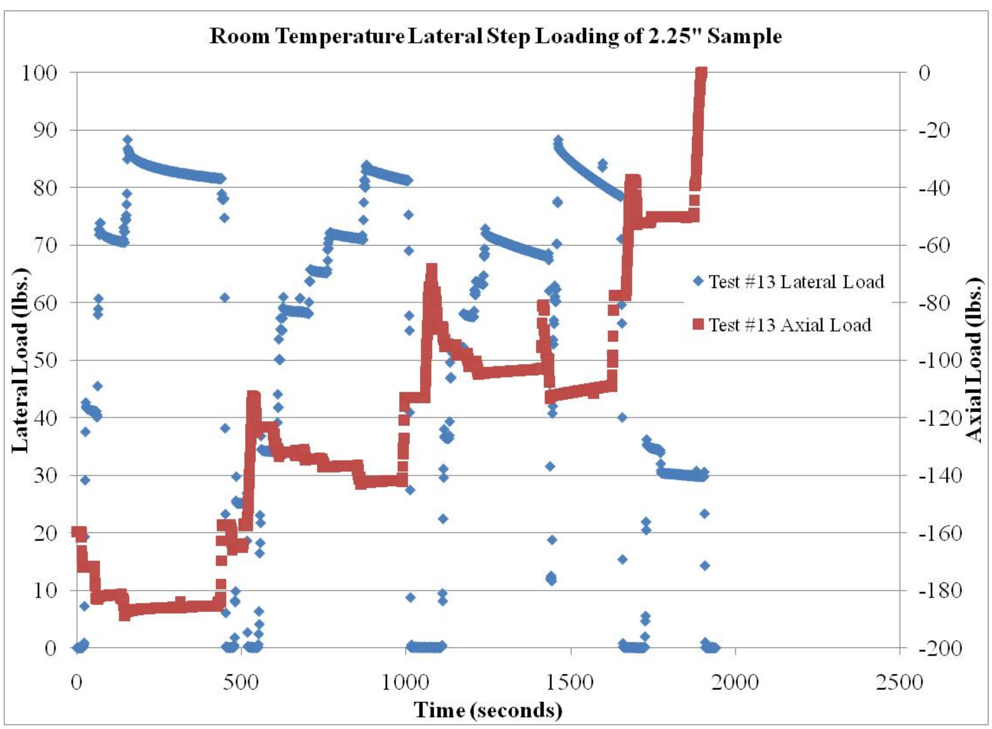

Figure 29. Results for Axial Step Loading of 2.25” Sample Using Lateral Load Testing Set-Up after Second Modification.

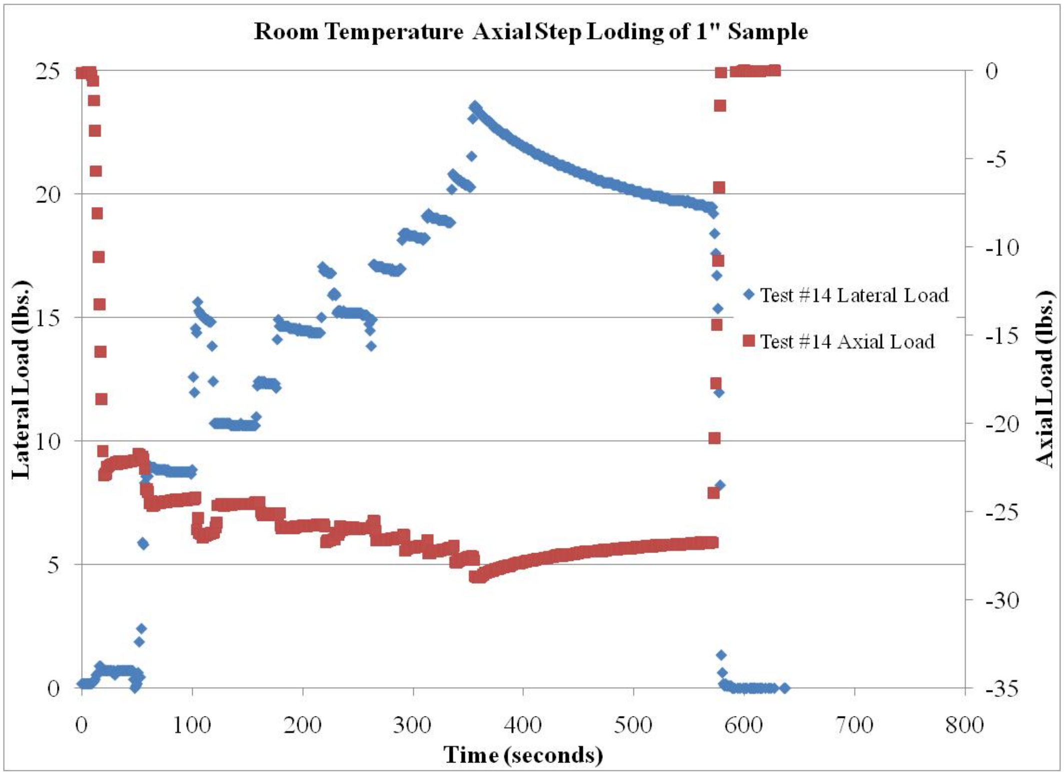

Figure 30. Results for Lateral Step Loading of 1" Sample Using Lateral Load Testing Set-Up after Second Modification.

After stiffening the test frame, Test #17 was run by axially loading a 1" (25.4 mm) square test sample to 65 lbs. (29.48 kg), then performing a lateral step loading as done for Tests #14-16. Results of this test are shown in Figure 31. The sample began to slip when the lateral load reached ≈60 lbs. (27.22 kg). The lateral load was then removed from the sample and the axial load was reduced to 15 lbs. (6.80 kg). The sample was then reloaded laterally in a step fashion while under 15 lbs. (6.80 kg) of axial load. The sample began to slip under this condition when the lateral load reached ≈20 lbs. (9.07 kg). At this time both the axial and lateral loads were removed and the test ended.

Tests #18-21 were also run using 1" (25.4 mm) square test samples. Test #18, 20, and 21 were axially loaded to 65 lbs. (29.48 kg), before being laterally loaded at steps of 10, 20, 30, 40, 50, 60 and 65+ lbs. (4.54, 9.07, 13.61, 18.14, 22.68, 27.22 and 29.48+ kg). An example of this testing is shown in Figure 32. These samples were all successfully loaded in excess of 60 lbs. (27.22 kg) without failure. For Test #19 an initial axial load of 65 lbs. (29.48 kg) was applied, immediately followed by a reduction of the axial load to 25 lbs. (11.34 kg). The sample was then stepped through the same lateral loading used above. This sample failed while going to 60 lbs. (27.22 kg) of lateral load as shown in Figure 33.

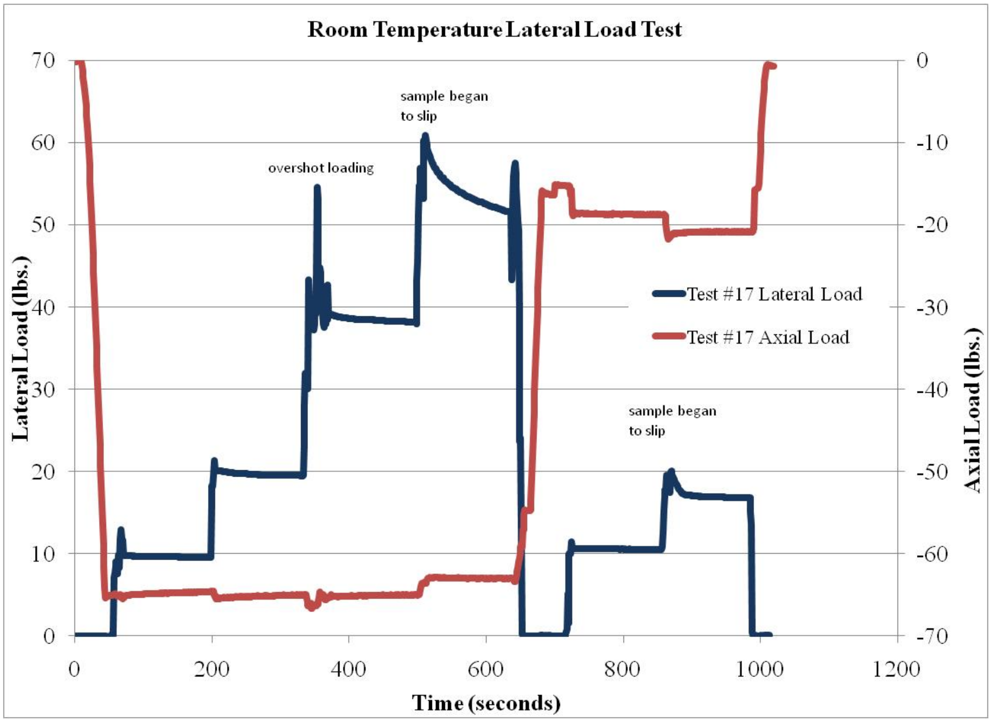

Figure 31. Results for Lateral Step Loading of 1" Sample Preloaded to 65 lbs. Axially Using Lateral Load Testing Set-Up after Second Modification.

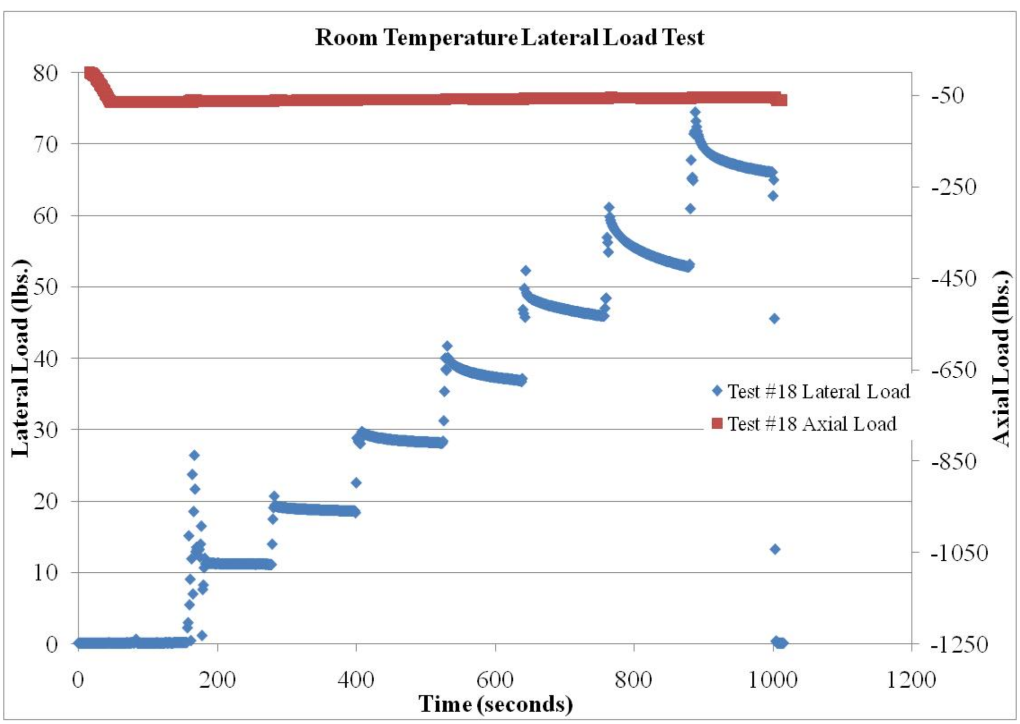

Figure 32. Characteristic Results for Lateral Step Loading of 1" Sample Loaded to 65 lbs. Axially.

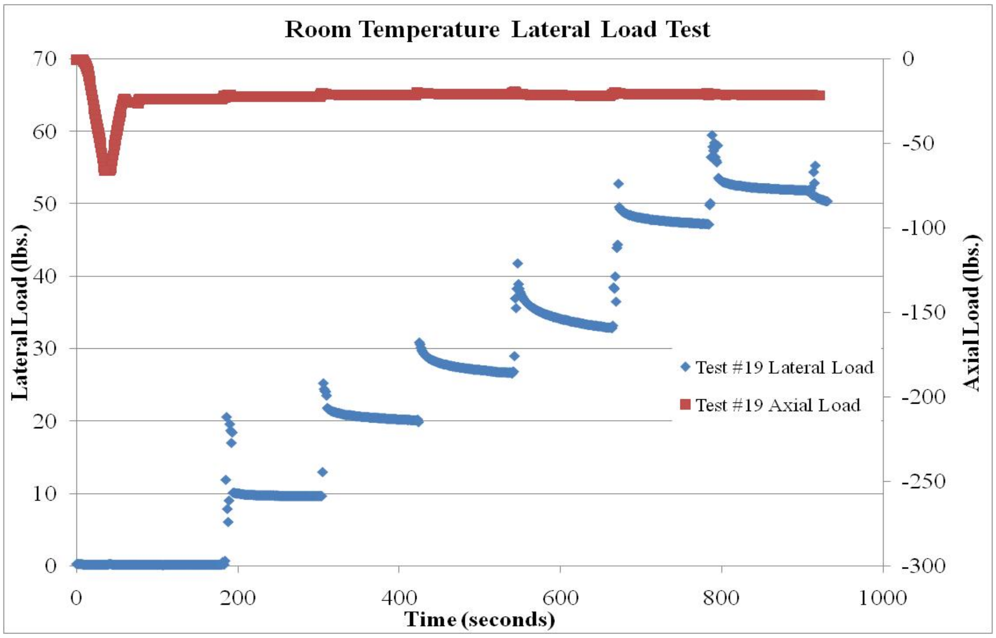

Figure 33. Results for Lateral Step Loading of 1" Sample Preloaded to 25 lbs. Axially After Being Subjected to Initial Axial Loading of 65 lbs.

Tests #22-24 were run using a 2.25" (57.15 mm) square test samples axially loaded to 270 lbs. or ≈55 psi (122.47 kg or ≈0.4 MPa) before being stepped through lateral loads of 50, 85, 115, 150, 170, 200, 250, and 285 lbs (22.68, 38.56, 52.16, 68.04, 77.11, 90.72, 113.40, and 129.27 kg). The samples in all of these tests began to fail while going to 250 lbs. or ≈50 psi (113.40 kg or ≈0.3 MPa) and fully failed while going to 285 lbs or >55 psi (129.27kg or >0.4 MPa) as shown in Figure 34.

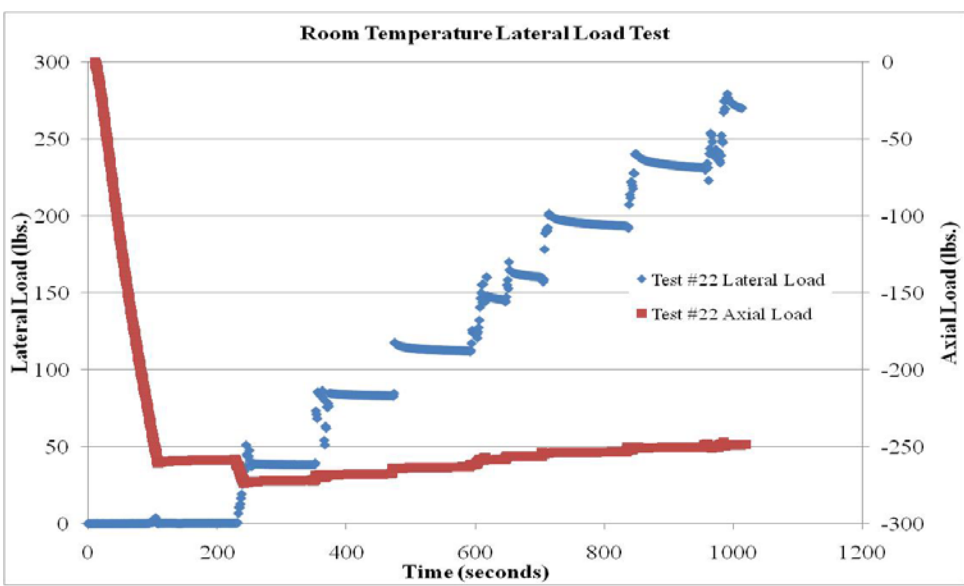

Figure 34. Results for Lateral Step Loading of 2.25" Sample Preloaded to 270 lbs. Axially.

Tests #25-27 were run at 400^oC using 1” (25.4 mm) square test samples. Test #25 was axially loaded after heating to 65 lbs. (29.48 kg) before being stepped through lateral loads of 10, 20, 40, and 50 lbs. (4.54, 9.07, 18.14, and 22.68 kg). The sample failed while going to 50 lbs. (22.68 kg) of lateral load as shown in Figure 35. This lateral load was thought to be low and possibly due to uneven loading. Test #26 was also axially loaded after heating to 65 lbs. (29.48 kg) before being stepped through lateral loads of 10, 20, 30, 40, 50, 60 and 70 lbs. (4.54, 9.07, 13.61, 18.14, 22.68, 27.22, and 31.75 kg). After successfully being loaded laterally, the lateral load was removed and the axial load was reduced to 25 lbs. (11.34 kg). The lateral load was then stepped through 10, 20, and 30 lbs. (4.54, 9.07, and 13.61 kg). The sample failed while going to 30 lbs. (13.61 kg) of lateral load as shown in Figure 36. For Test #27 an initial axial load of 65 lbs. (29.48 kg) was applied after heating, immediately followed by a reduction of the axial load to 25 lbs. (11.34 kg). The sample was then stepped through lateral loads of 10, 20, 30, 40, 50, 60, and 70 lbs. (.54, 9.07, 13.61, 18.14, 22.68, 27.22, and 31.75 kg). After successfully being loaded laterally, the lateral load was removed and the axial load was reduced to 15 lbs. (6.80 kg). The lateral load was then stepped through 10, 20, and 30 lbs. (4.54, 9.07, and 13.61 kg). The sample failed while going to 30 lbs. (13.61 kg) of lateral load as shown in Figure 37. The behavior exhibited by Tests #26 and 27 (at 400^oC) was found to be similar to that experienced at room temperature.

To confirm that the behavior of Min-K at elevated temperature (400^oC) was similar to that at room temperature additional testing was performed at 400^oC. Tests #28-30 were run using 1” (25.4 mm) square test samples. Test #28 was axially loaded to 65 lbs. (29.48 kg) after heating and then stepped through lateral loads of 10, 20, 30, 40, 50, 55, and 60 lbs. (4.54, 9.07, 13.61, 18.14, 22.68, 24.95, and 27.22 kg). The sample failed while going to 60 lbs. (27.22 kg) of lateral load. Test #29 was also axially loaded after heating to 65 lbs. (29.48 kg) before being stepped through lateral loads of 10, 20, 30, 40, 50, 55, 60, 65, and 70 lbs. (4.54, 9.07, 13.61, 18.14, 22.68, 24.95, 27.22, 29.48, and 31.75 kg). After successfully being loaded laterally, the lateral load was removed and the axial load was reduced to 25 lbs. (11.34 kg). The lateral load was then stepped through 10, 20, 30, 40, and 50 lbs. (4.54, 9.07, 13.61, 18.14, and 22.68 kg). The sample failed while going to 50 lbs. (22.68 kg) of lateral load as shown in Figure 38. For Test #30 an initial axial load of 65 lbs. (29.48 kg) was applied after heating, immediately followed by a reduction of the axial load to 25 lbs. (11.34 kg). The sample was then stepped through lateral loads of 10, 20, 30, 40, and 50 lbs. (4.54, 9.07, 13.61, 18.14, and 22.68 kg). The sample failed while going to 50 lbs. (22.68 kg) of lateral load as shown in Figure 39. Tests #31 and 32 were replicates of Tests #29 and 30, respectively. Data from these tests was nearly identical to that seen in Figure 38 and Figure 39, respectively.

Test #33 was run at 400^oC using a 1” (25.4 mm) square test sample. The sample was initially loaded axially to 65 lbs. (29.48 kg) after heating, then was immediately reduced to 15 lbs. (6.80 kg). The sample was then stepped through lateral loads of 10, 20, 30, 40, and 50 lbs. (4.54, 9.07, 13.61, 18.14, and 22.68 kg). The sample failed while going to 50 lbs. (22.68 kg) of lateral load as shown in Figure 40. The higher lateral load capability is thought to be due to the fact that the axial load was creeping up with the application of the lateral

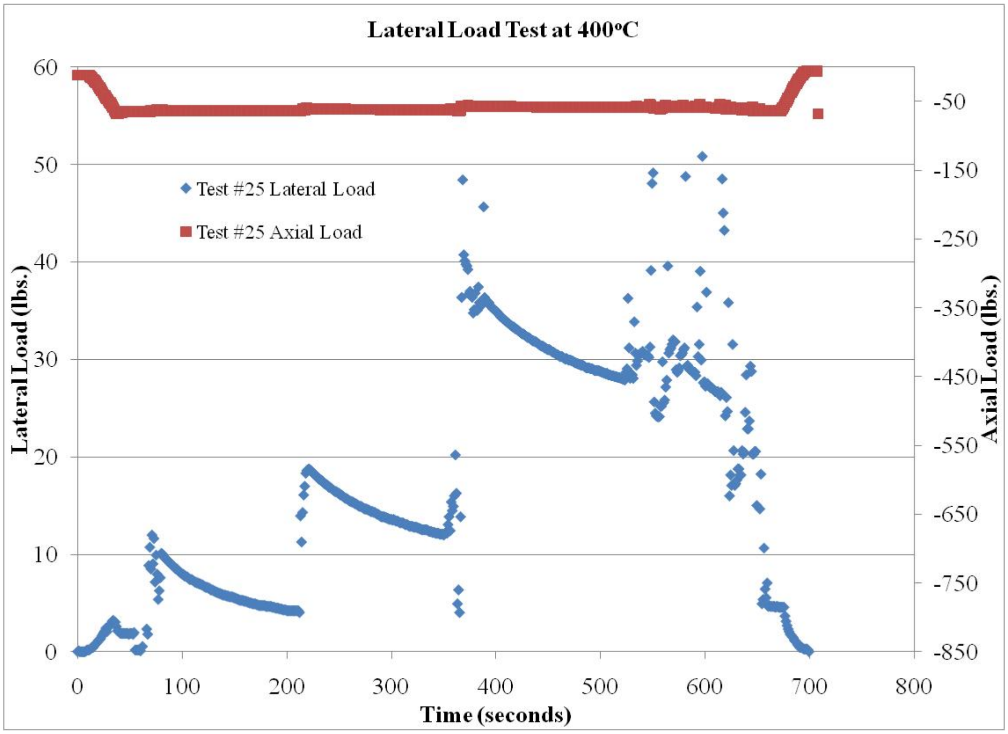

Figure 35. Results for Lateral Step Loading of 1" Sample at 400°C Preloaded to 65 lbs. Axially.

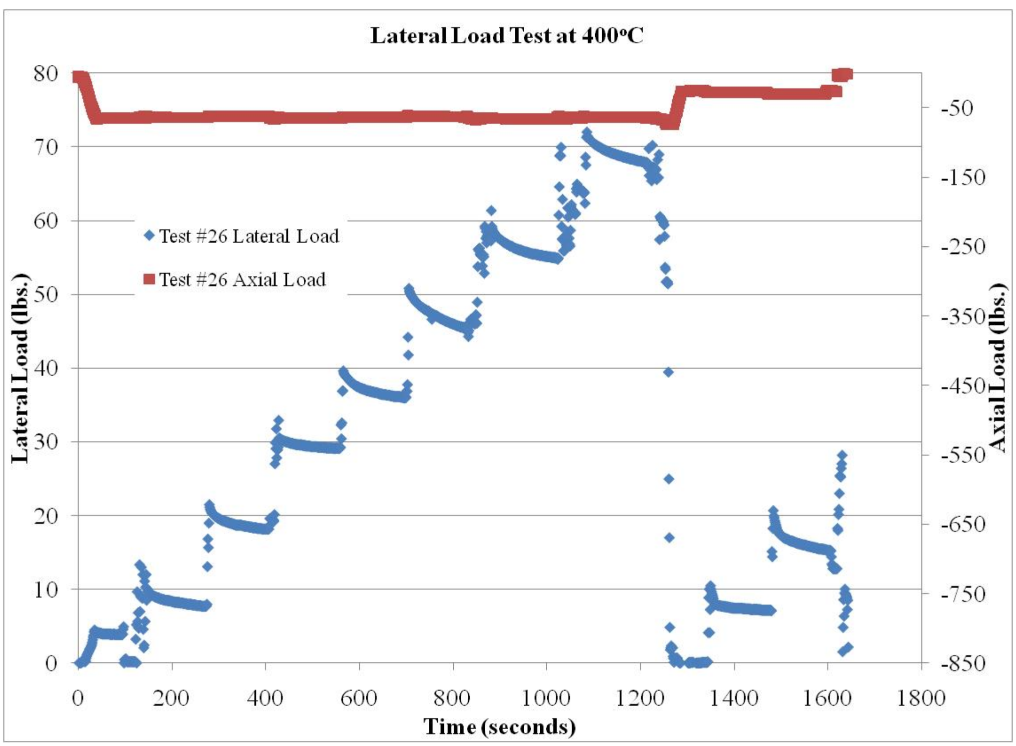

Figure 36. Results for Lateral Step Loading of 1" Sample at 400°C Preloaded to 65 and 25 lbs. Axially.

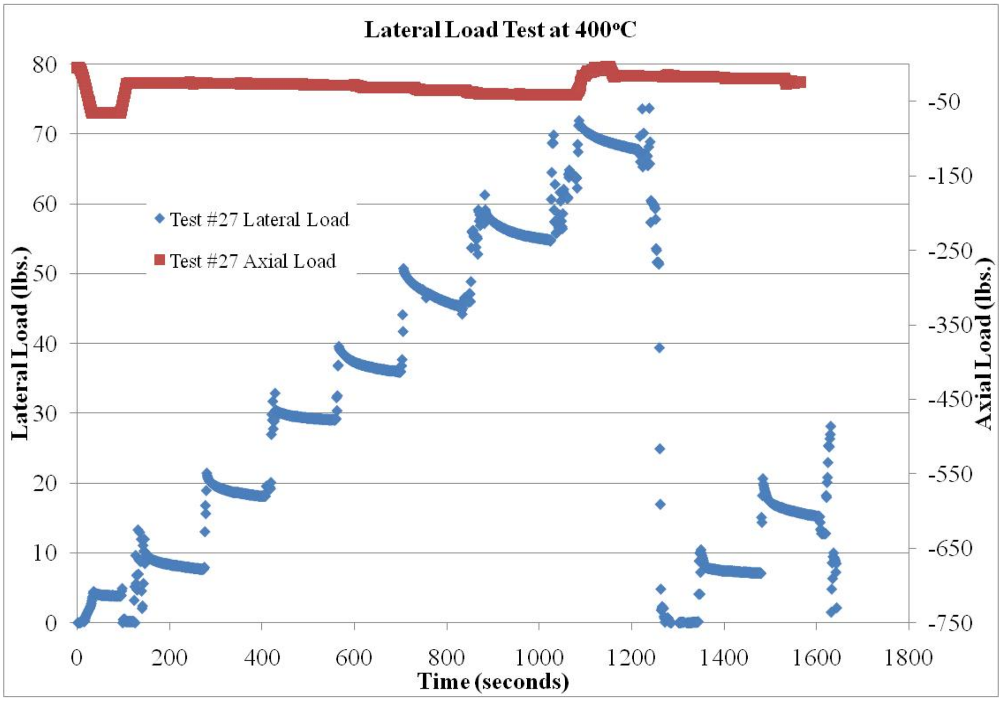

Figure 37. Results for Lateral Step Loading of 1” Sample at 400^{o}C Preloaded to 65, 25, and 15 lbs. Axially.

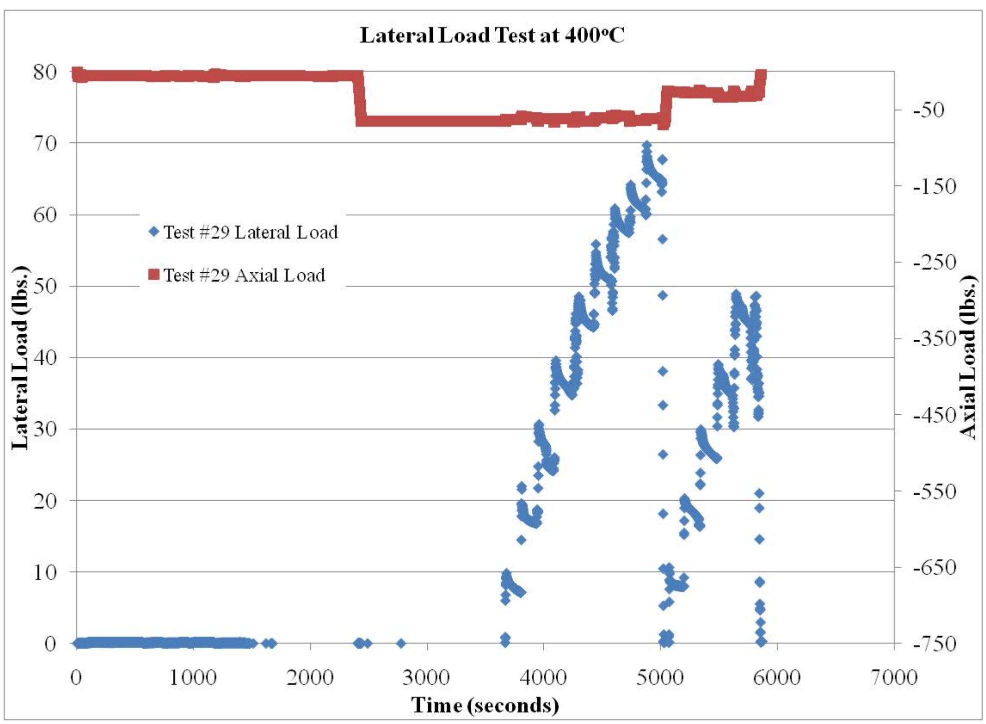

Figure 38. Results for Lateral Step Loading of 1” Sample at 400^{o}C Preloaded to 65 and 25 lbs. Axially After Heating.

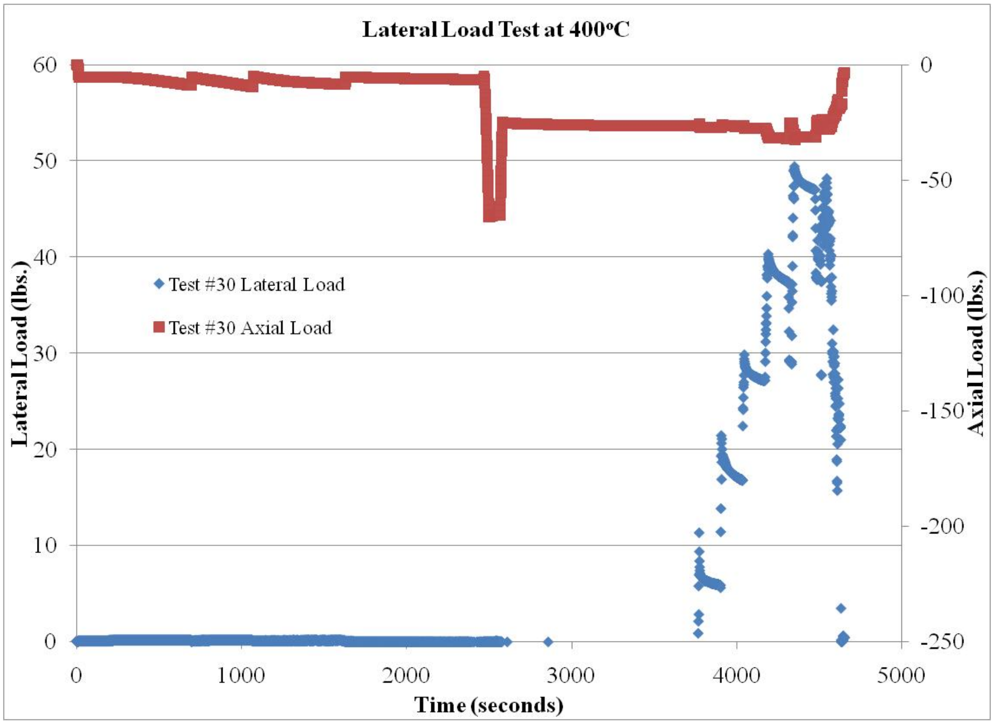

Figure 39. Results for Lateral Step Loading of 1" Sample at 400^{o}C Preloaded to 65 and 25 lbs. Axially After Heating.

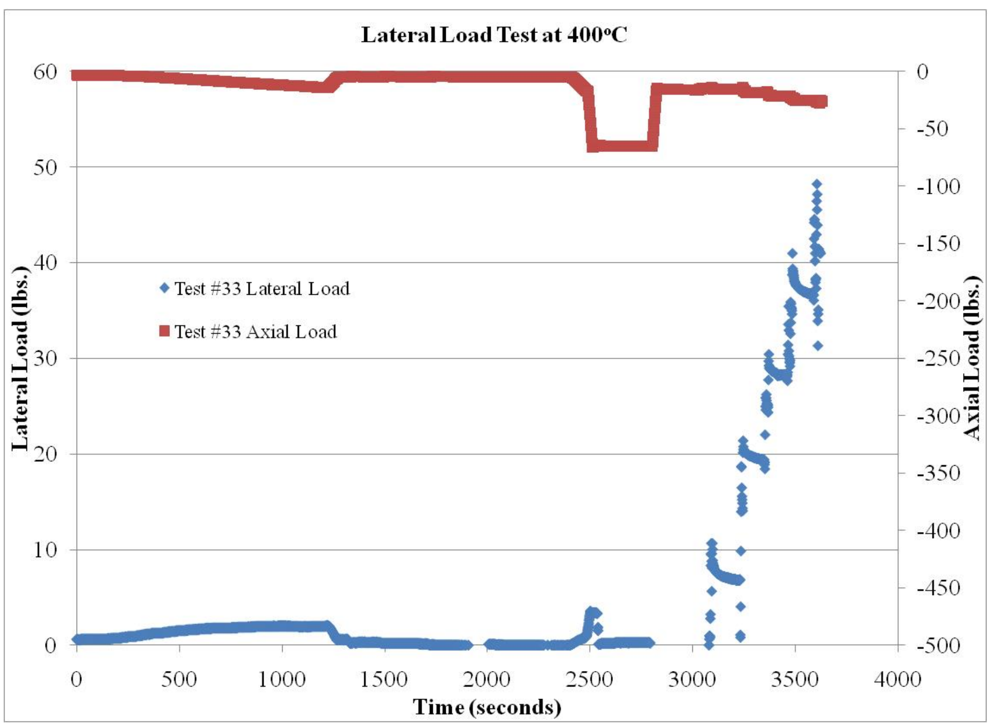

Figure 40. Results for Lateral Step Loading of 1" Sample at 400^{o}C Preloaded to 65 and 15 lbs. Axially After Heating.

load and was at a level of ≈25 lbs. (11.34 kg) at the time of failure. Tests #34 and 35 were replicates of Test #33. The axial load was maintained during these tests and these samples failed while going to a lateral load of 30 lbs. (13.61 kg) as shown in Figure 41, which is more of the level expected.

Test #36 was a replicate of Tests #29 and 31 and shows similar results to Figure 38. Test #37 and 41 were replicates of Tests #30 and 32. These test failed while attempting to load the sample to 50 lbs. (22.68 kg) laterally. Test #38 and 42 were replicates of Tests #33-35. Test #38 shows similar results to those seen for Tests #34 and 35 in Figure 41. Test #42 exhibited a creeping of the axial load with the application of the lateral load as seen in Test #33 and resulted in an axial load of ≈20 lbs. (9.07 kg) at the time the sample failed while going to a lateral load of 40 lbs. (18.14 kg) (results similar to those seen in Figure 40).

Test #39 was run at 400°C using a 1” (25.4 mm) square test sample. The sample was initially loaded axially to 65 lbs. (29.48 kg) after heating, then was immediately reduced to 10 lbs. (4.54 kg). The sample was then stepped through lateral loads of 10, 20 and 30 lbs. (4.54, 9.07, and 13.61 kg). The sample failed while going to 30 lbs. (13.61 kg) of lateral load as shown in Figure 42. Test #43 was a replicate of Test #39 and shows similar results to Figure 42.

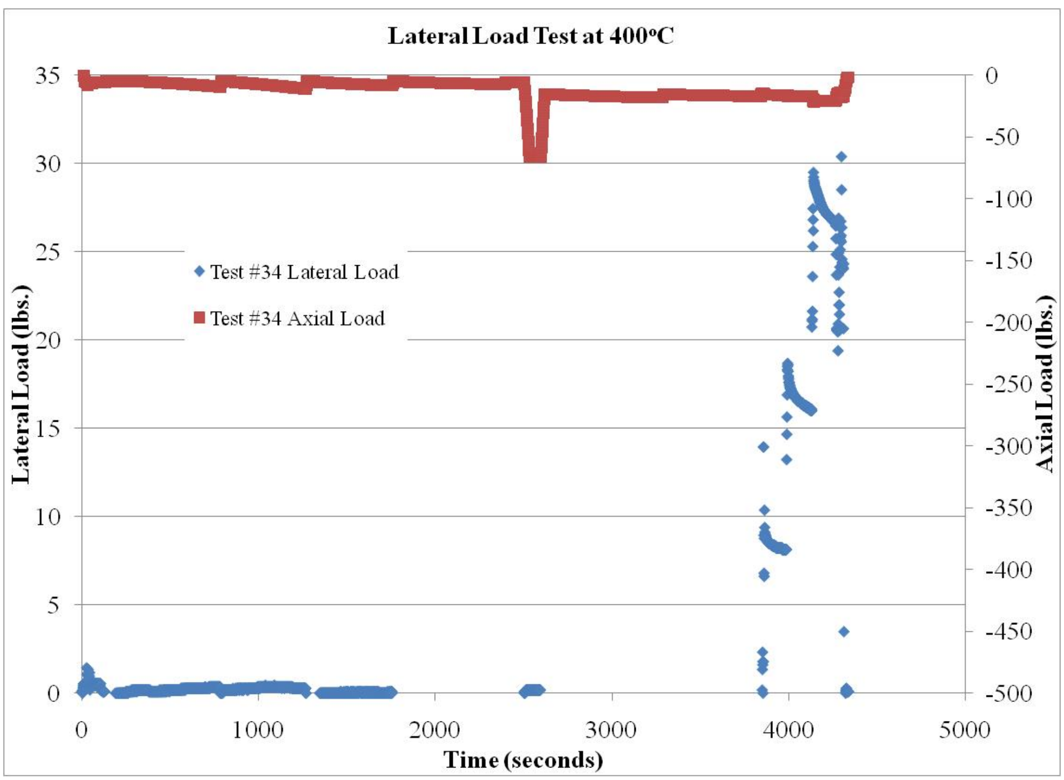

Figure 41. Results for Lateral Step Loading of 1” Sample at 400°C Preloaded to 65 and 15 lbs. Axially After Heating.

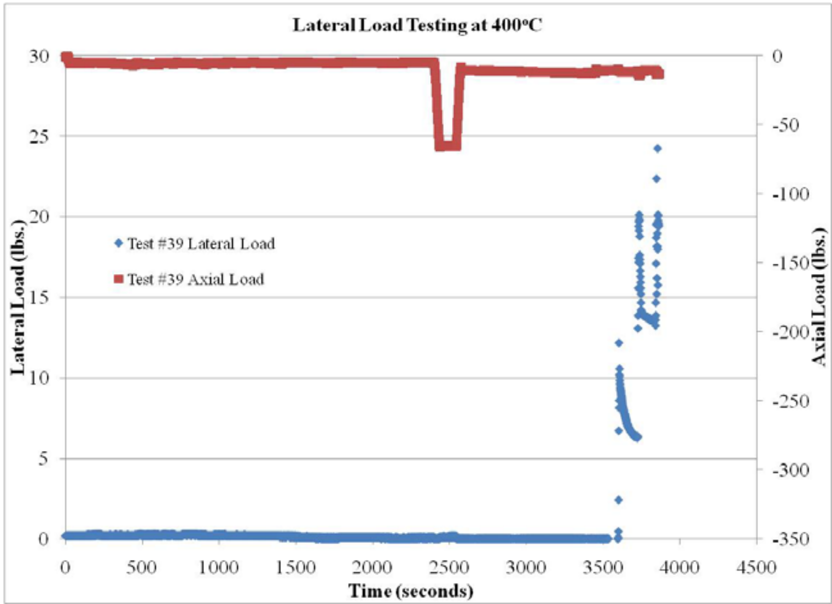

Figure 42. Results for Lateral Step Loading of 1" Sample at 400°C Preloaded to 65 and 10 lbs. Axially After Heating.

To ascertain dependence between the axial and lateral loads, Test #40 was run at 400°C using a 1" (25.4 mm) square test sample by initially loading the sample axially to 65 lbs. (29.48 kg) and laterally to 75 lbs. (34.02 kg) after heating. The lateral load was then removed while monitoring the axial load as shown in Figure 43. Both loads were found to fall off simultaneously.

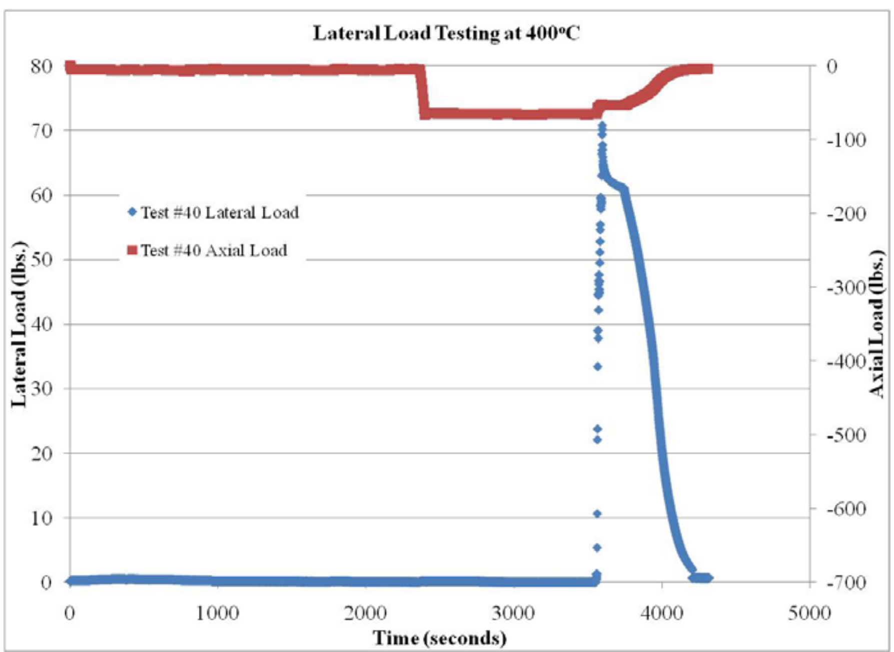

Figure 43. Results for 1" Sample Using Lateral Load Testing Set-Up at 400°C.

Tests #44, 45, and 46 were run at 400^{o}C using thinner (0.25”/6.35 mm thick) 1” (25.4 mm) square test samples. Test #44 was run under the same conditions as Tests #29 and 31 and showed similar results to Figure 38. Test #45 was run under the same conditions as Tests #30 and 32 and showed similar results to Figure 39. Test #46 was run under the same conditions as Tests #33-35. This test showed results more like that seen for Tests #33 and 42 though as a similar creeping of the axial load was experienced. These results would indicate that sample thickness does not significantly affect material performance in these instances.

Test #47-52 were run at room temperature using the thinner 1” (25.4 mm) square test samples. Test #47 was run under similar conditions to those used for Test #44. This test also showed similar results to those seen in Figure 38. Test #48 was run under similar conditions and exhibited similar behavior to Test #25, which failed while going to 50 lbs. (22.68 kg) of lateral load as shown in Figure 35. Test #49 and 50 were run under similar conditions and exhibited similar behavior to Test #46 above, with similar creeping axial load behavior resulting in a higher than expected lateral load capability. Test #51 was run under the same conditions as Tests #30 and 32, but failed while going to 60 lbs. (27.22 kg) of lateral load due to the creeping of the axial load up to 30 lbs (13.61 kg) during the second round of lateral load steps (initially under 25 lbs. (11.34 kg) axial load). Test #52 was loaded to 25 lbs. (11.34 kg) axially and then step loaded laterally to 10, 20, 30, 40, and 50 lbs. (4.54, 9.07, 13.61, 18.14, and 22.68 kg). The axial load was able to be kept constant during this test and the sample failed while going to 50 lbs. (22.68 kg) of lateral load as expected and shown in Figure 44. These results would indicate that sample temperature does not significantly affect material performance in these instances.

Test #53 was a replicate of Tests #29, 31, 36, 44, and 51. It behaved similar to previous tests as shown in Figure 38. Tests #54-56 were replicates of Tests # 30, 32, 37, 41, and 45. Tests #54 and 56 behaved similar to previous tests as shown in Figure 39. Test #55 failed while going to 40 lbs. (18.14 kg) of lateral load (as opposed to 50 lbs. (22.68 kg)). The failure at a lower lateral load is attributed to a flaw or defect in the sample.

To again verify that there were no size effects regarding testing of the Min-K samples, Tests #57 and 58 were run at room temperature using 2.5” (63.5 mm) square test samples. Test #57 was loaded axially to 152 lbs. or ≈30 psi (68.95 kg or ≈0.2 MPa), before being stepped through lateral loads of 77, 128, 181, 254, and 330 lbs. (34.93, 58.06, 82.10, 115.21, and 149.69 kg). The sample failed while going to 330 lbs. or 65 psi (149.69kg or 0.4 MPa) of lateral load as shown in Figure 45. Test #58 was loaded axially to 152 lbs. or ≈30 psi (68.95 kg or ≈0.2 MPa) and then immediately reduced to 102 lbs. (46.27 kg) of axial load (≈20 psi or 0.1 MPa), before being stepped through lateral loads of 77, 128, and 181 lbs. (34.93, 58.06, and 82.10 kg). The sample failed while going to 181 lbs. or 35 psi (82.10 kg or 0.2 MPa) of lateral load as shown in Figure 46.

Test #59-61 were run at room temperature using 1” (25.4 mm) square test samples. Test #59 was loaded axially to 25 lbs. (11.34 kg) and then immediately reduced to 10 lbs. (4.54 kg) of axial load before being stepped through lateral loads of 10, 20, and 30 lbs. (4.54, 9.07, and 13.61 kg). The sample failed while going to 30 lbs. (13.61 kg) of lateral load as shown in Figure 47. Test #60 was loaded to 25 lbs. (11.34 kg) and then immediately reduced to 15 lbs. (6.80 kg) of axial load, before being stepped through lateral loads of 10, 20, 30, and

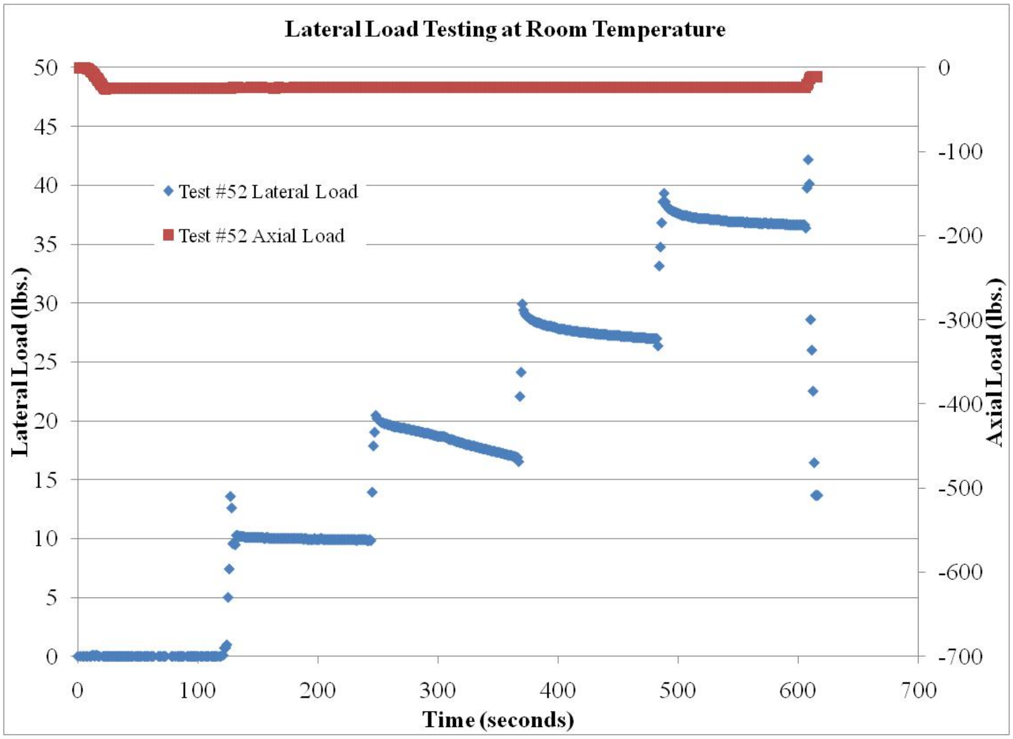

Figure 44. Results for 1” (0.25” Thick) Sample Preloaded to 25 lbs. Axially at Room Temperature.

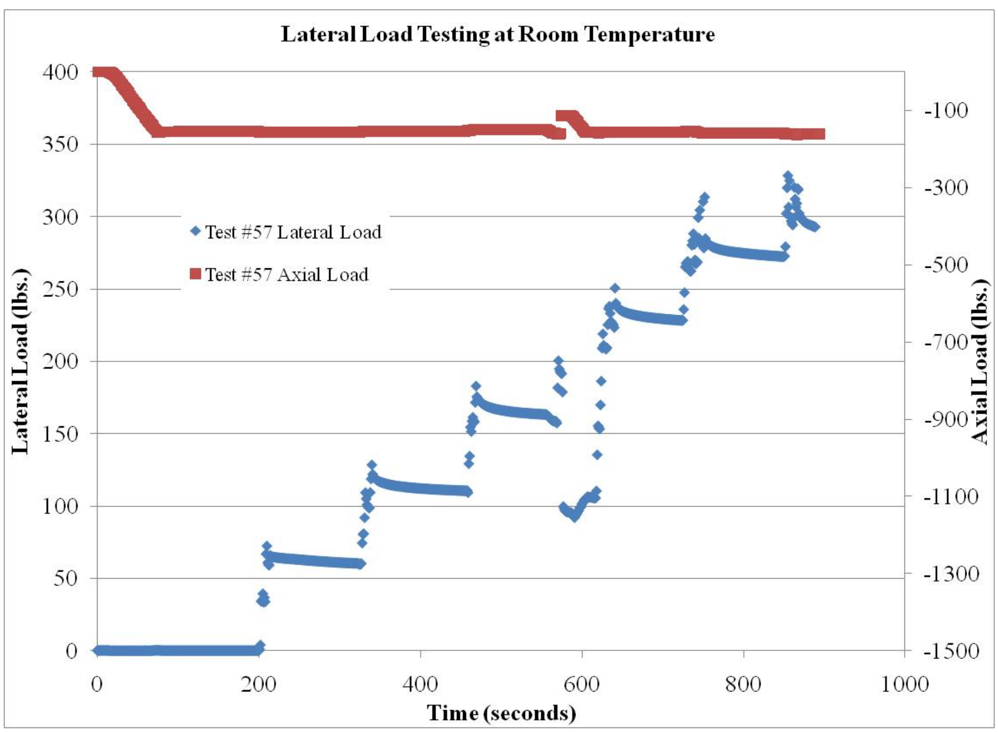

Figure 45. Results for 2.25” Sample Preloaded to 152 lbs. Axially at Room Temperature.

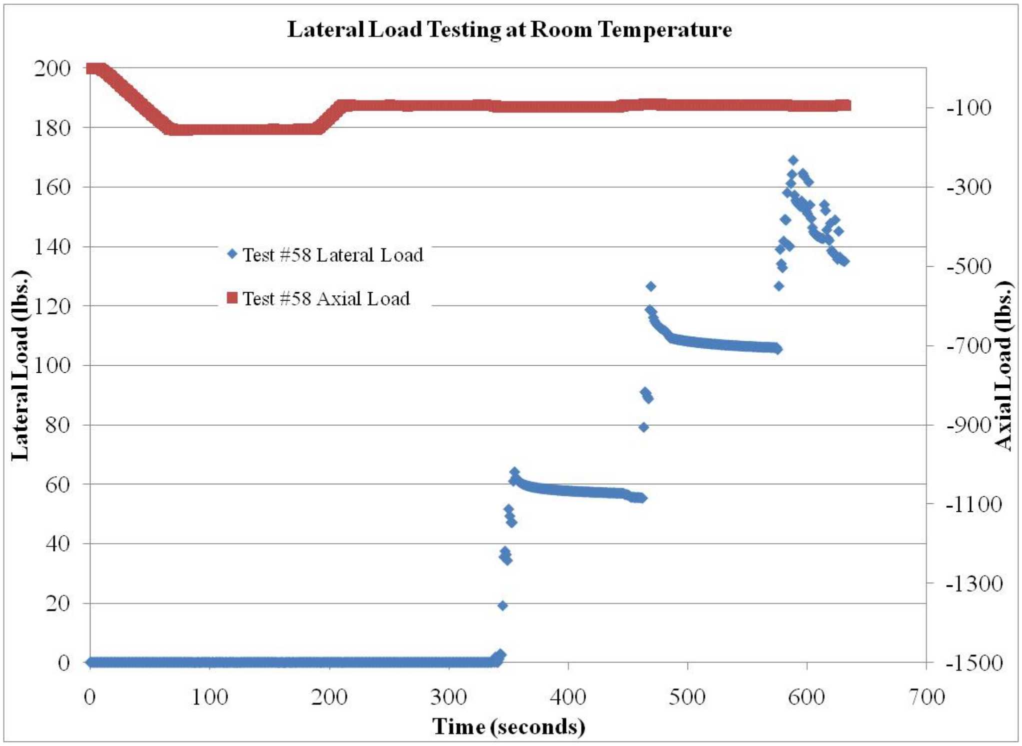

Figure 46. Results for 2.25” Sample Preloaded to 152 and 95 lbs. Axially at Room Temperature.

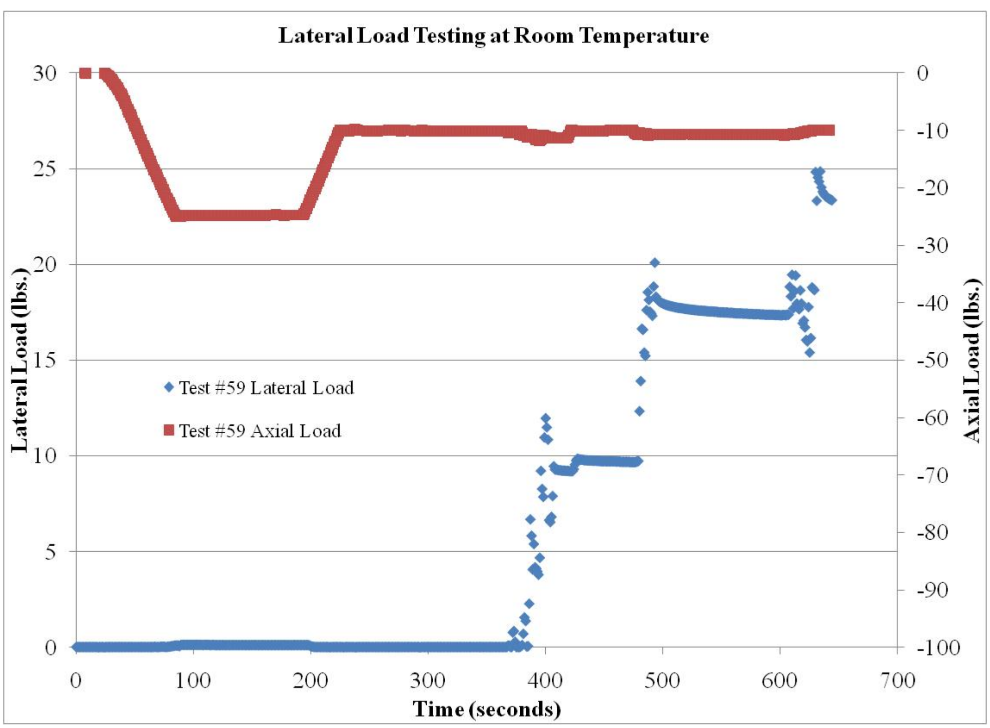

Figure 47. Results for 1” Sample Preloaded to 25 and 10 lbs. Axially at Room Temperature.

40 lbs. (4.54, 9.07, 13.61, and 18.14 kg). The sample failed while going to 40 lbs. (18.14 kg) of lateral load as shown in Figure 48. This is thought to be due to uneven loading of the sample due to not enough initial load being applied to embed the pyramoidal surfaces of the platens. Therefore, Test #61 was run by loading to 35 lbs. (15.88 kg) axially and then immediately reducing the load to 15 lbs. (6.80 kg). This sample failed while going to 30 lbs. (13.61 kg) of lateral load as expected and seen previously (see Figure 41).

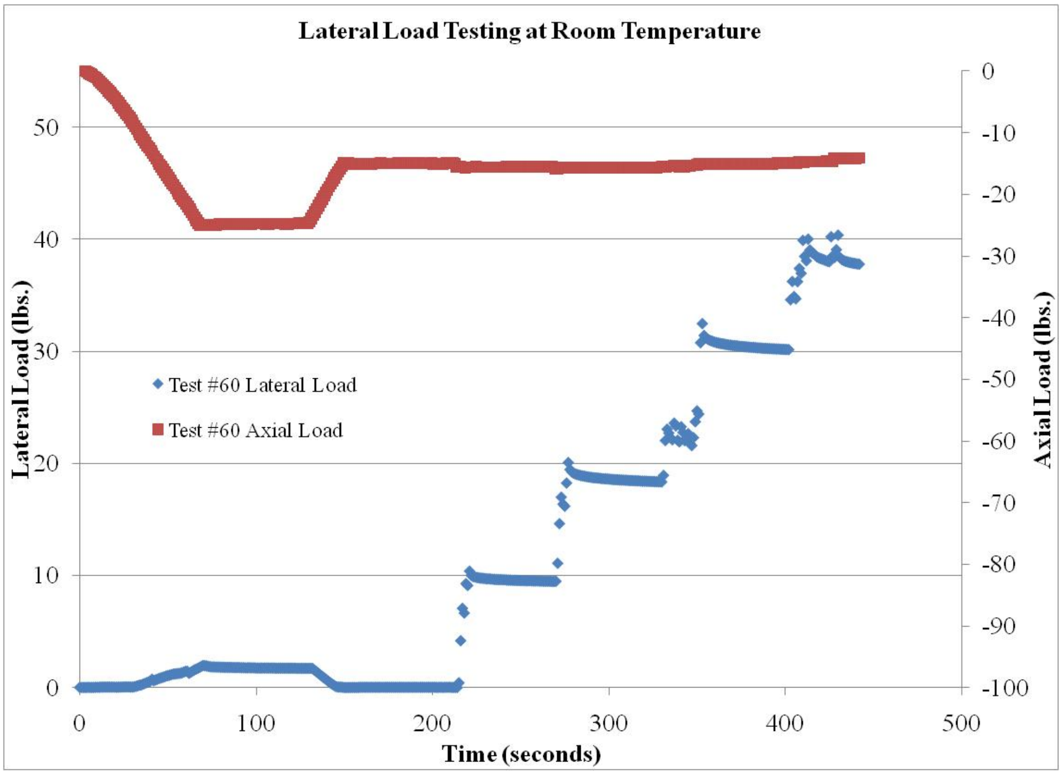

Figure 48. Results for 1" Sample Preloaded to 25 and 15 lbs. Axially at Room Temperature.

In summary, results of testing performed using the test set-up after the first modification (Tests #1-10) where samples were loaded axially and then laterally before the axial load was removed at a constant displacement rate showed a decrease in lateral load until a corresponding axial load was reached at which point the lateral load remained constant for a fixed period before the lateral load began to decrease to zero as the remainder of the axial load was removed. There was good repeatability found between repeat tests run under these conditions. Tests run under varying displacement rates during removal of the axial load indicated that the removal of the axial load at a faster rate resulted in the period of decreased lateral load loss occurring at a higher lateral load value. To confirm that the loss of lateral load was related to the removal of the axial load and not to some other source, a test was run which was loaded both axially and laterally with the axial load removed at a constant displacement rate with holds when the axial load reached set levels. As expected, the lateral load stopped decreasing when the axial load was held constant at each hold. A test was also run where the axial load was intermittently removed and reapplied at various levels again confirming the direct correlation between the axial and lateral loads, along with an increase in the lateral load with the axial reloading events. This indicated coupling between the axial and lateral loads due to problems with the test fixture which needed to be corrected for improved accuracy of the test data analysis. Therefore, the second modification of the test set-up was undertaken.

Results of testing performed using the test set-up after the second modification (Tests #11-61) showed that the lateral loads were found to decrease rapidly at a constant rate with the removal of the axial load, contrary to the behavior seen in previous testing. It was decided though that this test method was still not producing the desired data for analysis, therefore the test procedure was modified. The next tests were run by axially loading a sample in a step fashion and observing the corresponding lateral load. After each load step the loads (both axial and lateral) were allowed to relax as the sample was held under constant axial displacement. Tests were also run by applying a lateral load to a sample in a step fashion through turning of the frame turnbuckle assembly and observing the corresponding axial load. Again, after each load step the loads (both axial and lateral) were allowed to relax as the sample was held under the current conditions. It was found that coupling still existed between the axial and lateral load, which was thought to be due to deflection of the frame push rods. Subsequently, work was done to stiffen the frame by providing supports to the push rods.

After stiffening the test frame, Test #17 was run by axially loading a 1" (25.4 mm) square test sample to 65 lbs. (28.48 kg), then performing a lateral step loading as done for Tests #14-16. Results of this test are shown in Figure 31. The sample began to slip when the lateral load reached ≈60 lbs. (27.22 kg). The lateral load was then removed from the sample and the axial load was reduced to 15 lbs. (6.80 kg). The sample was then reloaded laterally in a step fashion while under 15 lbs. (6.80 kg) of axial load. The sample began to slip under this condition when the lateral load reached ≈20 lbs. (9.08 kg). At this time both the axial and lateral loads were removed and the test ended.

After stiffening the test frame, tests were run by axially loading samples to a set level, then performing a lateral step loading until the sample began to slip. A summary of the failure behavior of Min-K under this testing is shown in Table 4. In general, samples began to slip when the applied lateral load was roughly twice the applied axial load. This is as expected since a friction factor of ≈1 was expected for this material and the applied lateral load was split over two sample surfaces. Therefore, the lateral load at slippage should be roughly twice the applied axial load.

Table 4. Summary of General Lateral Load Test Results after Second Modification

Sample Size (inches)	Temperature	Axial Load (lbs.)	Failure Lateral Load (lbs.)
1.0 x 1.0	RT	65	No failure up to 70 lbs.
1.0 x 1.0	ET	65	No failure up to 70 lbs.
1.0 x 1.0	RT	65/25	50
1.0 x 1.0	ET	65/25	50
1.0 x 1.0	RT	65/15	40
1.0 x 1.0	ET	65/15	30
1.0 x 1.0	ET	65/10	30
1.0 x 1.0	ET	65/25/15	30
1.0 x 1.0	RT	25	50
1.0 x 1.0	RT	25/15	40
1.0 x 1.0	RT	35/15	30
2.5 x 2.5	RT	270	No failure up to 270 lbs.
2.5 x 2.5	RT	152	No failure up to 300 lbs.
2.5 x 2.5	RT	152/95	181

RT = room temperature, ET = 400°C

5. ISOTHERMAL STRESS RELAXATION TESTING

5.1 EXPERIMENTAL PROCEDURES

Additional Isothermal stress relaxation testing was performed at various temperatures and loads as indicated in Table 5. The purpose of this testing was to provide additional information on the isothermal stress relaxation behavior of Min-K at intermediate temperatures in the range of 400-500^{o}C. As found through previous testing[1], the behavior of Min-K transitions from “lower temperature behavior” to “higher temperature behavior” at these temperatures as characterized by the rate of stress relaxation.

Table 5. Isothermal Stress Relaxation Test Matrix

(all samples loaded to 200 psi – 1380 kPa)

Test #	Temperature (^{o}C)	Initial Load (lbf./N)	Test Duration (hours)
3_1	450	5,495/24,443	1,033
3_2	450	5,062/22,517	918
3_3	500	5,207/23,162	1,320
3_4	Not completed	NA	NA
3_5	450	5,479/24,372	570
3_6	500	5,695/25,333	1,006
3_7	550	5,663/25,190	456
3_8	550	5,664/25,195	749
3_9	650	5,664/25,195	724
3_10	600	5,658/25,168	24
3_11	650	5,658/25,168	1,487
3_12	600	5,728/25,479	4,676

Testing was performed using 6” (15 cm) diameter, 2” (5 cm) long cylindrical samples using the set-up shown in Figure 49. Each independent experimental station had a load capacity of 10,000 lbs. (4,536 kg). The experimental stations included a stiff frame, one load cell, one electromechanical actuator and a computerized system for data acquisition and control. In addition, each experimental station included a furnace to subject cylindrical test specimens of Min-K 1400 to a prescribed isothermal temperature. The operation of the furnace was controlled using a digital temperature controller and type-K thermocouples with the test set-up enclosed in an aluminum environmental chamber with helium flow (99.999% purity, flow rate of 70 mm) to maintain a prescribed atmosphere. Frames were connected to a back-up power supply similar to that shown in Figure 2 to provide uninterrupted power in the event of a laboratory power failure and a water chiller/circulator system to provide constant temperature cooling water to the test frames.

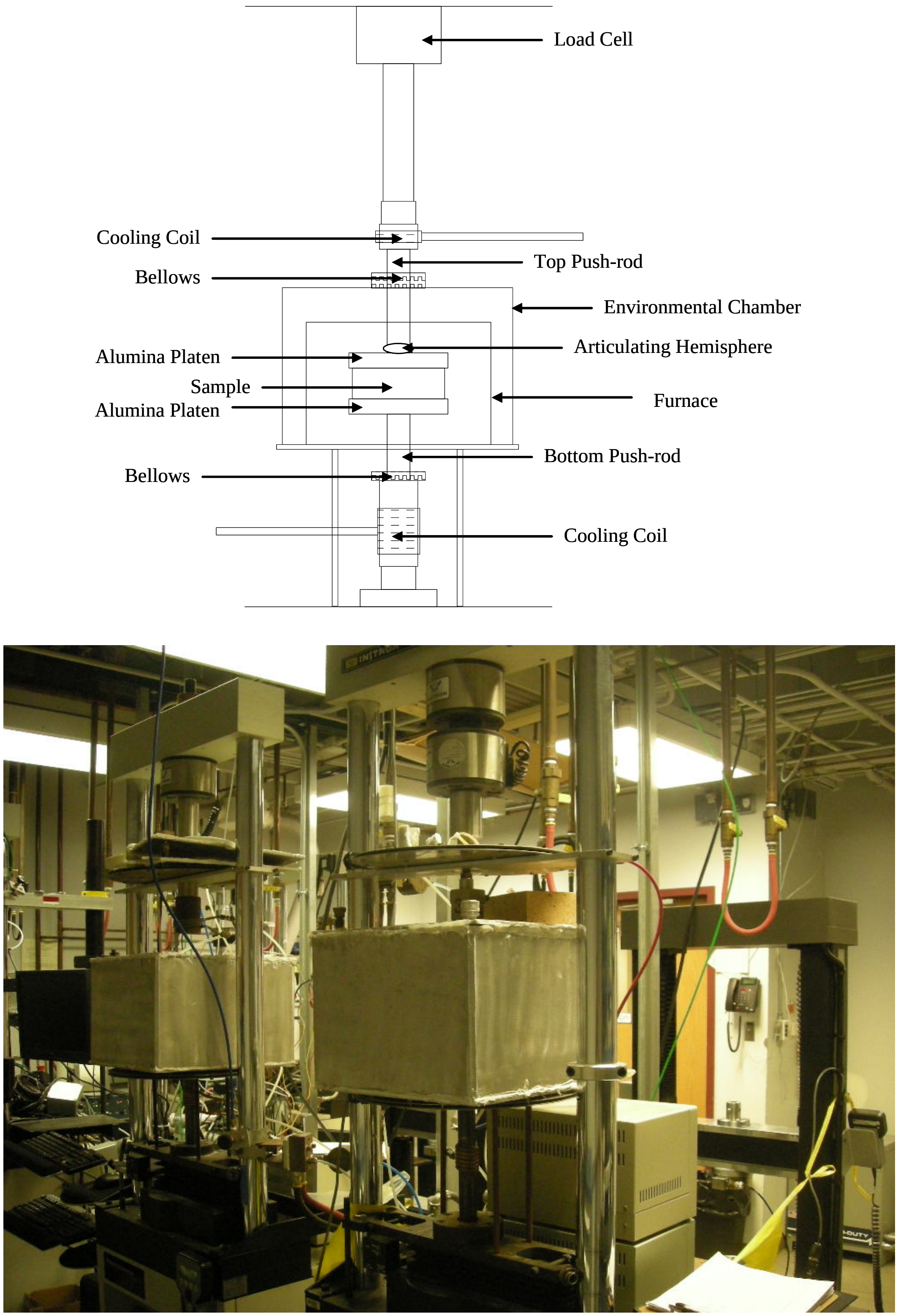

Figure 49. Isothermal Stress Relaxation Test Frame.

Sample loading was performed in strain control utilizing a twelve-step loading scheme with loading every half hour at a rate of 5.56% strain/hour as requested by the program sponsor to simulate actual system parameters. Samples were loaded between flat alumina platens and an alumina articulating semi-hemisphere was used for alignment purposes. Loading was then followed by stress relaxation under constant strain and the duration of the test was determined when the initial load was dissipated or had leveled off to a rate of change less than 0.25 psi/hour (1.7 kPa/hour).

5.2 RESULTS

Experimental testing of Min-K under isothermal stress relaxation conditions was completed at 450, 500, 550, 600, and 650^{o}C with an initial stresses of ≈200 psi (1,380 kPa). The duration of these tests spanned from 24 hours to in excess of 4,675 hours. Results from isothermal stress relaxation testing are shown in Figure 50 through Figure 60.

Figure 50 shows results from Test #3_1 which was performed at 450^{o}C. This test was ended after determining that enough data for accurate predictions had been collected. At the time the test was ended, it had been relaxing for over 1,025 hours and had reached a level of 164 psi (1,131 kPa).

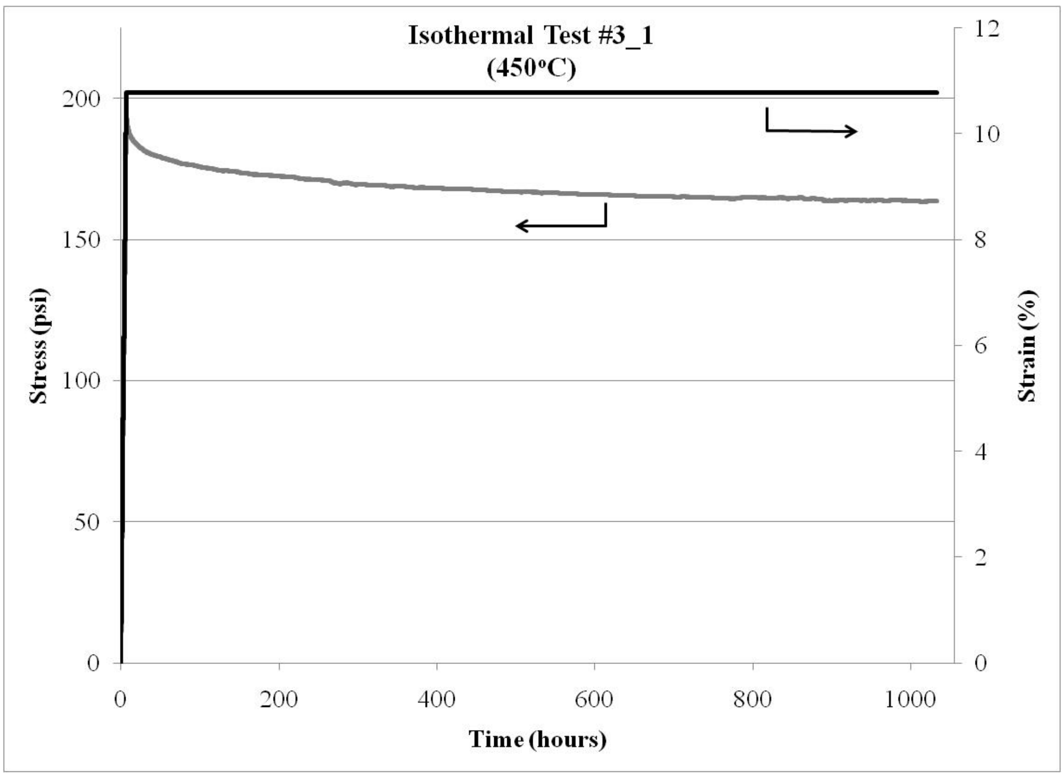

Figure 50. Isothermal Test #3_1 (450^{o}C).

The results from Test #3_2, which was also performed at 450^{o}C, are shown in Figure 51. This test was also ended after determining that enough data for accurate predictions had been collected. At the time the test was ended, it had been relaxing for over 905 hours and had reached a level of 173 psi (1,193 kPa).

Figure 52 shows the results from Test #3_3 which was performed at 500^{o}C. This test was also ended after determining that enough data for accurate predictions had been collected. At the time the test was ended, it had been relaxing for over 1,310 hours and had reached a level of 154 psi (1,062 kPa).

Isothermal Test #3_4 was heated but not run due to the breaking of the top ceramic platen attributed to thermal shock experienced during heating. Since the sample had been subjected to heating and some loading during preload and subsequent attempts to apply the actual test loads, the sample was thrown out.

The results from Test #3_5, which was performed at 450^{o}C, are shown in Figure 53. This test only relaxed for 560 hours, but was determined to have run for sufficient time to make accurate predictions in conjunction with the data previously collected at 450^{o}C. At the time the test was ended, it had relaxed to 167 psi (1,151 kPa).

Figure 54 shows the results from Test #3_6 which was performed at 500^{o}C. This test was ended after relaxing for over 1,000 hours which was determined to be a sufficient amount of time to make accurate predictions based on the collected data. At the time the test was ended, it had reached a level of 159 psi (1,096 kPa).

The results from Test #3_7, which was performed at 550^{o}C, are shown in Figure 55. This test lost temperature (and subsequently lost load to approximately 115 psi/793 kPa) after relaxing for approximately 70 hours due to a problem with the temperature controller. It was brought back up to temperature following identification of the problem and the load level was found to return to expected levels equivalent to those before the temperature loss. Upon being brought back up to temperature, the test was allowed to relax for another 375 hours (total relaxation time of over 445 hours) before being ended when it was determined that enough data for accurate predictions had been collected. At the time the test was ended, it had reached a level of 156 psi (1,076 kPa).

Figure 56 shows the results from Test #3_8 which was also performed at 550^{o}C. This test lost temperature (and subsequently lost load to approximately 110 psi/758 kPa) after relaxing for approximately 300 hours due to a problem with the cooling water supply system in the lab that activated the over-temperature controller on the test system furnace. It was brought back up to temperature following repair of the problem and the load level was found to return to expected levels equivalent to those before the loss of cooling water. Upon being brought back up to temperature, the test was allowed to relax for another 440 hours (total relaxation time of over 740 hours) before being ended when it was determined that enough data for accurate predictions had been collected. At the time the test was ended, it had reached a level of 153 psi (1,055 kPa).

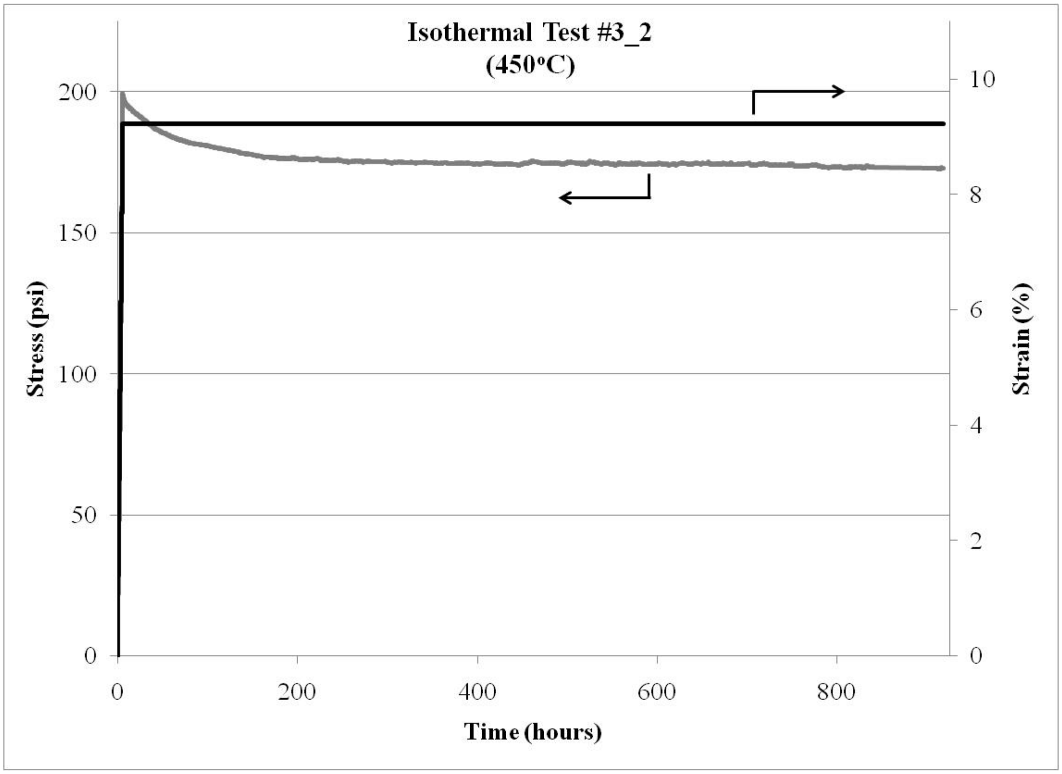

Figure 51. Isothermal Test #3_2 (450^{o}C).

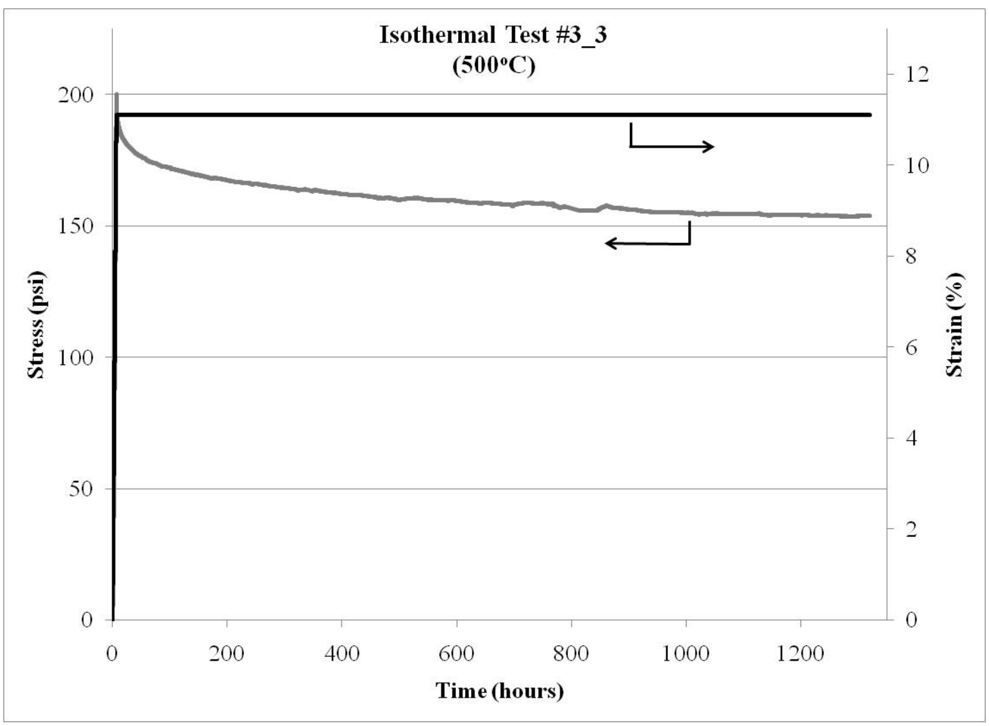

Figure 52. Isothermal Test #3_3 (500^{o}C).

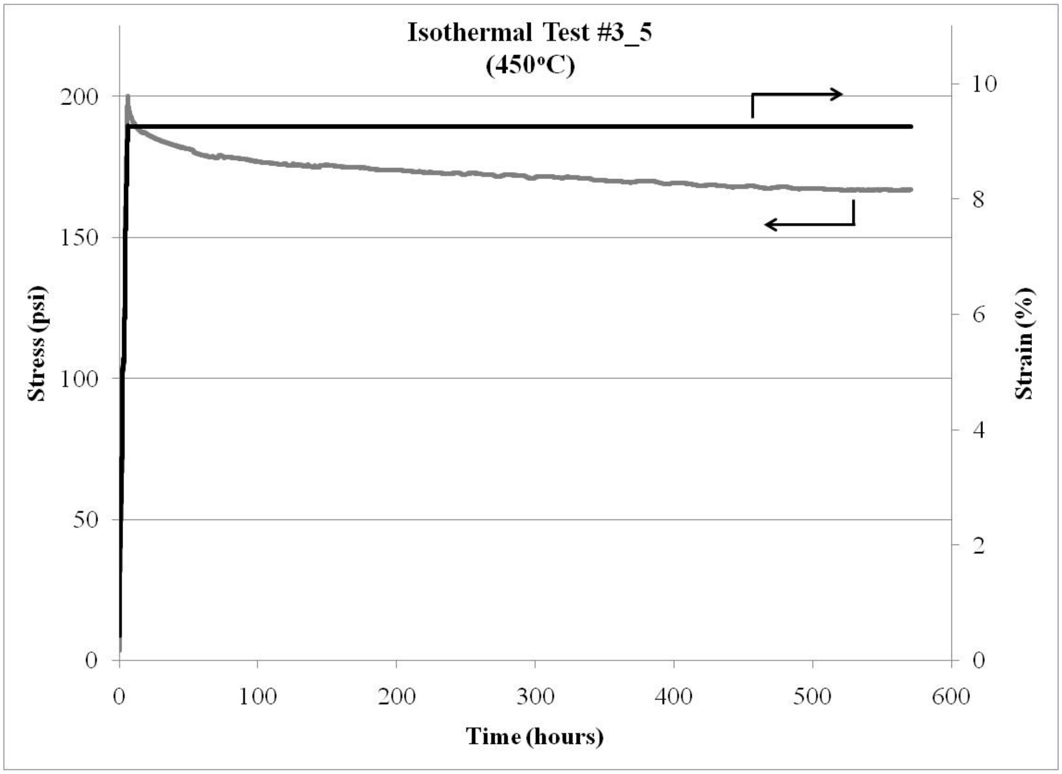

Figure 53. Isothermal Test #3_5 (450^{o}C).

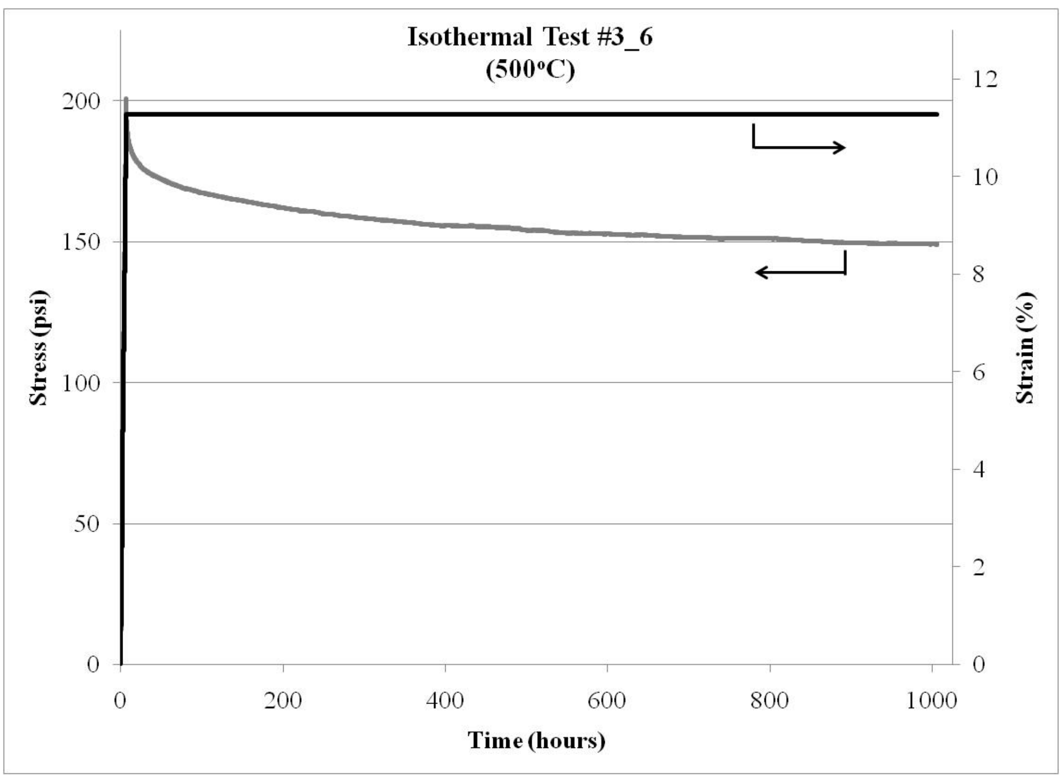

Figure 54. Isothermal Test #3_6 (500^{o}C).

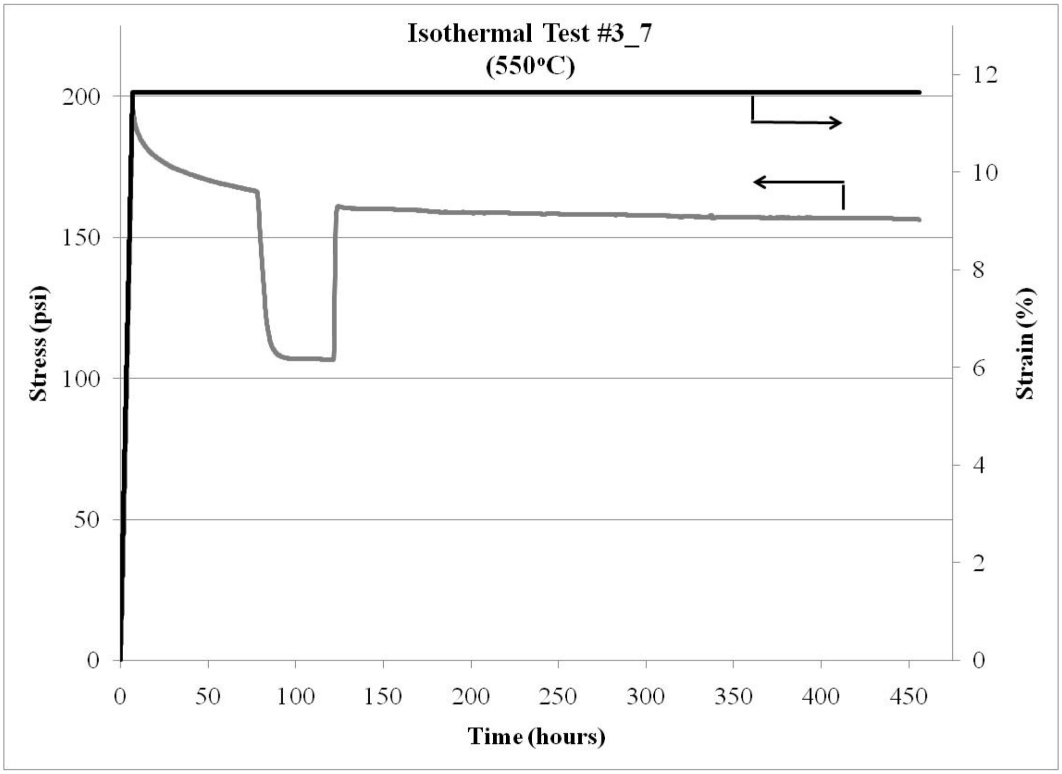

Figure 55. Isothermal Test #3_7 (550°C).

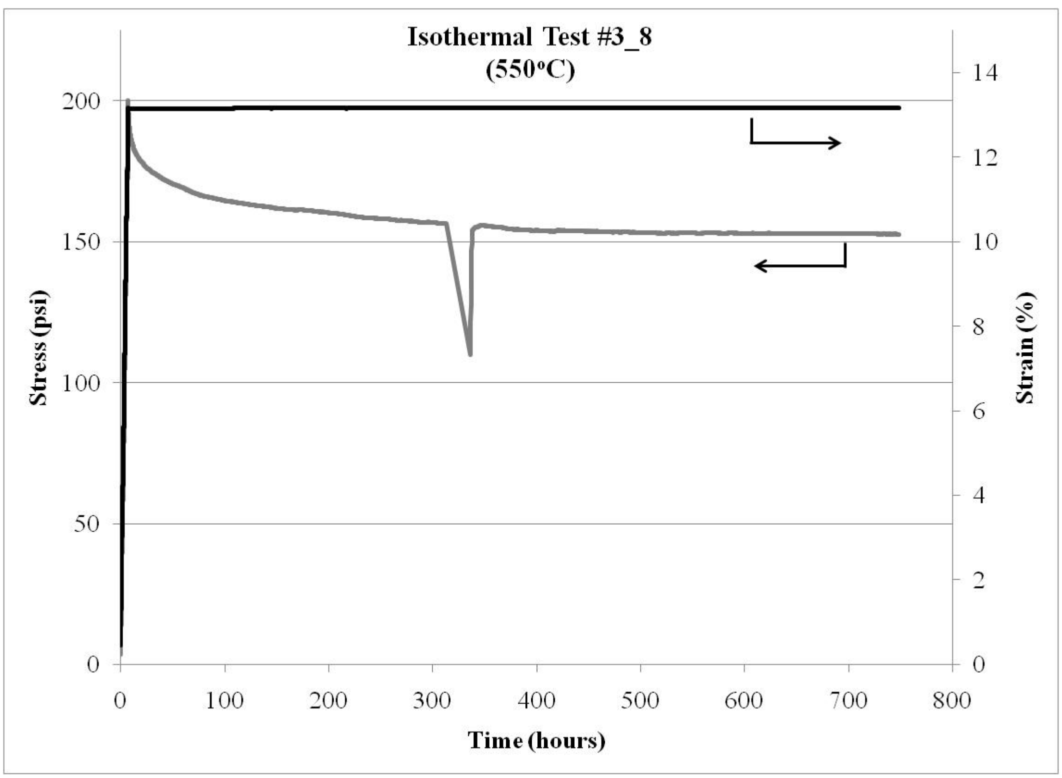

Figure 56. Isothermal Test #3_8 (550°C).

The results from Test #3_9, which was performed at 650^{o}C, are shown in Figure 57. This test lost temperature (and subsequently lost load to approximately 110 psi/758 kPa) after relaxing for approximately 375 hours due to the same problem with the cooling water supply system in the lab noted for Test #3_8, which in turn activated the over-temperature controller on the test system furnace. The test was brought back up to temperature following repair of the problem and the load level was found to return to expected levels equivalent to those before the loss of cooling water. Upon being brought back up to temperature, the test was allowed to relax for another 340 hours (total relaxation time of over 715 hours) before being ended when it was determined that enough data for accurate predictions had been collected. At the time the test was ended, it had reached a level of 116 psi (800 kPa).

Figure 57 shows the results for Test #3_10 which was performed at 600^{o}C. This test only relaxed for 20 hours before it was ended due to a frame communication error. At the time the test was ended, it had relaxed to 169 psi (1,165 kPa).

The results of Test #3_11, which was performed at 650^{o}C, are shown in Figure 59. This test was allowed to relax for over 1,480 hours and to a level of 82 psi (565 kPa) before being ended due to fluxuations in the test data.

Figure 60 shows the results for Test #3_12 which was performed at 600^{o}C. This test was allowed to continue until the end of the project, therefore substantially more relaxation data than collected for the other tests was obtained. The test relaxed for over 4,670 hours and to a level of 102 psi (703 kPa).

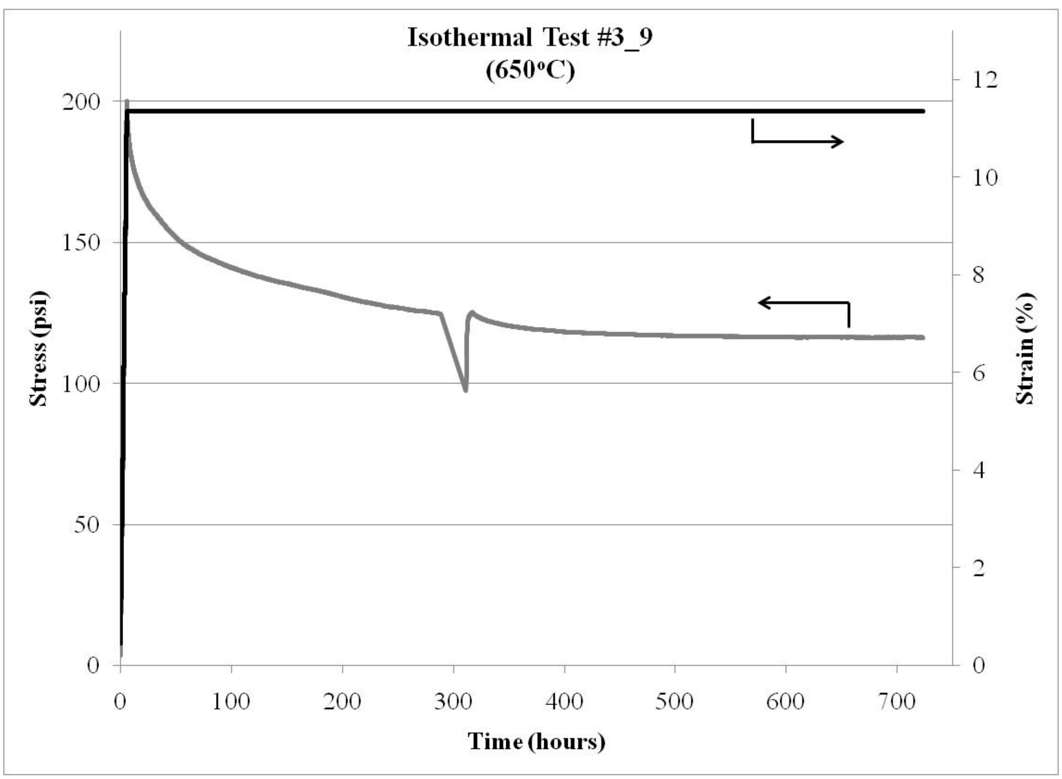

Figure 57. Isothermal Test #3_9 (650^{o}C).

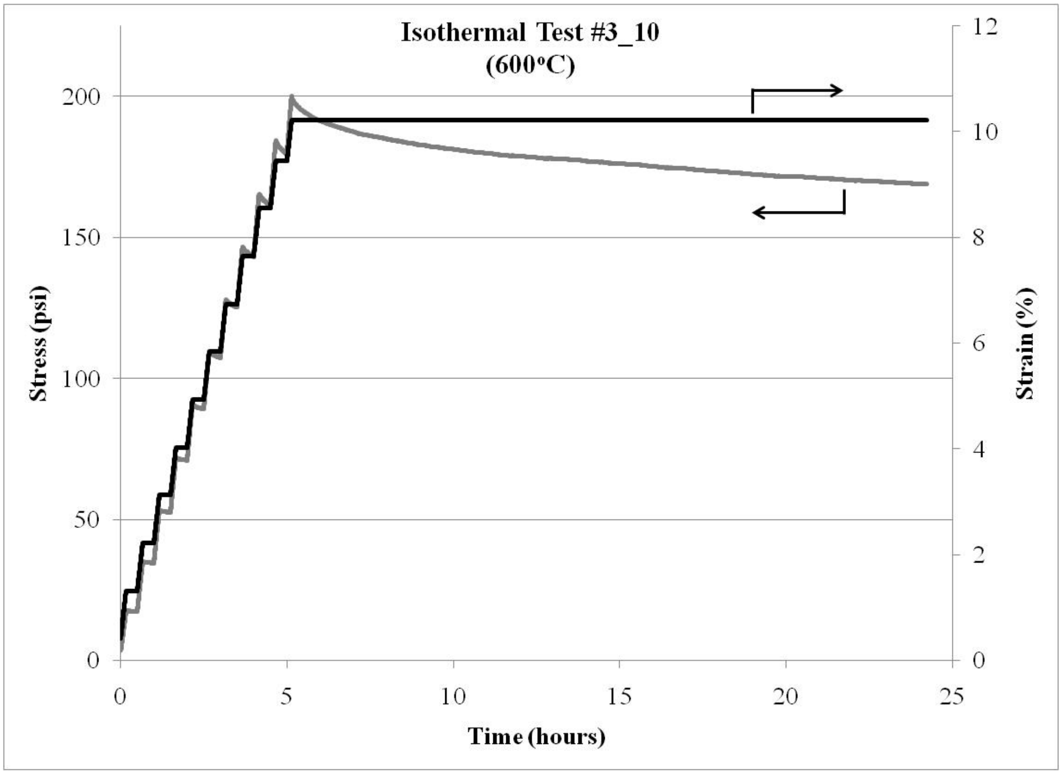

Figure 58. Isothermal Test #3_10 (600°C).

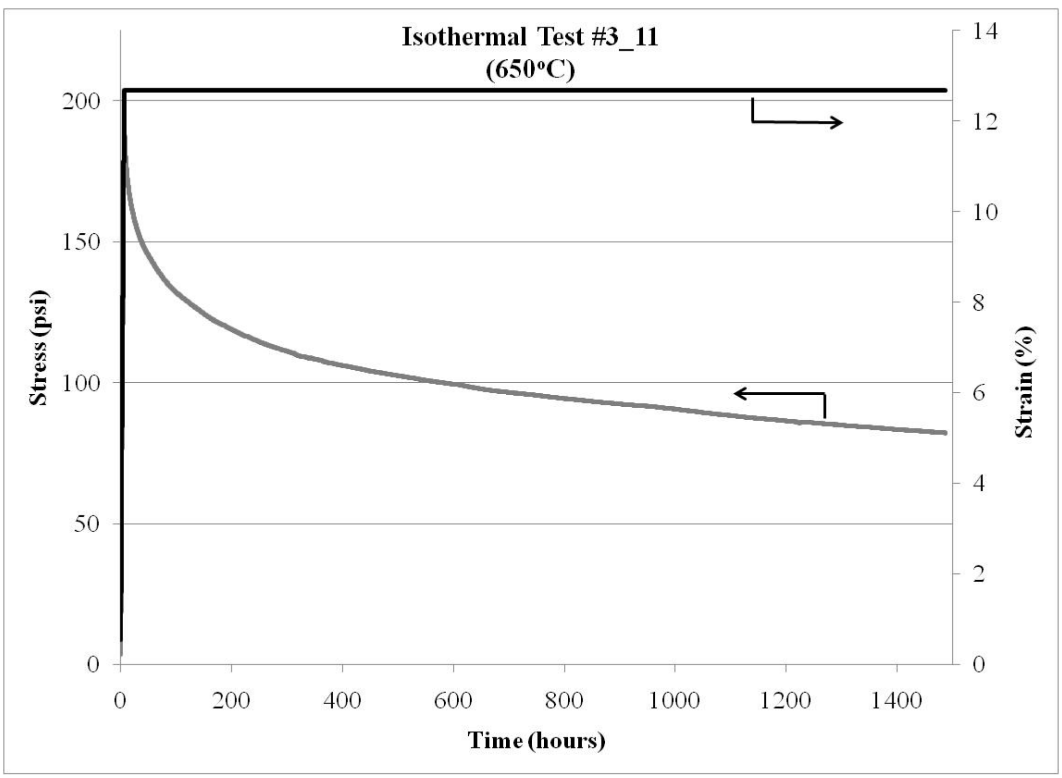

Figure 59. Isothermal Test #3_11 (650°C).

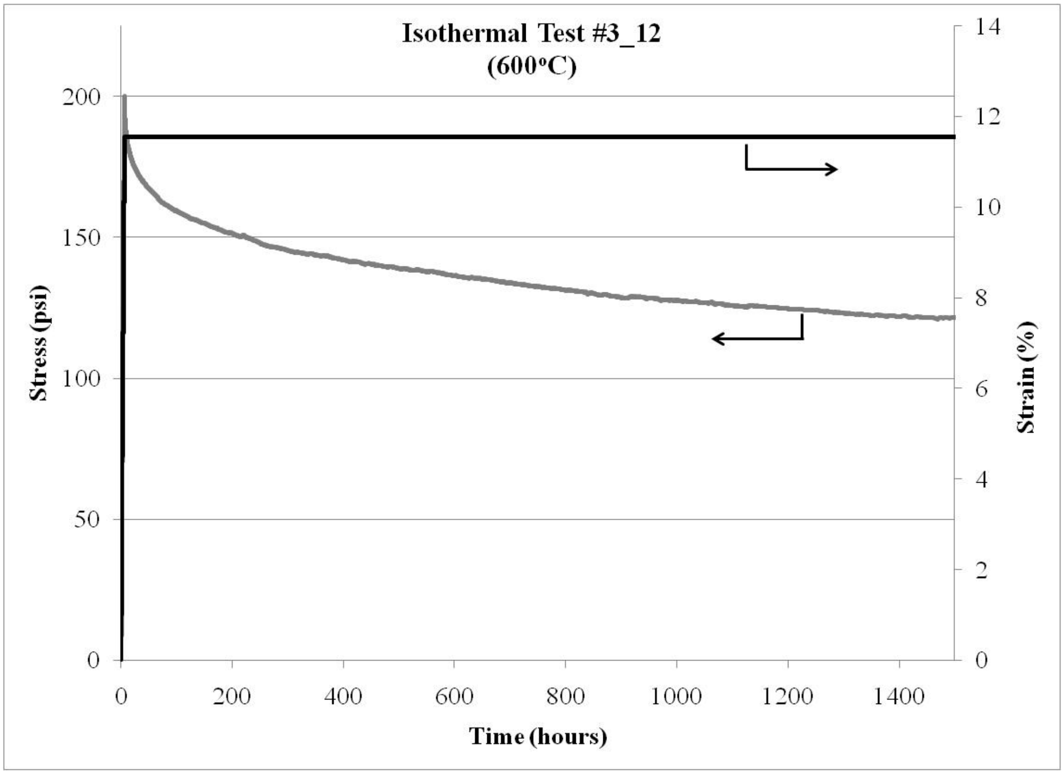

Figure 60. Isothermal Test #3_12 (600^{o}C).

6. LESSONS LEARNED

- For the Changing Environments Tests, the rate of stress relaxation did not appear to be affected by either the first or second changing environment event, nor by the TSE event. After each of these events, the rate of stress relaxation appeared to return to a level similar to that before the event.

- Lateral Load Testing was performed to provide information on the friction created between two pieces of Min-K or a piece of Min-K and a textured aluminum surface at both room temperature and at elevated temperatures. The original test set-up required modification to eliminate lateral loading created when axial loads were applied to the test assembly. The original rear support assembly was replaced with a turnbuckle system connected to the center aluminum plate and load cell by hooks and eyelets. Additionally, the original metal loading plates were replaced with new plates incorporating aluminum inserts with the same "pyramoidal" texture as the center plate. Also, supports were added to confine lateral movement of the push rods due to flexure. The use of the hooks and eyelets allowed the sample assembly to move without creating a lateral load during the application of the axial loading and by manipulating the turnbuckle, a lateral load could now be applied to the test assembly.

  Results of initial testing performed at room temperature using the original test set-up provided information on the amount of axial stress that the test assembly could accumulate for a specific dead axial load and test speed (speed of actuator to apply lateral load) before slipping between the Min-K layers occurred represented by the maxing out of the measured axial stress. Results of testing performed using the test set-up after the first modification showed a decrease in lateral load until a corresponding axial load was reached at which point the lateral load remained constant for a fixed period before the lateral load began to decrease to zero as the remainder of the axial load was removed. There was good repeatability found between repeat tests run under these conditions. Tests run under varying displacement rates during removal of the axial load indicated that the removal of the axial load at a faster rate resulted in the period of decreased lateral load loss occurring at a higher lateral load value. Results of testing performed using the test set-up after the second modification showed that the lateral loads were found to decrease rapidly at a constant rate with the removal of the axial load, contrary to the behavior seen in previous testing. After stiffening the test frame, testing showed that in general, samples began to slip when the applied lateral load was roughly twice the applied axial load. This is as expected since a friction factor of $\approx$1 was expected for this material and the applied lateral load was split over two sample surfaces. Therefore, the lateral load at slippage should be roughly twice the applied axial load. No difference in material behavior was seen when using different sample sizes nor when testing at room temperature or 400^{o}C.

- Isothermal Stress Relaxation testing performed at 450, 500, 550, 600, and 650^{o}C provided additional information on the isothermal stress relaxation behavior of Min-K at intermediate temperatures. As found through previous testing, the behavior of Min-K transitions from "lower temperature behavior" to "higher temperature behavior" at these temperatures as characterized by the rate of stress relaxation.

7. ACKNOWLEDGEMENTS

The authors acknowledge the work of ORNL Technical Intern Zach Burns who contributed to the set-up and maintaining of the long-term testing. Technical advisement and input was provided by Al Lewis, Xinhong Zheng, Michael Lauer, and Nora Low (United Technologies) and Russell Bennett (Teledyne Energy Systems, Inc.). The authors would also like to thank Jy-An John Wang, Andrew Wereszczak, and Edgar Lara-Curzio for reviewing the manuscript.

References

1. J.G. Hemrick, E. Lara-Curzio, and J.F. King, "Characterization of Min-K TE-1400 Thermal Insulation", ORNL Technical Report, ORNL/TM-2008/089, (2008).

2. J.G. Hemrick, E. Lara-Curzio, and J.F. King, "Characterization of Min-K TE-1400 Thermal Insulation (Two-Year Gradient Stress Relaxation Testing Update)", ORNL Technical Report, ORNL/TM-2008/157, (2009).

3. W.E. Osmeyer, "Selenide Isotope Generator for the Galileo Mission – SIG Thermal Insulation Evaluation Tests", TES-33009-50, (1979).

INTERNAL DISTRIBUTION

1.	B. R. Friske	7.	R. G. Miller
2-4.	J. G. Hemrick	8.	G. B. Ulrich
5.	J. F. King	9.	S. M. Wilson
6.	E. Lara-Cruzio	10.	ORNL Laboratory Records—OST

EXTERNAL DISTRIBUTION

11-12. U. S. DEPARTMENT OF ENERGY, NE-43/Germantown Building, 1000 Independence Avenue S. W., Washington, District of Columbia 20585-1290

D. A. Cairns-Gallimore
W. S. Yoon

13-14. IDAHO NATIONAL LABORATORY, P. O. Box 1625, Idaho Falls, ID 83415

S. G. Johnson
K. L. Lively

15. LOS ALAMOS NATIONAL LABORATORY, P. O. Box 1663, NMT-9, MS E502, Los Alamos, NM 87545

D. L. Armstrong

16-18. ORBITAL SCIENCES CORPORATION, INC., 20030 Century Blvd., Suite 102, Germantown, MD 20874

R. T. Carpenter
A. Rabeau
E. A. Skrabek

19. TELEDYNE ENGINERING SYSTEMS, 10707 Gilroy Road, Hunt Valley, MD 21031

R. Bennett
M. McKittrick

21-24. UNITED TECHNOLOGIES, 6633 Canoga Avenue, Canoga Park, CA 91309

M. Lauer
A. Lewis
N. Low
X. Zheng

25-26. UNIVERSITY OF DAYTON RESEARCH INSTITUTE, 300 College Park, Dayton, OH 45469-0162

C. D. Barklay
D. P. Kramer